



UNIVERSITÀ  
DEGLI STUDI  
DI PADOVA

Sede Amministrativa: Università degli Studi di Padova

Dipartimento di Biologia

---

SCUOLA DI DOTTORATO DI RICERCA IN BIOSCIENZE E BIOTECNOLOGIE  
INDIRIZZO: BIOTECNOLOGIE  
CICLO: XXV

**BIOCHEMICAL AND FUNCTIONAL CHARACTERIZATION OF P23  
A REGULATORY CO-CHAPERONE OF HSP90 IN ARABIDOPSIS**

**Direttore della Scuola:** Ch.mo Prof. Giuseppe Zanotti

**Coordinatore d'indirizzo:** Ch.mo Prof. Giorgio Valle

**Supervisore:** Ch.ma Prof.ssa Fiorella Lo Schiavo

**Co-Supervisore:** Dott.ssa Michela Zottini

**Dottorando:** Stefano D'Alessandro







## Index

<b>Abstract</b>	1
<b>Introduction</b>	3
<b>Results and Discussion</b>	25
Biochemical characterization of the two isoforms of p23	
The p23 co-chaperone is a novel substrate of CK2 in <i>Arabidopsis</i>	29
p23-1 co-chaperone shows a specific pattern of phosphorylation in <i>Arabidopsis</i>	41
Functional analysis of p23 co-chaperones of <i>Arabidopsis</i>	53
A technical note on the use of cPTIO as NO scavenger and EPR probe	75
<b>Conclusions</b>	89
<b>Materials and Methods</b>	97
<b>Collaborations and Acknowledgments</b>	
<b>Bibliography</b>	
<b>Evaluations</b>	

---



## Abstract

In the present Ph.D. thesis it is reported a molecular and functional study of the *Arabidopsis* p23, a key component of the HSP90 complex. Homologues of the p23 co-chaperone of HSP90 have been found in all eukaryotes, suggesting conserved functions for this protein throughout evolution. While p23 has been well studied in animals, little is known about its function in plants. *Arabidopsis* owns two isoforms of p23 and their expression pattern was analysed *in planta*. We characterized the expression profile of the two isoforms founding redundant functions in the analysed pathway. In order to determine the function of the two p23 paralogue genes, we selected knockout homozygous insertional mutant lines and overexpressing transgenic lines for both genes. The analysis of the knockout mutant and overexpressing lines showed these proteins as involved in Nitric oxide production both in physiological processes and in stress induced conditions. All the lines showed alteration in root growth parameters, suggesting a likely involvement of p23 in auxin regulation. So to understand the molecular mechanisms underlying the growth alterations observed in p23 knockout mutants, the involvement of auxin and Nitric Oxide was investigated.



# *Chapter I:*

## *Introduction*



### ***Arabidopsis thaliana*: a plant model organism**

*Arabidopsis thaliana* is an herbaceous plant belonging to *Brassicaceae*, well studied since the end of the 19<sup>th</sup> century, which has become a model organism for plant science since the 80s. *Arabidopsis* is the first plant whose genome (125Mbp in five chromosomes) has been sequenced (published in 2000), and this acquired knowledge has finally corroborated the use of this species as model plant. Its life cycle which is only of six weeks, the small size of its genome and the easy processing techniques, have also contributed to the emergence of mutant collections such as NASC (<http://arabidopsis.info/>) and databases, such as TAIR ([www.arabidopsis.org](http://www.arabidopsis.org)), enabling the integrated management of many data collected throughout the world.



### ***Arabidopsis* p23, a co-chaperone of HSP90**

P23 is a small acidic protein, identified in animal system as a component of the progesterone-receptor HSP90 complex [Johnson J. et al. 1994]. P23 binds to the N-terminal domain of HSP90 in the ATP-bound state of the HSP90 dimer (Figure I.1.B) and stabilizes the active closed-conformation of the complex, by inhibiting the ATPase activity [Chadli A. et al., 2000; Ali M.M. et al., 2006]. *Arabidopsis* genome shows two paralogues of p23: the *At4g02450* and the *At3g03773* loci. These two loci encode for two proteins of different length called respectively p23-1 (241 AA 25.47 kDa) and p23-2 (150 AA 17.4 kDa) that have a medium similarity level (ClustalW2 score: 36, 60% positive AA), and show a 38-60% range of identities with other plant-p23 (Fig. I.3). The difference in length between p23-1 and p23-2 is due to a long glycine rich (MG/GA) segment of 70 amino acids in the C-terminal region of the protein, whose function is not yet understood. Both plant p23 isoforms, and the chimeric protein p23-1-d (deleted of the glycine rich tail) are able to bind HSP90 but unlike their animal counterpart, they do not slow the ATPase activity rate of the chaperone [Zang Z. et al., 2010].

A

Bnp23	...MSRHPTVWQKRS.....DKVYITVQLFCAEIVYKLEK...EKK	37
Atp23-1	...MSRHPEVWQKRT.....EKIPLTVVLAQIKITKVNLDG...EAV	37
Atp23-2	...MSRNPEVLWQKRS.....DKVYLVVLAEDAKDESVKCEP...DQL	37
Osp23	...MSRHPEVWQKRI.....DKVYITVQADAKTAKVNLEP...EIV	37
Lep23	...MSRHPTIWRQMS.....DKIPLTVVLEFDANNVKLEK...EKK	37
Dgp23	...MSRHSTIWRQRS.....DKVYLVVLEEDAKIVKLNLEK...DQH	37
Sba1p	MSDKVINQVAVWQKRSSTTDPERNYVLIIVVSLADCCDAPELTIKSYIEN	50
p23	...MQPSAIVWYDR.....EYVEIEFCMRSKIVNVNFE...KER	35
Consensus	.....w.....d.....	
Bnp23	EFYKRTSGASKTLVYVDELDLDSVIVNESKASVSS...RSVLYLVKRAAS	84
Atp23-1	EDFAKVGPFENHVYELKLEFLADKRVNVESSKINIGE...RSFFCIIEKRAF	84
Atp23-2	EFPSALGAGQGERYEFSLDLYGKI.MTYEYKRVGL...RNIIFSIQEER	82
Osp23	ESFDATAGTGNLYESKLEKLNKVNVESSKISVGV...RSFFCIIEKRAA	84
Lep23	ELFRATAGADNVPYVVDLDFDKINVDESSSTTS...RSVYLVKRAED	84
Dgp23	ENFSAKVGSDDMQYELDLELDFDAVWVESSKAAVAP...RTICYLVKRAAS	83
Sba1p	AQSKFHVGDENVVHQLHLDLYKEIIPKTMHKVANGCHYELKLYKOLE	100
p23	LTFSCLGSSDNFK.HLNEIPLFHCILPKNSKHKRTD...SSLCCERKES	82
Consensus	.....q.....l.....k.....	
Bnp23	.KHWNLTPPEGRHPLYLKYVDWQWVDEDEED.....	115
Atp23-1	.EYNNQLR.VKKPPHYVKVDWQWVDEDEGSAGAADMDMAGMEGMGGH	132
Atp23-2	.SKWTDLLKSEKPAPIRYDWNWVDEDEEVN.....	114
Osp23	.KHWKLVVDDQKAPNFVKVDWQWVDEDDDG...ADVNVDGMD.FSNF	128
Lep23	.KHWSPVWQKGLRPVFLKYVDWQWVDEDEED.....	115
Dgp23	.TWWPILKKGKPPVFLKYVDWQWVDEDEED.....	114
Sba1p	SEYMPPEEK.EKVKYPYIIEFDWVDEDEQDE.....	132
p23	GQSPFRTIY.EKRAKLNWLSNDENWVWVDEDDG.....	113
Consensus	.....w.....l.....d.....w.....d.....	
Bnp23	...KGGEGDMDDFGDFP.FNGLN.....MGD.....TDE	139
Atp23-1	GGMGGMGGMGGMGGMGGMGGMEGMDFSKLMGGMGGMGGLEGLGGMG	182
Atp23-2	.....	114
Osp23	GGMGGMGGMGGMGM.....MGGMG.....GMGGMGMAEM.MGG	162
Lep23	...SKPEPDMDFGDMDFSKLN.....MDEG.....PSN	140
Dgp23	...AGFGG...DFGDMDFSKLG.....MGDD...GDE	138
Sba1p	VEAEGNDVAQQNDFSCMMGAG.....GAGGAGGMDFSQMMGG	170
p23	.....DEMSNFDRESMM.....	127
Consensus		
Bnp23	IG.....EEVAEEDG..DGEGETAAETREKKIDGKDEEGVNAKED....	178
Atp23-1	MGGMGGMGGMGMEFEFESDDEESTAKSGDKKIDAVKKEGPATERAPAAE	232
Atp23-2	.....SETASDDE...SAFVNDSESSODDGLLYLPLEKARNK.....	150
Osp23	MGGMGGMGGMGMEFEFEDESDDDEEVSK.PQDAEKAAEAGNSQESDAKAE	211
Lep23	FD.....VDVPEGDD...DSDTEEIEEENSEPKAAPPSTEPGVAA....	179
Dgp23	IE.....EDEDEDDNMVDSANKEVEIVRPEGSKGEAPATTDEAKP...	180
Sba1p	AGG.AGSPDMAQLQLLAQSGGNLDMGDFKENDEEDEEEIEPEVKA...	216
p23	.....NNMGGCEVDLPEVDEADEDSQDSDEKMPLE.....	160
Consensus		
Bnp23	.....	178
Atp23-1	ETTSVKEDK	241
Atp23-2	.....	150
Osp23	TS.....	213
Lep23	.....	179
Dgp23	.....	180
Sba1p	.....	216
p23	.....	160
Consensus		

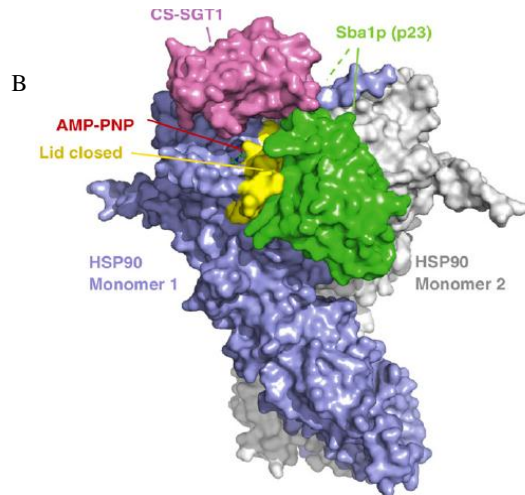


**Fig. I.1: A)** Figure adapted from [Zhang Z. et al., 2010]. Amino-acid sequence alignment of p23-like proteins of plant, yeast and human origins. Bnp23 (AAG41763), Atp23-1 (CAC16575), Atp23-2 (NP\_683525), Osp23 (NP\_001061631.1), Lep23 (AAG49030), Dgp23 (ABA60373.1), Sba1p (NP\_012805.1), and p23 (AAA18537) were aligned using DNAMAN software. The numbers on the side indicate the amino acid positions in the proteins. Black, gray, and light gray shading indicates 100%, 75%, and 50% conservation of amino acids, respectively.

**B)** Figure adapted from [Kadota Y. et al., 2009]. A hypothetical model of a full-length HSP90 dimer with different co-chaperones, extrapolated from the structures of HSP90–Sba1p (p23) (PDB:2CG9) and CS domain–HSP90-ND (PDB:2JKI) complexes. Although the SGT1 CS domain and p23 are structurally similar, each protein binds a distinct, non-overlapping site of HSP90.

### HSP90 co-chaperones

Various co-chaperones associate dynamically with HSP90 during the chaperone cycle. In eukaryotic cells the complex is regulated by more than 20 co-chaperones (Figure I.2.B).

These proteins have a pivotal role in the regulation of the complex and in the specificity of HSP90 activity and they can be divided in two main groups: the TPR (tetratricopeptide) and the non-TPR domain co-chaperones. TPR containing co-chaperones include HOP (HSP70-HSP90 Organizing Protein), PP5 (Protein Phosphatase 5), and the PPIase (Prolyl Isomerase) family, such as FKBP51 and FKBP52 (FK506 Binding Protein), while the non-TPR containing co-chaperones include AHA1 (Activator of HSP90 ATPase), p23 and Cdc37 (Cell Division Cycle protein) [Li J. et al., 2011].

HOP binds and stabilizes the open conformation of HSP90 and mediates the interaction with HSP70. P23 is a co-chaperone essential for the folding of the steroid receptor that binds specifically to the closed conformation of HSP90, mainly with the ND and the MD, and that stabilizes the active conformation of the dimer by lowering the ATPase rate of HSP90. Cdc37 is a co-chaperone of HSP90 that slows the ATPase rate, like p23, specific for the folding of kinases: it interacts with kinases by the N-terminal domain and binds to the ND of HSP90 through its C-terminal domain. Cdc37 controls the HSP90 complex regulating the folding of signaling kinases, and it competes for the binding site with p23, responsible for the regulation of the steroid receptor foldosome. AHA1 (activator of the ATPase activity of HSP90) is a co-chaperone that upon the binding with HSP90, induces a domain re-orientation in which the ND reaches the closed conformation and by so doing accelerates the progression of the ATPase cycle. PP5 is a protein phosphatase that associates with HSP90 by its N-terminal TPR containing domain. The binding with

HSP90 induces the activation of PP5 activity that can specifically dephosphorylate HSP90 and Cdc37.

### **The Heat Shock Protein 90 complex**

Heat shock protein 90 (HSP90) is an highly abundant protein that represents 2% to 4% of total proteins in eukaryotic cells, and controls many fundamental cellular processes regulating a plethora of kinases, hormone receptors and transcription factors [Pearl L. H. and Prodromou C., 2006; Kadota Y. and Shirasu K., 2012].

In eukaryotes, HSP90 localizes mainly to the cytosol, but it can be found also in organelles and into the nucleus. In animals, there are two main cytosolic isoforms: an inducible isoform (HSP90- $\alpha$ ) and a constitutive one (HSP90- $\beta$ ). In plants several additional isoforms are present [Krishna P. and Gloor G., 2001]. Organelle-localized HSP90 proteins are part of the same family: TRAP1 in mitochondria, HSP90-6 in the chloroplast, and GRP94 in the endoplasmic reticulum. Moreover, recent studies show that HSP90 is present also at the external cell surface and secreted in the extracellular space [Sidera K. and Patsavoudi E., 2008].

HSP90 is structured in three main domains: the N-terminal ATPase domain (ND), followed by a charged region of variable length, the middle domain (MD), where client proteins are accommodated, and the C-terminal dimerization domain (CD) containing the MEEVD motif. The MEEVD motif allows HSP90 to interact with a rich cohort of co-chaperones containing the TPR (Tetratricopeptide) domain, and this domain confers an extraordinary plasticity of function to the chaperone. In the apo-state, HSP90 is in an open V-shaped conformation and upon the binding of the ATP to the N-terminal domain, the lid portion of the HSP90-ND rotates in order to enclose ATP (first intermediate state). Then, the ND of the two HSP90 monomers come in contact and associate with the MD, by so doing the HSP90 dimer reaches the closed conformation (second intermediate) [Ali M.M. et al., 2006; Li J. et al., 2011]. In the closed conformation of the HSP90 dimer, the ATP is brought to ATPase active site of the HSP90-MD, where it is hydrolyzed. Once ATP is hydrolyzed the lid segment rotates back and the HSP90 dimer returns to the open conformation, releasing ADP and phosphate (Figure I.1.A). By this way ATP generates an ordered sequence of conformational changes in the chaperone complex that is essential for its chaperoning functions and regulates the binding of the co-chaperones and the one with its clients [Li J. et al., 2011].

As HSP90 is extremely abundant and is able to recognize more than 200 clients, the probability of encountering between the chaperone and its substrates is very high so HSP90 has to maintain an exceptional specificity. This is due to the ATP conformational cycle of the HSP90 complex and the rich cohort of co-chaperones that modulates its function. The composition of the complex, in terms of co-chaperones interacting with HSP90, is strictly regulated at several levels, including post-translational modifications. During the chaperone cycle several complexes are formed which differ in the co-chaperones associated with HSP90 [Li J. et al., 2011]. So the complex conformation is regulated by the ATP cycle, by HSP90-dimer intermediates that allow specific binding of the co-chaperones, even in an asymmetrical manner, and by the binding with the clients. Altogether, the ATP cycle, the binding with the co-chaperone or the binding with clients stabilize the HSP90 complex in many different conformational states and this is the main feature that confers an exceptional specificity to this protein [Li J. et al., 2011].

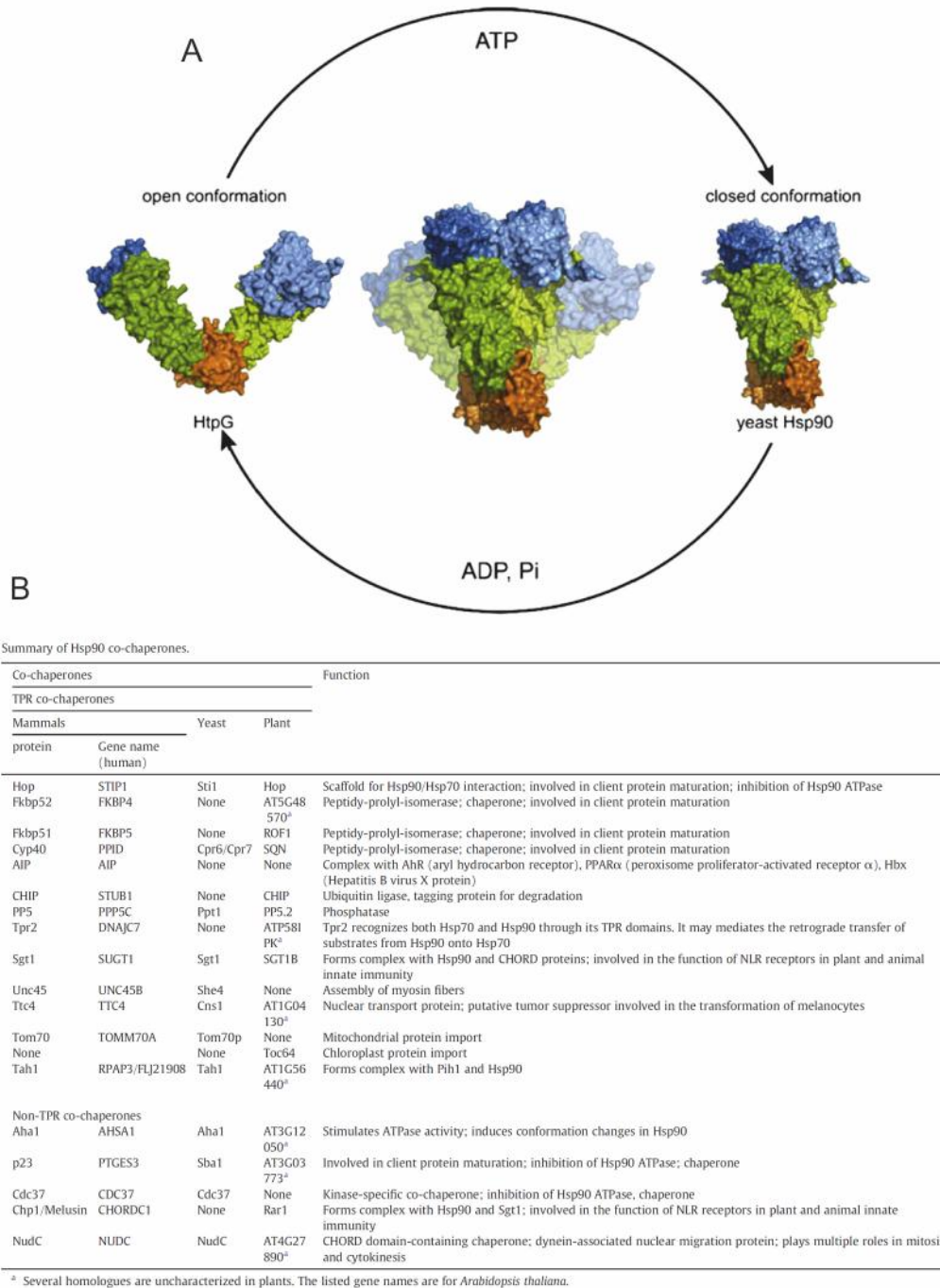


**Fig. I.2:** Figure adapted from [Li J. et al., 2011]

**A)** HSP90 crystal structures of full length HSP90 from *E. coli* (HtpG) in the open conformation (left, PDB 2IOQ) and nucleotide-bound yeast HSP90 in the closed conformation (right, PDB 2CG9). The N-domain is depicted in blue, the M-domain in green and the C-domain in orange.

**B)** Summary of HSP90 co-chaperones

## HSP90 chaperone cycle

The chaperone cycle of HSP90 is a finely orchestrated process, under control of the ATP cycle and of many co-chaperones. HSP90 has to exhibit the right conformation in order to accept the client protein, to facilitate the folding and to extrude the folded protein. Each of these steps is stabilized by specific co-chaperones that allow the encountering between the HSP90 dimer and the client protein. In particular, Cdc37 is fundamental for the folding of the so-called signaling kinases, while p23 is essential in the maturation of the steroid receptor (SHR).

The assembly of the SHR involves the chronological progression through three complexes: while HSP90 is in the V-shaped apo-state, HSP70 and HSP40 binds the native receptor and by the adaptor protein HOP they form a quaternary complex. The open conformation of the early complex can accommodate ATP and a PPIase co-chaperone forming an asymmetric complex. Upon the binding of ATP, the complex reaches the first intermediate complex that releases and accommodates p23. After the release of HOP and so of HSP70 and HSP40, the complex reaches a symmetrical second intermediate state in which ATP can be hydrolyzed. The hydrolysis of ATP and the release of ADP and phosphate bring the dimer back to the open conformation (Figure I.3.A).

## Plant HSP90

Seven members of the HSP90 family were identified in *Arabidopsis* [Krishna P. and Gloor. G., 2001]. The seven members share at least 45% sequence identity, reaching 96% between HSP90-2, HSP90-3 and HSP90-4 that, together with HSP90-1, are the isoforms localized to the cytosol. All the cytosolic isoforms share the MEEVD C-terminal sequence and have a long charged linker region of variable length [Buchner J., 1999] in which a CK2 phosphorylation site is present. The other three isoforms HSP90-5, HSP90-6 and HSP90-7 show specific targeting peptides. HSP90-5 is addressed to the mitochondrion by a 48-residue N-terminal pre-sequence, HSP90-6 is targeted to the chloroplast by a 60-residue N-terminal transit peptide and HSP90-7 shows the C-terminal KDEL retention motif [Krishna P. and Gloor. G., 2001]. Although the cellular localization patterns are distinct, the amino acid sequence identities between *Arabidopsis*

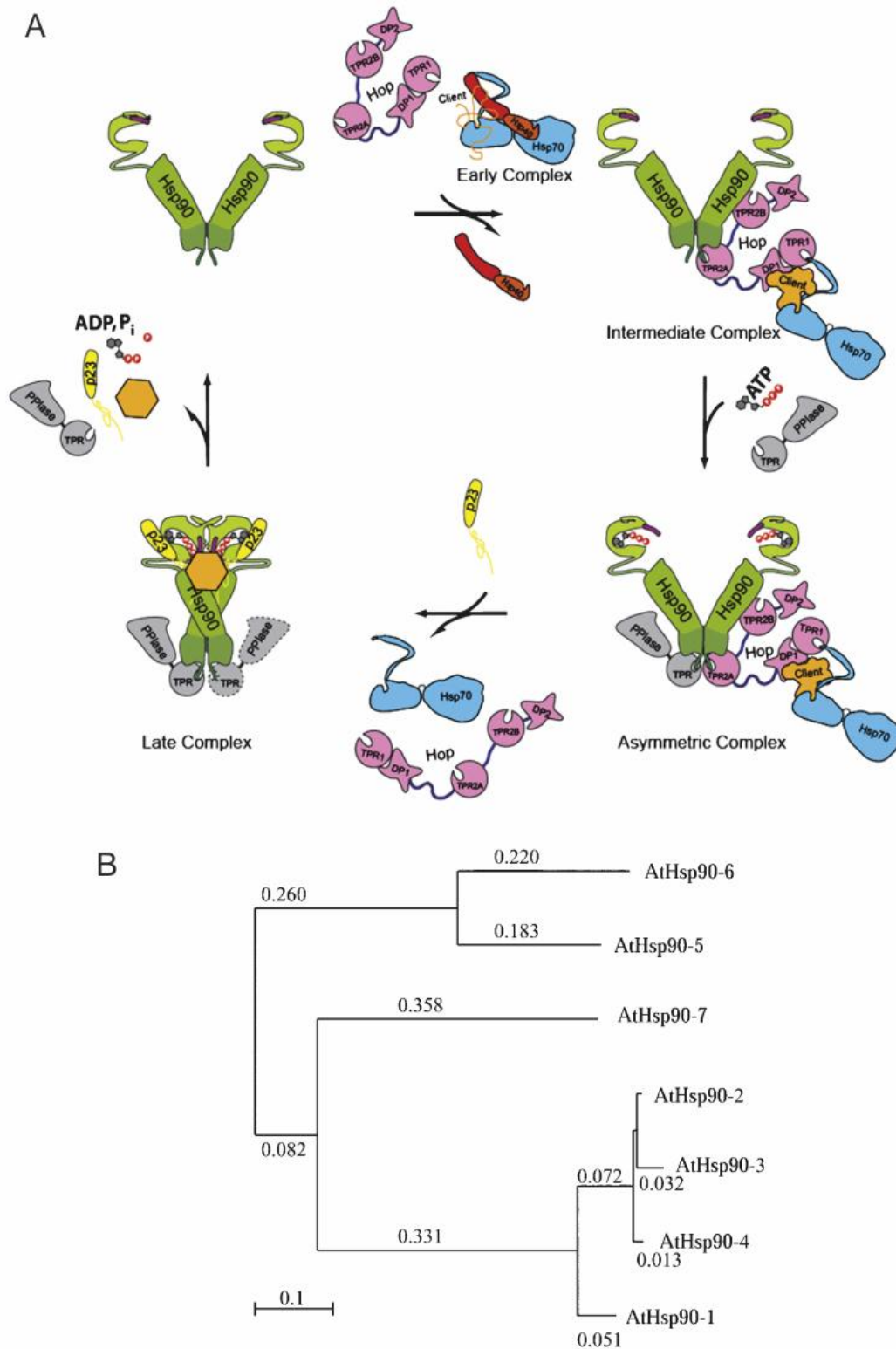


**Fig. I.3:** Figure adapted from [Li J. et al., 2011]

**A)** Co-chaperone cycle of the HSP90 machinery HSP70, HSP40 and a client protein form an ‘early complex’. The client protein is transferred from HSP70 to HSP90 through the adaptor protein HOP. One HOP bound is sufficient to stabilize the open conformation of HSP90. The other TPR-acceptor site is preferentially occupied by a PPIase, leading to an asymmetric intermediate complex. HSP90 adopts the ATPase-active (closed) conformation after binding of ATP. p23 stabilizes the closed state of HSP90, which weakens the binding of

HOP and promotes its exit from the complex. Potentially another PPIase (dashed-line) associates to form the 'late complex' together with HSP90 and p23. After the hydrolysis of ATP, p23 and the folded client are released from HSP90.

**B)** Figure adapted from [Krishna P. and Gloor. G., 2001]. Molecular phylogeny of the AtHsp90 family of genes. This diagram shows the number of amino acid substitutions per amino acid position that is observed between a given protein and the inferred ancestral protein sequence represented as the node to which the protein is joined. For example, it is estimated that an average of 0.22 amino acid substitution occurred at each position in the sequence of the AtHsp90-6 protein since it diverged from the common ancestor, leading to both it and the AtHsp90-5 protein. Branches without an associated substitution number have fewer than 0.01 substitution per position.

HSP90 proteins and the other HSP90 are significant, suggesting that the biochemical function of all these isoforms could be similar [Kadota Y. and Shirasu K., 2012].

In plant cells, HSP90s are developmentally regulated but they can also be modulated by external stimuli such as abiotic stresses or hormone treatments [Sangster T.A. and Queitsch C., 2005]. HSP90-1 transcript is detected only in roots of *Arabidopsis* under normal physiological conditions while it is strongly induced in all plant tissues under heat stress or heavy metals treatment. HSP90-2 and HSP90-3 transcripts are present at basal level in all plant organs but abundant only in roots and flowers. Moreover, they increase after treatment with IAA (Indole-3-acetic acid, the most abundant auxin) or heavy metals [Sangster T.A. and Queitsch C., 2005]. HSP90 is involved in many physiological and pathological signaling pathways and mutants of the different isoforms show specific and redundant functions. Mutation in the chloroplast specific HSP90-5 causes altered response to red light, chlorate resistance and delayed chloroplast development. Mutation in the ER-specific HSP90-7 produces floral and shoot meristem phenotypes [Kadota Y. and Shirasu K., 2012]. Mutation of both HSP90.1 and HSP90.2 is lethal [Sangster T.A. and Queitsch C., 2005]. HSP90 is an essential protein whose interaction with many co-chaperones is pivotal for its functions. Co-chaperones control the cycle of the HSP90 dimer by inhibiting or accelerating the cycle at defined position and set the stage for the client binding. HSP90 complex relies on the participation of many co-chaperones such as p23, HOP, AHA1, PP5 and the FKBP (PPIases) [Zhang Z. et al., 2010; Kadota Y. et al., 2008; Geisler M. and Bailly A., 2007]. Plant HSP90 and its co-chaperones resemble their mammalian counterparts in their structure but they can participate in diverse and unique pathways such as defense mechanisms against pathogens, regulation of gene expression, transport of pre-proteins into organelles and response to heat stress. Moreover there is increasing evidence on the role of HSP90 and its co-chaperone in hormone homeostasis. Auxin homeostasis, for example, is controlled by TWD1 as shown by its mutant *Twisted*

*dwarf 1* (*twd1*). TWD1 is a FKBP (PPIase) that interacts with HSP90 and this complex regulates the auxin efflux by modulating ABC transporters [Geisler M. et al., 2005; Bailly A. et al., 2006]. ABC transporters are membrane transporters not specific for auxin that can associate with the PIN family transporters and enhance and direct the auxin specific efflux [Blakeslee J.J. et al., 2007; Mravec J. et al., 2008]. TWD1 is a perfect example of how a co-chaperone of HSP90 can be essential for the regulation of the homeostasis of an hormone, and the *twd1* knockout line shows severe dwarfism and a strong impairment in the auxin transport leading to the characteristic twisted short root (Figure I.4) [Bailly A. et al., 2006].

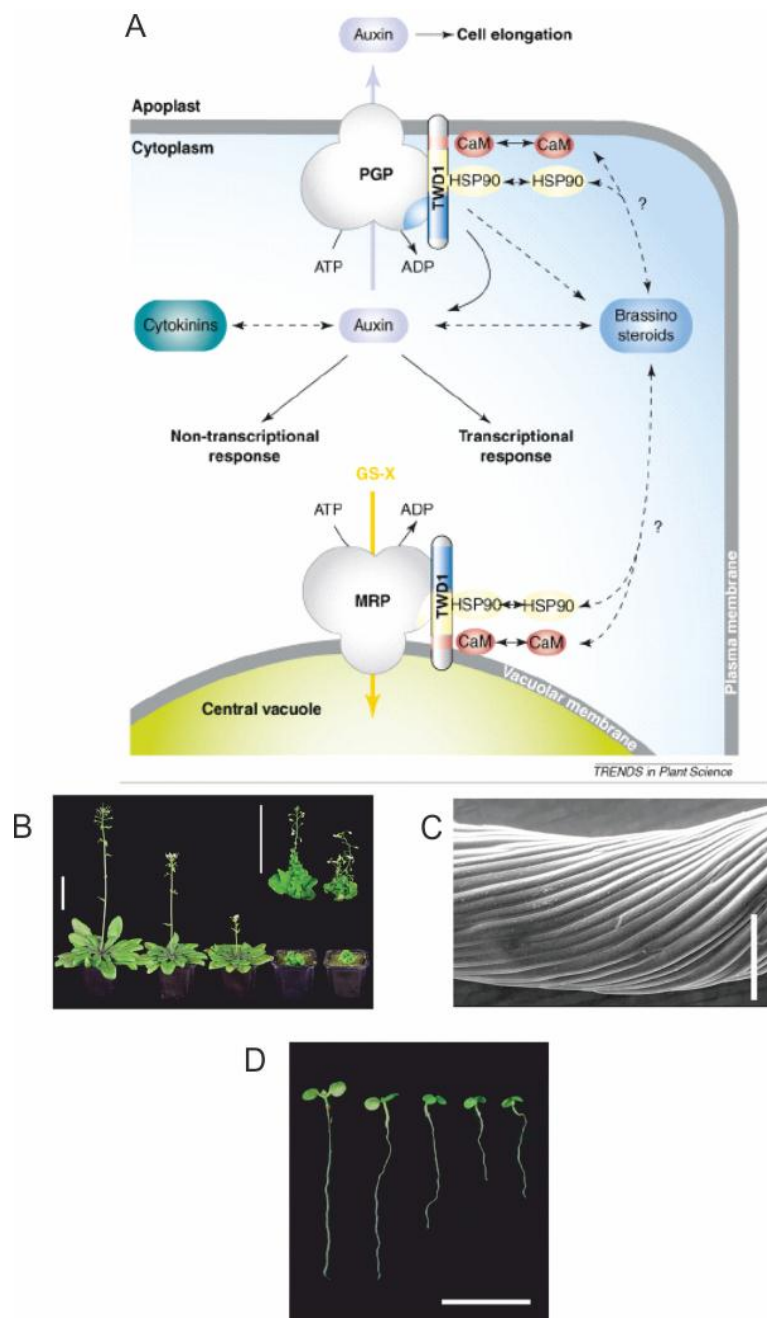


**Fig. I.4:** Figure adapted from [Geisler M. and Bailly A., 2007] and [Bailly A. et al., 2006]

**A)** Model of TWD1 action. TWD1 forms functional ABC transporter complexes on both the vacuolar and plasma membrane. Whereas the positive regulatory role of TWD1 on PGP-mediated auxin transport has been demonstrated, the modulation of MRP-mediated vacuolar import was established using mammalian test substrates [glutathione conjugates (GS-X)] because the *in planta* substrates remain unknown. Direct TWD1-mediated (solid lines) and indirect (dashed lines) signal transduction and hormone crosstalk are indicated by arrows. Functional domains and interactor proteins are as follows: blue, FKBD; yellow, TPR domain and HSP90; red: CaM(-BD); and gray, membrane anchor. Question marks indicate expected or controversial functional connections that await experimental confirmation.

**B)** The twisted dwarf1 (*twd1*) mutant displays a pleiotropic developmental phenotype that correlates with reductions in auxin transport. Growth phenotypes of one-month-old soil-grown plants; from left to right: wild-type (ecotype Wassilewskija), *pgp1*, *pgp19*, *pgp1/pgp19* and *twd1*. Inset: mature *pgp1/pgp19* and *twd1* plants. Bars, 5 cm.

**C)** Electron micrograph of the *twd1* hypocotyl. The “twisted syndrome” of all organs is perceptible at the epidermal level. Bar, 100  $\mu$ m.

**D)** Growth phenotypes of light-grown seedlings 5 dag; from left to right: wild-type, *pgp1*, *pgp19*, *pgp1/pgp19* and *twd1*. Bar, 1 cm.

## Post-translational modifications of the complex

The regulation of the HSP90 complex is strongly dependent on the exchange of the many chaperones during the cycle. The interaction between HSP90 and its co-chaperones is additionally regulated by post-translational modifications both of HSP90 and its co-chaperones [Miyata Y. 2009]. Transient post-translational modifications such as phosphorylation, acetylation and nitrosylation, ensure fast and efficient responses to extracellular and intracellular stimuli and further contribute to the extraordinary plasticity of the function of HSP90 [Li J. et al., 2011].

Acetylation is a prominent HSP90 modification and its influence on HSP90 is still under investigation. It has been reported by [Yang Y. et al., 2008] that p300 is an acetyltransferase responsible for the acetylation of HSP90 and HDAC6 is an HSP90 deacetylase [Kovacs J. J. et al., 2005; Bali P. et al., 2005]. This modification is important for HSP90 function and influences client protein maturation [Scroggins B. T. et al., 2007]. Furthermore there is a physical interaction between HDAC6 and HSP90 and different studies links HSP90 acetylation with cell signaling, nuclear transport and gene expression.

S-nitrosylation of HSP90 C-terminus was shown to affect HSP90 function, negatively influencing HSP90 ATPase activity *in vitro* and reducing association with eNOS in endothelial cells [167, 168].

## Regulation of HSP90 complex by phosphorylation

Phosphorylation is the most frequent post-translational modification of HSP90 being phosphorylated at multiple sites, mainly on serines. It has been shown that dynamic phosphorylation – dephosphorylation events represent a key regulatory mechanism for chaperone function and the phosphorylation of key residues specifically modulates conformational rearrangements during the ATPase cycle [Li J. et al., 2011].

In particular, the protein kinase CK2 can phosphorylate many components of the complex and so can regulate the chaperone cycle of HSP90. Both isoforms of animal HSP90 can be constitutively phosphorylated by protein kinase CK2 *in vitro* and *in vivo* at two serine residues in a highly charged region of the molecule [Lees-Miller S. P. and Anderson C. W., 1989] and a link between HSP90 phosphorylation and its chaperoning function was

shown for different client proteins [Szyszka R. et al., 1989; Mimnaugh E. G. et al., 1995; Zhao Y. G. et al., 2001; Miyata Y. et al., 1997; Cox M. B. et al., 2007].

The case of the two PPIases: FKBP51 and FKBP52 is of particular interest in order to understand the fine regulation of the HSP90 chaperone cycle by CK2. Despite structural and biochemical similarities between FKBP51 and FKBP52, they have opposing effects on steroid hormone action [Yong W. et al., 2007]. One structural distinction between the two FKBP5s lies in a linker loop (hinge region) between the first and second FK506-binding domains, where FKBP52 possesses a well-conserved putative CK2-phosphorylation site, while FKBP51 does not. FKBP52 is a substrate of CK2 both *in vitro* and *in vivo*, and an *in vitro* reconstitution experiments suggest that CK2-phosphorylated FKBP52 has lower HSP90-binding activity, indicating that phosphorylation by CK2 weakens FKBP52 function [Miyata Y. et al., 1997]. Moreover, the activity of FKBP52, to potentiate steroid hormone receptors in yeast and in mouse cells, is greatly diminished by the phospho-mimicking mutation in the CK2-phosphorylation site [Cox M. B. et al., 2007].

Thus, HSP90 phosphorylation is a crucial part of the finely regulated chaperone cycle and it plays an important role in the chaperoning function.

## The protein kinase CK2

Protein kinase CK2 (formerly known as Casein Kinase II) is an ubiquitous and constitutively active Ser/Thr protein kinase in animal cells, usually organized as a tetrameric complex, consisting of two catalytic ( $\alpha$ ) and two regulatory ( $\beta$ ) subunits (Figure I.5.C) [Pinna L.A., 2002]. *Arabidopsis* owns four  $\alpha$  subunit (Figure I.5.A and B) and four  $\beta$  subunit genes [Salinas P. et al., 2006]. They are essential for cell viability even though the biological roles of CK2 subunits have not been fully characterized yet [Mulekar J. J. et al., 2012]. CK2 phosphorylates many proteins: more than 300 substrates are known so far, most in mammals, with a strict site specificity requiring a precise consensus including acidic residues, in particular at the  $n + 3$  position downstream from the target Ser/Thr [Pinna L.A. and Ruzzene M., 1996]. Among the CK2 numerous substrates, several chaperone proteins have been identified which deserve special attention: in fact, it has been demonstrated that CK2, by phosphorylating this class of proteins, can regulate levels and functions of many other proteins, thus controlling different cellular processes [Miyata Y., 2009].

Expression profile experiments revealed that *Arabidopsis* CK2 subunits are ubiquitously expressed in almost all the tissues. Interestingly, the chloroplastic localized subunit ( $\alpha$ cp) is expressed at higher levels compared to the other nuclear/cytosolic subunits (Figure I.6) [Salinas P. et al., 2006]. CK2 is involved in several crucial processes, including cell cycle and proliferation, circadian rhythm, auxin signaling pathways, dark/light-dependent enzyme regulation, translation, and the salicylic acid (SA)-mediated defense response [Moreno-Romero J. et al., 2008; Moreno-Romero J. and Martínez M.C., 2008; Espunya M.C. et al., 2005; Zottini M. et al., 2007].



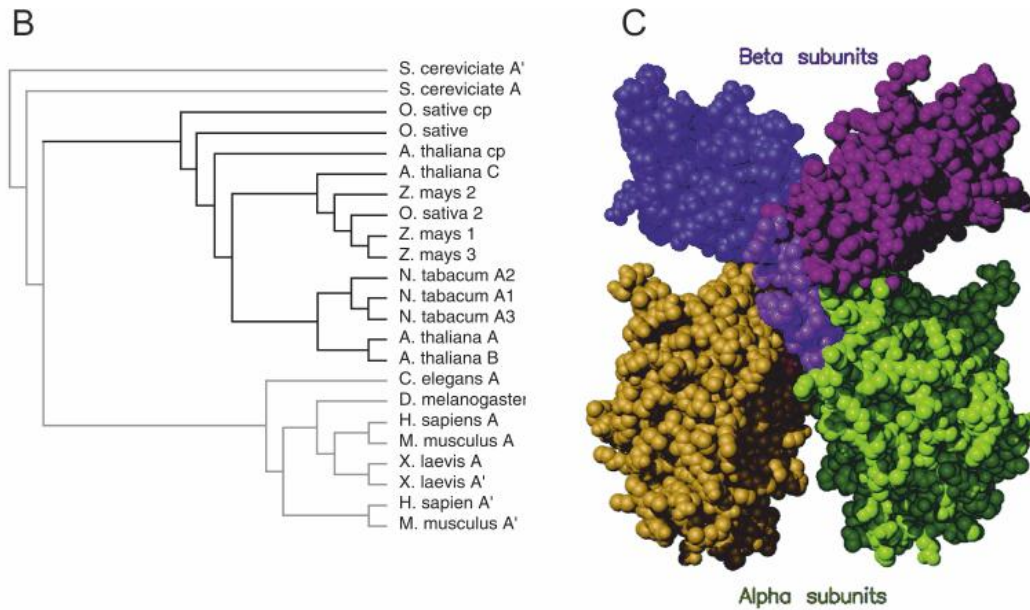


**Fig. I.5: A)** Figure adapted from [Salinas P. et al., 2006]. Protein sequence analyses of CK2 $\alpha$  subunits from Arabidopsis. CK2 $\alpha$  subunits encoded in the Arabidopsis genome (A.t. $\alpha$ A, At5g67380; A.t.  $\alpha$ B, At3g50000; A.t.  $\alpha$ C, At2g23080; and A.t.  $\alpha$ cp, At2g23070) were aligned with two CK2 $\alpha$  subunits already crystallized from other species: CK2A1 from Homo sapiens (H.s  $\alpha$ A, AAH50036, CSNK2A1 protein) and CK2 $\alpha$ 2 from Zea mays (Z.m  $\alpha$ 2.CAA72290 ZMCK2 protein). Invariant residues are indicated by \*, similar residues by: and semi-conservative changes by (according to Blosom62-12-2). Functional domains conserved in these proteins are underlined: ATP-binding site, the basic stretch (NLS), the catalytic loop and the activation segment.

**B)** Cladogram showing the evolutionary divergence of CK2 $\alpha$  subunits from different species. The cladogram was generated using the deduced full-length protein sequence of the genes indicated (the predicted destination peptide for A.t. $\alpha$ cp was excluded for this analysis). The PAM250 evolutionary matrix was used for the alignment and sorting of the sequences.

**C)** Figure adapted from [Battistutta R. et al., 2000], Hypothetical model of the naturally occurring maize CK2 tetrameric holoenzyme. The model shown is based on the structure of the complex between two  $\alpha$  subunits (in the lower part) with two C-terminal  $\beta$ [181–203] peptides (in magenta, in the center of the entire complex) presented in this work and the structure of the truncated [1–182]  $\beta$ -dimer (upper part) determined by [Chantalat et al., 1999]. The model was assembled in such a way to minimize the distances between the C-terminal ends of the  $\beta$ -dimer and the N-terminal ends of the  $\beta$  peptides. The location of a the nucleotides binding site is indicated by red atoms of residues Arg47 and Lys122.

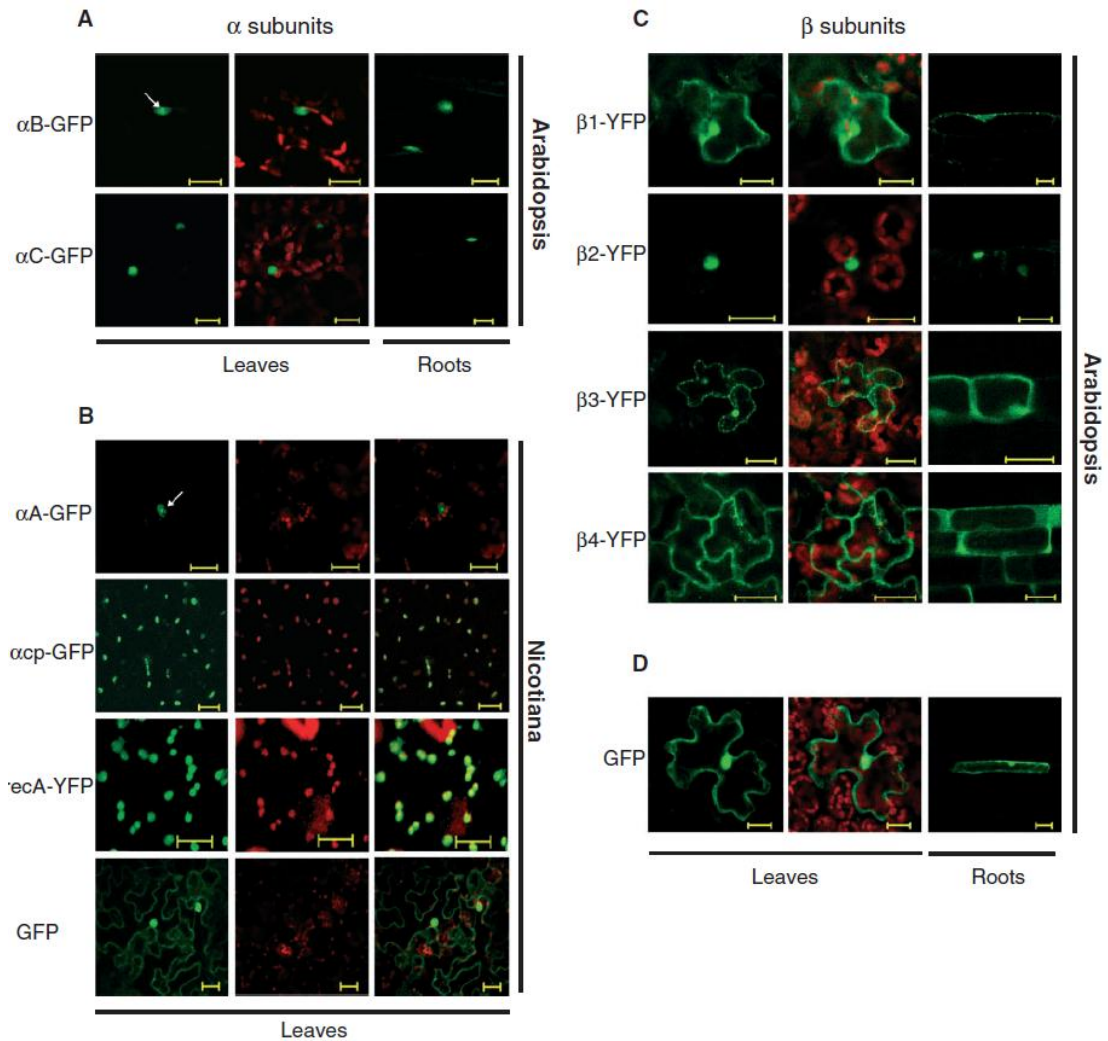


**Fig. I.6:** Figure adapted from [Salinas P. et al., 2006]. **A)** Subcellular localization of CK2:YFP/GFP fusion proteins. Transgenic Arabidopsis plants transformed with XVE inducible constructs coding for CK2 $\alpha$ :GFP fusion proteins (for  $\alpha$ B,  $\alpha$ C) were obtained. Before processing leaf and root samples for confocal microscopy, transgenic plants were treated for 48 h with 50 mM 17- $\beta$  estradiol to induce the transgene expression.

**B)** Leaves from *N. benthamiana* plants were transiently transformed by agroinfiltration with constructs coding for the fusion proteins  $\alpha$ A:GFP,  $\alpha$ cp:GFP and recA:YFP controlled by a constitutive promoter (35S CaMV). At 16 h post-agroinfiltration, leaf samples were analyzed by confocal microscopy.

**C)** Transgenic Arabidopsis plants transformed with XVE inducible constructs coding for CK2 $\beta$ :YFP fusion proteins ( $\beta$ 1,  $\beta$ 2,  $\beta$ 3 and  $\beta$ 4) were obtained. Plants were treated and analyzed as described in A.

**D)** Leaf and root samples from a representative Arabidopsis transgenic plant expressing GFP alone under the control of the XVE inducible promoter. Plants were treated and analyzed as described in A).

Green: GFP or YFP fluorescence. Red: chlorophyll fluorescence. White arrow: discrete structure within the nucleus, presumably the nucleolus. Bar=20  $\mu$ m.

## HSP90 and NO signaling

NO is a small diatomic molecule exhibiting hydrophobic properties with high diffusive abilities ( $4,8 \times 10^{-5} \text{ cm}^2 \text{ s}^{-1}$  in water). So NO may migrate to the hydrophilic regions of the cell and freely diffuse through the plasma membrane [Floryszak-Wieczorek, 2007].

In animal systems, nitric oxide acts as endothelium-derived relaxing factor of vascular tissues. It derives from the oxidation of L-arginine by the endothelial NO synthase (eNOS) [Hecker M. et al., 1991]. Endothelium-derived NO is a critical regulator of cardiovascular homeostasis through its profound effects on blood pressure, vascular remodeling, platelet aggregation, and angiogenesis [Ignarro Lj. et al., 1999]. It has been demonstrated that HSP90 can modulate the activity of eNOS, so regulating the NO signaling pathway [Sud N. et al., 2007].

While NO is generated mainly by nitric oxide synthases (NOS) in animals, in plants there are many possible sources. Nitrification and de-nitrification cycles provide NO as byproduct of  $\text{N}_2\text{O}$  oxidation from the atmosphere, NO could be generated also by non-enzymatic mechanisms such as chemical reduction of  $\text{NO}^2$ , and the major origin of NO production in plants is by the action of NAD(P)H-dependent nitrate and nitrite reductases; moreover NOS-like activities have been detected in plant tissues, even if no protein or gene has been identified so far [Durner J. and Klessig D. F. 1999; Cooney et al., 1994; Crawford, 2006; Yamasaki et al., 1999; Besson-Bard et al., 2008;].

NO is a pivotal signaling molecule in plants and it is involved in many physiological and pathological processes. It acts as a signaling molecule by modulating protein activity and by modulating gene expression. The covalent attachment of NO to the thiol side chain of a cysteine (S-nitrosylation) has been considered the most widespread and functionally important NO-dependent posttranslational modification. Such reaction is not enzymatically catalyzed and depends on the local concentration of NO, so from the equilibrium between NO synthesis and scavenging rates [Hess et al., 2005; Crawford 2006].

NO can react rapidly with thiol and transition metal-containing proteins and more than 100 proteins have been identified as targets for NO *in vitro* and *in vivo*, such as catalases, ascorbate peroxidases, glyceraldehyde 3-phosphate dehydrogenase, and in particular the guanylate cyclase controlling the cGMP-dependent pathway [Stamler et al., 2001; Besson-Bard 2008; Durner et al., 1998].

Moreover NO is able to activate both plasma membrane and intracellular  $\text{Ca}^{2+}$ -permeable channels via signaling cascades involving membrane depolarization and protein kinases,

and it lead to elevated levels of cytosolic calcium [Lamotte et al., 2004; Garcia-Mata and Lamattina, 2003].

Furthermore NO has a pivotal role in plant defense both in the Salicylic acid acquired resistance (SAR) and in the Hyper sensitive response. NO acts at different levels in the SAR, as a matter of fact it has been demonstrated that inhibition of NOS-like activity reduced the SAR. Moreover NO activate the Salicylic acid-induced protein kinase (SIPK) and is fundamental in the induction of the Pathogen related protein 1 (PR1) [Floryszak-Wieczorek, 2007, DelleDonne M. et al., 2001].

The interplay between SA and NO was further demonstrated by the discovery that SA induce NO production in roots of *Arabidopsis* seedlings, and this induced NO production is dependent on a NOS-like activity [Zottini et al., 2007].

Furthermore NO is involved in the action of plant hormones and it is pivotal for Auxin and ABA action, while it antagonizes ethylene [Kolbert et al., 2008; Zhu and Zhou, 2007]. In particular, NO is involved in the auxin-induced adventitious and lateral root formation and in auxin-induced cell division [Otvos K. et al., 2005]. Furthermore NO influences auxin signaling through nitrosylation of TIR1, an auxin receptor [Terrile M. C. et al., 2012 ].

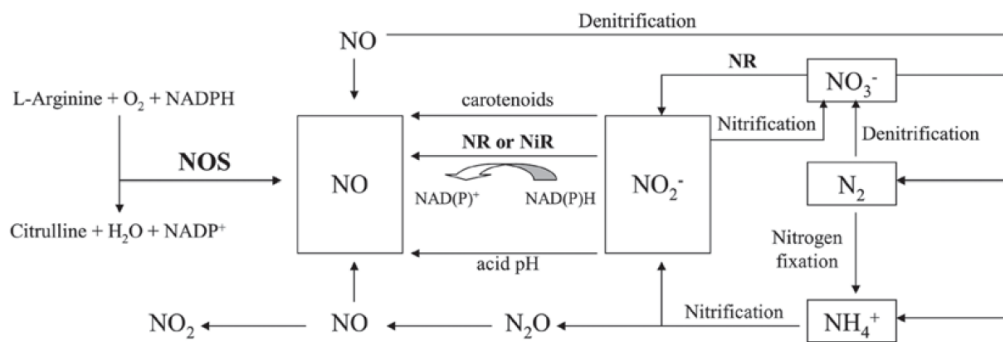


**Fig. I.7:** Possible sources of NO. NO: nitric oxide; N2O: nitrous oxide; NO3<sup>-</sup>: nitrate; NO2<sup>-</sup>: nitrogen dioxide; NH4<sup>+</sup>: ammonium; NR: nitrate reductase; NiR: nitrite reductase; NOS: nitric oxide synthase.



*Chapter II:*

*Results*

*&*

*Discussion*



While p23 has been well studied in animals, little is known about its function in plants where the knowledge of this protein is poor and the role far to be understood.

The aim of the Ph.D. project was to deep the knowledge on *Arabidopsis* p23, probably the most important regulative co-chaperone of HSP90 in plants, being lacking Cdc37, the other main regulative co-chaperone present in animals.

A wide range analysis of p23 protein in *Arabidopsis* has been performed initially with the biochemical characterization of the phosphorylation process, then analysing the phenotype of knockout and overexpressing mutant lines. Some hypotheses have been tested to understand the molecular mechanisms underlying the physiological behaviour of the mutants. Last a quantitative approach for an *in vivo* NO measurement has been addressed.

Results are structured in three parts: “Biochemical characterization of the two isoforms of p23”, “Functional analysis of p23 co-chaperones of *Arabidopsis*” and “A technical note on the use of cPTIO as NO scavenger and EPR probe”.

In the first part I have analysed the phosphorylation pattern of the two p23 isoforms by a biochemical point of view, starting from p23-2, that was the only documented isoforms of p23 before this study. Then the phosphorylation pattern of p23-1, recognized as p23 isoform by [Zhang Z. et al. 2010], is investigated. The analysis of these proteins lead to the discovery of interesting aspects of the regulation by phosphorylation of these proteins.

In the second part, I present a wide analysis of the expression of the two isoforms of p23 in *Arabidopsis* and, for the first time, a role for these proteins in plants is proposed.

In the last part of the thesis, I present a technical review on the use of cPTIO as NO scavenger and EPR probe.



***Biochemical characterization of the two isoforms of p23:***

***The p23 co-chaperone is a novel substrate of CK2 in Arabidopsis***



## The p23 co-chaperone protein is a novel substrate of CK2 in *Arabidopsis*

Kendra Tosoni · Alex Costa · Stefania Sarno ·  
Stefano D'Alessandro · Francesca Sparla ·  
Lorenzo A. Pinna · Michela Zottini · Maria Ruzzene

Received: 13 June 2011 / Accepted: 24 June 2011 / Published online: 7 July 2011  
© Springer Science+Business Media, LLC. 2011

**Abstract** The ubiquitous Ser/Thr protein kinase CK2, which phosphorylates hundreds of substrates and is essential for cell life, plays important roles also in plants; however, only few plant substrates have been identified so far. During a study aimed at identifying proteins targeted by CK2 in plant response to salicylic acid (SA), we found that the *Arabidopsis* co-chaperone protein p23 is a CK2 target, readily phosphorylated in vitro by human and maize CK2, being also a substrate for an endogenous casein kinase activity present in *Arabidopsis* extracts, which displays distinctive characteristics of protein kinase CK2. We also demonstrated that p23 and the catalytic subunit of CK2 interact in vitro and possibly in *Arabidopsis* mesophyll protoplasts, where they colocalize in the cytosol and in the nucleus. Although its exact function is presently unknown, p23 is considered a co-chaperone because of its ability to associate to the chaperone protein Hsp90; therefore, an involvement of p23 in plant signal transduction pathways, such as SA signaling, is highly conceivable, and its phosphorylation may represent a fine mechanism for the regulation of cellular responses.

**Keywords** CK2 · Casein kinase 2 · *Arabidopsis* · p23 · Chaperone proteins · Salicylic acid

### Introduction

Protein kinase CK2 [1, 2] is a ubiquitous and constitutively active Ser/Thr protein kinase, usually organized as a tetrameric complex, consisting of two catalytic and two regulatory subunits. It is essential for cell viability and it plays a special function in tumor cells as a pro-proliferative and anti-apoptotic kinase [3–5]. It phosphorylates many proteins: more than 300 substrates [6] are known so far, most from mammals, with a strict site specificity requiring a precise consensus including acidic residues, in particular at the  $n + 3$  position downstream from the target Ser/Thr [7]. Among the CK2 numerous substrates, several chaperone proteins have been identified which deserve special attention: in fact, it has been demonstrated [8] that CK2, by phosphorylating this class of proteins, can regulate the levels and the functions of many other proteins, thus controlling different cellular processes.

CK2 is well conserved in all eukaryotes, and it has been studied also in plants, where multiple forms of CK2 subunits exist: indeed, while in mammals only two catalytic ( $\alpha$  and  $\alpha'$ ) and one regulatory ( $\beta$ ) subunits are present, in *Arabidopsis* four genes coding for  $\alpha$  (denoted as A, B, C, and D) and four for  $\beta$  (1, 2, 3, and 4) have been described [9].

CK2 is essential for cell viability also in plants [10], where it is involved in several crucial processes, including cell cycle and proliferation [11], circadian rhythm [12–15], auxin signaling pathways [16], dark/light-dependent enzyme regulation [17], translation [18], and the salicylic acid (SA)-mediated defense response [19, 20].

Kendra Tosoni and Alex Costa equally contributed to this work.

K. Tosoni · S. Sarno · L. A. Pinna · M. Ruzzene (✉)  
Department of Biological Chemistry and Venetian Institute of  
Molecular Medicine (VIMM), University of Padova, Viale G.  
Colombo, 3, 35131 Padova, Italy  
e-mail: maria.ruzzene@unipd.it

A. Costa · S. D'Alessandro · M. Zottini  
Department of Biology, University of Padova, Padova, Italy

F. Sparla  
Department of Experimental Evolutionary Biology, University  
of Bologna, Bologna, Italy

We have recently investigated the SA signaling pathway, and, in contrast to what observed by others [19], we did not find any change in CK2 catalytic activity induced by SA [20]; we therefore reasoned that CK2 intervenes in SA signaling by specifically modulating the phosphorylation level of only one or few proteins among its substrates, which become available as targets only upon an SA-mediated event, such as changing in protein expression, cellular translocations, or post-translational modifications catalyzed by other enzymes. Based on this premise, we performed a study where a proteomic approach was exploited for the identification of SA-dependent CK2 substrates (manuscript in preparation). During this study, we identified a novel CK2 substrate in *Arabidopsis*, the co-chaperone protein p23, whose phosphorylation was investigated in detail.

### Experimental procedures

#### Materials

The CK2 inhibitor TBB (4,5,6,7-tetrabromo benzotriazole) was synthesized as in [21]. Quinalizarin was provided by Produits Chimiques ACP Chemicals. Staurosporine and K252a were from Sigma-Aldrich. Recombinant human and maize CK2 were produced and purified as described in [22]. Purified proteins were dialyzed against 25 mM Tris pH 7.5 and 50% of glycerol and stored at  $-20^{\circ}\text{C}$ . Radioactive ATP was from PerkinElmer.

#### Plant material and growth conditions

*Arabidopsis thaliana* Columbia ecotype plants were used in this study. Plants were grown on MS/2 0.8% agar medium [23] with 16/8 h cycles of light ( $70 \mu\text{E m}^{-2} \text{s}^{-1}$ ) at  $22^{\circ}\text{C}$  and 75% RH. Seeds of *Arabidopsis* lines overexpressing the CK2B3 subunit (ox18 and ox41 [12]) were kindly provided by Prof. Tobin from UCLA (Los Angeles, CA). For the treatment, *Arabidopsis* 8-day-old seedlings were transferred into 5 cm Petri dishes and washed with LB buffer (5 mM MES-KOH, pH 5.7, 1 mM  $\text{CaCl}_2$ , 0.25 mM KCl). The LB buffer was then replaced with the same buffer supplemented with  $30 \mu\text{M}$  TBB or DMSO as control. The proteins were then extracted as described in [20].

#### Cloning, expression, and purification of recombinant p23-2

The coding sequence of *Arabidopsis* p23-2 protein (At3g03773) was amplified by PCR using the following primers: p23-2-For-NdeI CATGCATATGAGTCGTAATCCGGAGTTCTT (forward primer), p23-2-Rev-NdeI CATGCATATGCTACTTGTCTTTCCTTTTCCA (reverse primer).

The template for PCR reactions was cDNA obtained by the retrotranscription of total RNA extracted from 8-day-old *Arabidopsis* seedlings as previously described [24]. The PCR was performed by using the Phusion<sup>®</sup> DNA Polymerase (Finnzymes). The amplified fragment was inserted into NdeI pre-digested expression vector pET28a(+) (Novagen). The p23 cDNA was placed in frame with a His-tag and a cleavable thrombin site at the 5'. The recombinant plasmid was amplified into *E. coli* XL1Blue (Stratagene) cells and sequenced before the transfer into BL21(DE3) *E. coli* cells for expression. Heterologous expression, purification of the recombinant protein, and removal of the His-tag were performed as in [25]. The purification grade of recombinant proteins was checked by SDS-PAGE and Coomassie staining.

#### Vector construction for subcellular localization and BiFC analyses

For the subcellular localization analyses of p23-2 (At3g03773.1) and CK2 $\alpha\text{C}$  (At2g23080) the coding sequences of the two genes were cloned in front of YFP and GFP in a modified pGreen 0029 vector [26] and pSAT-EGFP-N1 vector, respectively [27] by using the following primers: p23-2-For-NcoI CATGCCATGCCATGAGTCGTAATCCGGAGGTTCTT and p23-2-Rev-NcoI CATGCCATGCCCGCCTTGTCTTTCCTTTTCCA; CK2 $\alpha\text{C}$ -For-SacI CATGGAGCTCAATGTCGAAAGCTAGGGTTATACAGAT and CK2 $\alpha\text{C}$ -Rev-BamHI CATGGGATCCCTGCCTGAGTTCGTAGTCTGCTGCT. For the BiFC analysis the p23-2 coding sequence was subcloned in front of the splitted N-terminal part of the Venus in the pSAT1A-nVenus-N pE3231 vector, whereas the CK2 $\alpha\text{C}$  was inserted in front of the splitted C-terminal part of the CFP in the pSAT1-cFP-N pE3449 vector [28]. The p23-2 coding sequence was amplified by PCR using the following primers: p23-2-For-SacI CATGGAGCTCATGAGTCGTAATCCGGAGGTTCTT and p23-2-Rev-BamHI CATGGGATCCCGCCTGTTTCTTGCCTTTTCCA; the CK2 $\alpha\text{C}$  was directly subcloned from the pSAT-CK2 $\alpha\text{C}$ -EGFP-N1 vector. In all the constructs made the coding sequences were amplified by using as template the same cDNA described above by using the Phusion<sup>®</sup> DNA Polymerase (Finnzymes). The vectors were then sequenced to verify that no mistakes were introduced. All the cloned genes were under control of a double CaMV35S promoter.

#### Protoplasts transformation and confocal analyses

The *Arabidopsis* mesophyll protoplasts were isolated and transformed following the Jen Sheen's protocol [29]. Briefly, 20 leaves from 4-week-old *Arabidopsis* plants grown in Giffy pots [24] were cut in thin slices and placed

in enzymatic solution. Protoplasts were then isolated at a density of  $1\text{--}2 \times 10^5/\text{ml}$  and a PEG-calcium transfection was performed. The protoplasts were then maintained at  $22^\circ\text{C}$  for 16 h in the dark before the analyses.

The Confocal microscopy analyses were performed using a Nikon PCM2000 (Bio-Rad, Germany) laser scanning confocal imaging system. For the green fluorescence protein (GFP) detection the excitation was at 488 nm and emission between 515 and 530 nm, for yellow fluorescence protein (YFP), and reconstituted nVenus, detection, the excitation was still at 488 nm but the emission between 530 and 560 nm. For the chlorophyll detection, excitation was at 488 nm and detection over 600 nm. Image analyses were done with the IMAGEJ BUNDLE software (<http://rsb.info.nih.gov/ij/>).

#### In vitro phosphorylation assays

Protein substrates (p23 or  $\beta$ -casein) were incubated at  $30^\circ\text{C}$  with recombinant human monomeric ( $\alpha$ ) or tetrameric ( $\alpha_2\beta_2$ ) CK2 or maize CK2  $\alpha$ , in a phosphorylation mixture containing 50 mM Tris-HCl, pH 7.5, 10 mM  $\text{MgCl}_2$ , 20  $\mu\text{M}$  [ $\gamma$ - $^{33}\text{P}$ ] ATP (or GTP) (1000–2000 cpm/pmol) according to the  $K_m$  value for ATP of human CK2 (10  $\mu\text{M}$ ) in a total volume of 20  $\mu\text{l}$ . 100 mM NaCl was added when tetrameric CK2 was used. Further details are specified in the figure legends. After incubation, samples were loaded on a SDS-PAGE, which was stained with Coomassie blue, and analyzed by autoradiography with the Cyclone Plus Storage Phosphor System (PerkinElmer). When quantization was required, [ $\gamma$ - $^{32}\text{P}$ ] ATP instead of [ $\gamma$ - $^{33}\text{P}$ ] ATP was used, radioactive bands were excised and counted in a scintillation counter. For the calculation of kinetic values, initial rate data were fitted to the Michaelis–Menten equation with the program Prism (GraphPad Software).

Recombinant p23 phosphorylation by *Arabidopsis* lysates was performed as described above, but without the addition of any kinase.

#### In-gel kinase assay

For this assay, a protein substrate (500  $\mu\text{g}/\text{ml}$   $\beta$ -casein or 10  $\mu\text{g}/\text{ml}$  p23) was included into a 11% SDS-PAGE where cytosolic proteins (5–20  $\mu\text{g}$ ) from *Arabidopsis* seedling extracts were separated according to Laemmli [30]. After the electrophoresis, SDS was removed and protein renatured, as elsewhere described [31]. Then gel was incubated with a phosphorylation mixture containing 50 mM Tris-HCl, pH 7.5, 10 mM  $\text{MgCl}_2$ , 20  $\mu\text{M}$  ATP, [ $\gamma$ - $^{33}\text{P}$ ]ATP (specific radioactivity  $\sim 1000\text{--}5000$  cpm/pmol). After Coomassie blue staining, the gel was analyzed by autoradiography for the detection of radioactive bands.

#### BIAcore experiments

For the surface plasmon resonance (SPR) analysis, a BIAcore X system (GE Healthcare) was used, as described in [32]. Human CK2 $\alpha$  was covalently coupled to a CM5 sensor chip (carboxymethylated dextran surface), by the amine-coupling chemistry, to a final density of 1600 RU (resonance units); a flow cell with no immobilized protein was used as a control. His-tagged p23 solutions were injected at the indicated concentrations in HBS-EP buffer (10 mM HEPES, pH 7.4, 0.15 M NaCl, 3 mM EDTA, 0.005% (v/v) P20) at a flow rate of 10  $\mu\text{l}/\text{min}$ ; the same buffer flowed before injections and during the dissociation phase; after each injection the surface was regenerated by injecting 1 M NaCl for 1 min; this treatment restored the baseline to the initial resonance unit value. Each sensorgram (time course of the SPR signal) was corrected for the response obtained in the control flow cell, and normalized to baseline.

## Results

### Identification of p23 as a CK2 substrate in *Arabidopsis*

During a proteomic study where extracts from 8-old-day *Arabidopsis* seedlings treated with SA were analyzed for their CK2-dependent phosphorylations (manuscript in preparation), we found a major protein identified as the *Arabidopsis* p23. This protein is defined as a co-chaperone protein, since, similarly to its animal homologous [33], it has been demonstrated to associate to Hsp90 [34]. Two isoforms of p23 are expressed in *Arabidopsis*, denoted as p23-1 (At4g02450.1) and p23-2 (At3g03773.1). Their sequences were analyzed looking for CK2 consensus sites [7], and revealed the presence of putative CK2 targets, more numerous in the p23-2 isoform (Fig. 1). We therefore decided to verify and characterize the p23-2 phosphorylation by CK2 in vitro. We cloned the coding sequence of At3g03773.1 locus (whose product will be hereafter denoted as p23) into a prokaryotic expression vector to produce a His-p23 protein, which was then purified and subjected to thrombin digestion to cleave the His-tag and obtain a 17.4 kDa p23 recombinant protein (Fig. 2). Although preliminary experiments showed that the His-tag did not affect the phosphorylation degree, we preferred to use this thrombin-digested protein as kinase substrate; we performed a first set of experiments with human CK2, using the model substrate  $\beta$ -casein as a comparison: we found that indeed human CK2 phosphorylates the recombinant p23 in vitro, with an efficiency similar to that obtained with a sixfold higher concentration of  $\beta$ -casein (Fig. 3a). The stoichiometry of phosphorylation reached



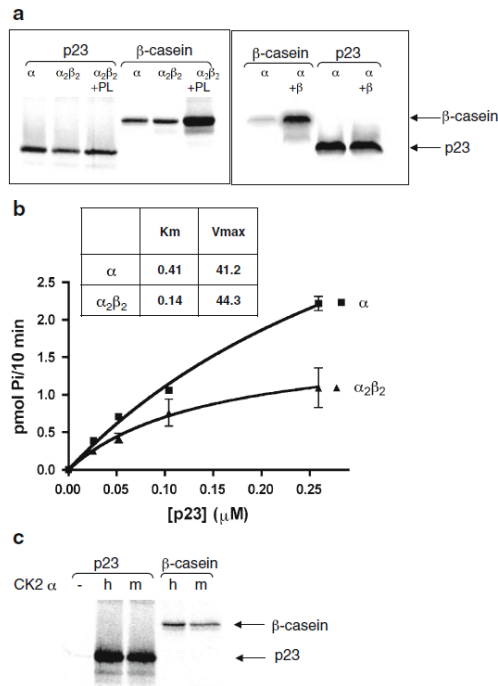


**Fig. 3** Phosphorylation of p23 by recombinant CK2. **a** Recombinant *Arabidopsis* p23 (0.1  $\mu$ g, 0.29  $\mu$ M) was incubated with monomeric  $\alpha$  (15 ng in the left panel, 100 ng in the right panel) or tetrameric  $\alpha_2\beta_2$  (4.4 ng) human CK2, as indicated, for 10 min in a radioactive phosphorylation mixture (total volume 20  $\mu$ l). Where present, polylysine (PL, 400  $\mu$ g) and human CK2 $\beta$  subunit (100 ng), were added at the beginning of the incubation time. Where indicated,  $\beta$ -casein (1  $\mu$ g, 1.72  $\mu$ M) replaced p23. After incubation, samples were analyzed by SDS-PAGE and autoradiography. **b** The kinetics is shown, obtained by phosphorylating increasing amounts of recombinant p23 with  $\alpha$  (15 ng) or  $\alpha_2\beta_2$  (4.4 ng) human CK2, as described above. The kinetic values are also shown:  $K_m$  is expressed in  $\mu$ M,  $V_{max}$  in pmol of phosphate (Pi)/min/ $\mu$ g enzyme. **c** Recombinant *Arabidopsis* p23 (0.29  $\mu$ M) or  $\beta$ -casein (1.72  $\mu$ M) were phosphorylated for 10 min by human (*h*) or maize (*m*) CK2  $\alpha$  (40 or 20 ng, respectively, to ensure a similar degree of  $\beta$ -casein phosphorylation), as described above. The first lane corresponds to p23 incubated in the absence of any enzyme

when TBB was added in vitro during the phosphorylation assay, or in vivo to the *Arabidopsis* seedlings. A corroborating experiment was performed by incubating p23 with extracts from two transgenic *Arabidopsis* lines overexpressing CK2 $\beta$ 3 and reported to display a higher CK2 activity [12]; as shown in Fig. 4a, indeed, a higher p23 phosphorylation degree was observed in both transgenic lines compared to wt *Arabidopsis* line. These data strongly suggest that p23 phosphorylation was catalyzed by endogenous CK2 in *Arabidopsis* lysates. To further confirm

these results, we compared the efficacy of different protein kinase inhibitors and effectors on this reaction: as shown in Fig. 4b, the phosphorylation level of p23 was decreased by two different CK2 inhibitors (TBB and quinalizarin [37]), but very weakly by general protein kinase inhibitors not effective on CK2 (staurosporine and K252a) [20, 38] or by calcium deprivation by EGTA. Moreover, the phosphorylation of p23 was also observed when ATP was replaced by GTP, a phosphate donor that can be used by CK2, but not by the majority of the other protein kinases [39].

Next, to assess if the main endogenous enzyme responsible for p23 phosphorylation was able to phosphorylate casein and displays a size consistent with that of CK2 catalytic subunit, we performed a set of in-gel kinase assays, including either casein or p23 in the gel, and performing the radioactive phosphorylation of these substrates by enzymes present at certain migration positions, after SDS-PAGE and protein renaturing. These experiments (Fig. 4c) demonstrated that the only kinase phosphorylating p23 in *Arabidopsis* migrates at about 39 kDa; at the same size, also a band able to phosphorylate casein is present, strongly suggesting that the major p23 kinase in *Arabidopsis* is a casein kinase with the size expected for CK2 $\alpha$ C (At2g23080.1). Interestingly, a higher Mw band phosphorylating casein is also present in the *Arabidopsis* extract (Fig. 4c, right panel), whose size roughly corresponds to that expected for the other CK2  $\alpha$  isoforms expressed in *Arabidopsis* (At5g67380 and At3g50000); however, this activity towards casein is not accompanied by activity towards p23, indicating that CK2 $\alpha$ C is the major CK2 isoform responsible for the p23 phosphorylation.

#### Physical association between CK2 and p23

Considering that p23 is phosphorylated in vitro by CK2, we wondered if also a stable association can occur, in vitro and in vivo, between the two proteins. To assess this point, we first performed BIAcore experiments, where recombinant p23 was flowed over a surface where human CK2 $\alpha$  was immobilized. As shown in Fig. 5, a concentration-dependent signal was observed, corresponding to p23 binding to CK2 $\alpha$ .

In order to test if an in vivo association of the *Arabidopsis* CK2 and p23 proteins also occurs, we first assessed the subcellular localization of these two proteins. In *Arabidopsis*, three non plastidial CK2  $\alpha$  subunits have been identified (A, B, C) [9] and among them the CK2  $\alpha$ C (At2g23080.1) is the one expected to phosphorylate p23, as judged from the size displayed in the in-gel kinase assay (see Fig. 4c). We then fused the GFP at the C-terminal end of the CK2 $\alpha$ C and expressed it in *Arabidopsis* mesophyll protoplasts. The confocal microscopy analyses showed that the GFP signal was clearly detectable in the cytoplasm and nucleus (Fig. 6a–c), confirming published data [9]. We then tested the subcellular localization of p23 by fusing it to the

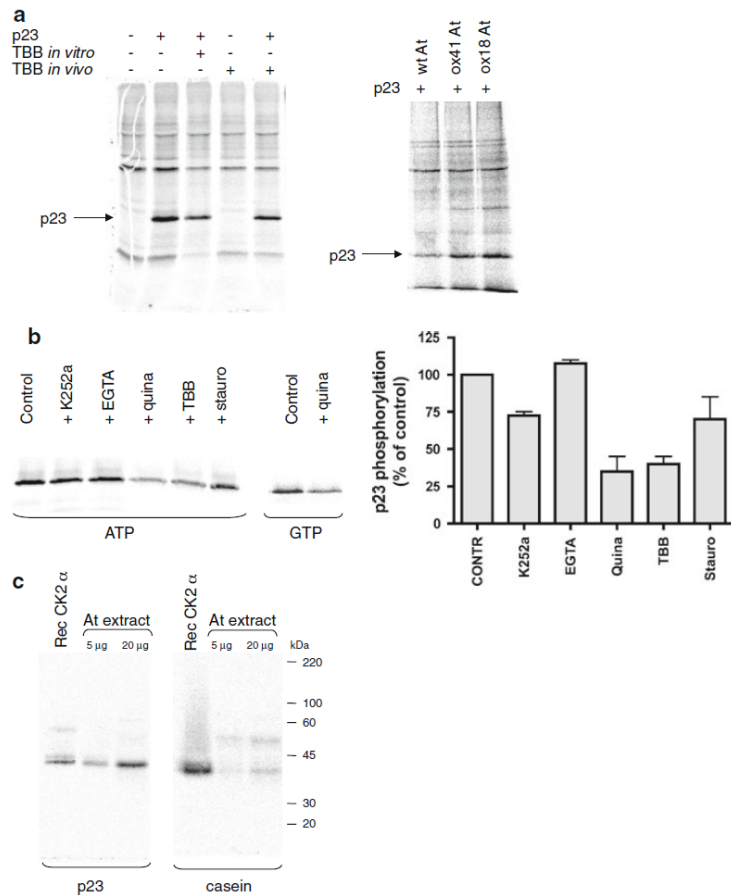


**Fig. 4** Phosphorylation of p23 by *Arabidopsis* cytosolic extracts. **a** 10 μg of proteins from cytosolic extracts of *Arabidopsis* seedlings (previously treated with 30 μM TBB, where indicated as in vivo), were incubated for 10 min at 30°C with a radioactive phosphorylation mixture, in the presence, where indicate (+), of recombinant p23 (0.1 μg). If added during the phosphorylation reaction (in vitro), TBB was 2 μM. Proteins were separated by SDS-PAGE and radioactivity detected by autoradiography. On the right panel, phosphorylations obtained with cytosolic extracts from wt *Arabidopsis* and from transgenic plants overexpressing CK2β3, indicated as ox41At and ox18At as in [12], are compared. **b** Recombinant p23 (0.1 μg) was phosphorylated by proteins from *Arabidopsis* extracts as in **a**, with the addition of the indicated protein kinase effectors as follows: 0.1 μM K252a, 500 μM EGTA, 2 μM quinalizarin (Quina), 2 μM TBB, 1 μM

staurosporine (Stauro). Where indicated, radioactive GTP replaced ATP as phosphate donor. The autoradiography corresponding to the migration of p23 is shown on the left, while quantification of p23 phosphorylation (expressed as percentage of control, obtained without any effector) is shown by the graph on the right; vertical bars indicate the standard deviation to the mean obtained from three separated experiments. **c** For the in-gel kinase assay, 5 or 20 μg of proteins from *Arabidopsis* cytosolic extracts were loaded on a gel containing 10 μg/ml p23 (left) or 500 μg/ml β-casein (right). The gels, after incubation with a radioactive phosphorylation mixture, were analyzed by autoradiography. 10 ng of recombinant human CK2α, truncated at the C-terminus (1-336 sequence), were loaded as a positive control. The migration positions of Mw markers are shown on the right. At, *Arabidopsis thaliana*

YFP and expressed it in *Arabidopsis* mesophyll protoplast, and, also in this case, the confocal microscopy analyses show its presence in cytoplasm and nucleus (Fig. 6d–f).

Having demonstrated that CK2αC and p23 localize in the same subcellular compartments (cytoplasm and nucleus) we then wanted to assess their in vivo interaction

by means of bimolecular fluorescence complementation technique (BiFC) [40]. To this purpose, the CK2αC protein was fused upstream to the C-terminal portion of the cyan fluorescence protein (cCFP) and the p23 upstream the N-terminal portions of Venus (nVenus) [28]. The two constructs were then introduced in *Arabidopsis* mesophyll

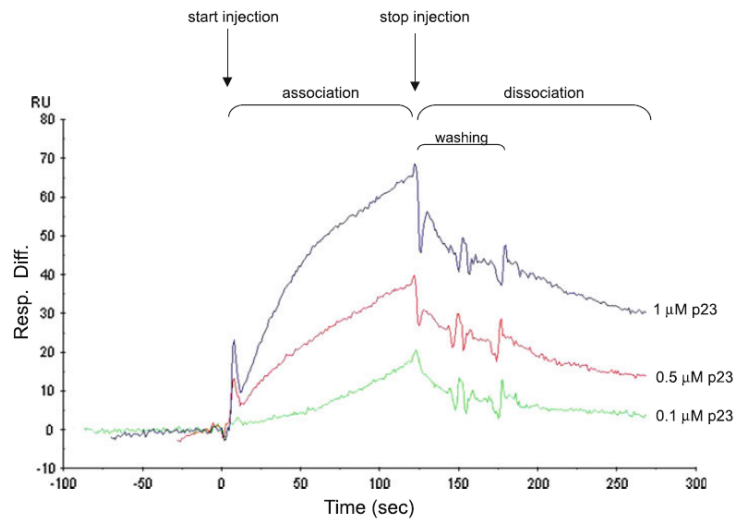


**Fig. 5** Detection of CK2  $\alpha$ /p23 interaction by means of SPR. On a BIAcore X system, p23 solutions were injected at the indicated concentrations in HBS buffer, over a surface where human CK2  $\alpha$  was covalently coupled. Injection time was 2 min (association phase), then HBS buffer started to flow (dissociation phase). The variation of the response in the SPR signal is shown as response difference (Resp.

diff.), after subtraction of the signal of the control cell. For this kind of experiments, His-tagged p23 solutions were used, since they were available at higher concentrations than thrombin-cleaved p23 solutions; however, single concentration experiments performed with p23 devoid of His-tag confirmed the binding (not shown)

protoplasts and analyzed by means of confocal microscopy. The results presented in Fig. 6g–i show that indeed we were able to recover a fluorescence signal, denoting the reconstruction of a functional fluorophore generated by the interaction between the cCFP and nVenus portions. In accordance with the subcellular localization analyses of CK2 $\alpha$ C and p23, the signal was present in the cytoplasm and nucleus. However, when we tried to obtain negative controls by co-expressing p23-nVenus with the cCFP alone, a fluorescence signal was recovered as well (not shown), possibly due to system pitfalls [40]. Therefore, at present, our results are not conclusive for an in vivo interaction between CK2 $\alpha$ C and p23; however, they clearly confirm the presence of the two proteins in the same subcellular compartments.

## Discussion

CK2 is a highly pleiotropic kinase whose importance has been extensively described also in plant physiology; however, despite the huge number of substrates reported so far, only a minority of these are from plants [6].

In this study we identify the *Arabidopsis* p23 protein as a novel substrate for CK2. p23 is a co-chaperone protein homologous to the human p23 protein, which was first

identified as a Hsp90 partner [41], with the role of assisting it in the chaperoning of steroid receptors [42, 43]. The molecular characterization of the *Arabidopsis* p23 has been recently published [34], showing that it binds to Hsp90 in its ATP-bound conformation; however, p23 has no effect on the Hsp90 ATPase activity, and, since the Hsp90/p23 client proteins in plants are unknown, no evident function of p23 has been described so far. Human p23, which shares only a 25–27% sequence identity with the *Arabidopsis* protein [34], was already reported as a CK2 substrate, in a paper where it was considered a prostaglandin E synthase [44]; in that work, the phosphorylated sites were also identified on Ser113 and Ser118.

Here we show that *Arabidopsis* p23 is phosphorylated by human and maize recombinant CK2, with high stoichiometry and favorable kinetic values; at difference to what observed for most of the CK2 substrates, the  $\beta$  regulatory subunit does not have a significant stimulatory effect on the p23 phosphorylation; on the other hand, this substrate does not match the features of the class II CK2 substrates, whose phosphorylation in the presence of the  $\beta$  subunit is inhibited, but completely rescued by the addition of polycationic effectors such as polylysine [2], which instead has no effect on p23 phosphorylation.

Our investigation was mainly performed in vitro with recombinant proteins, but we have also demonstrated that

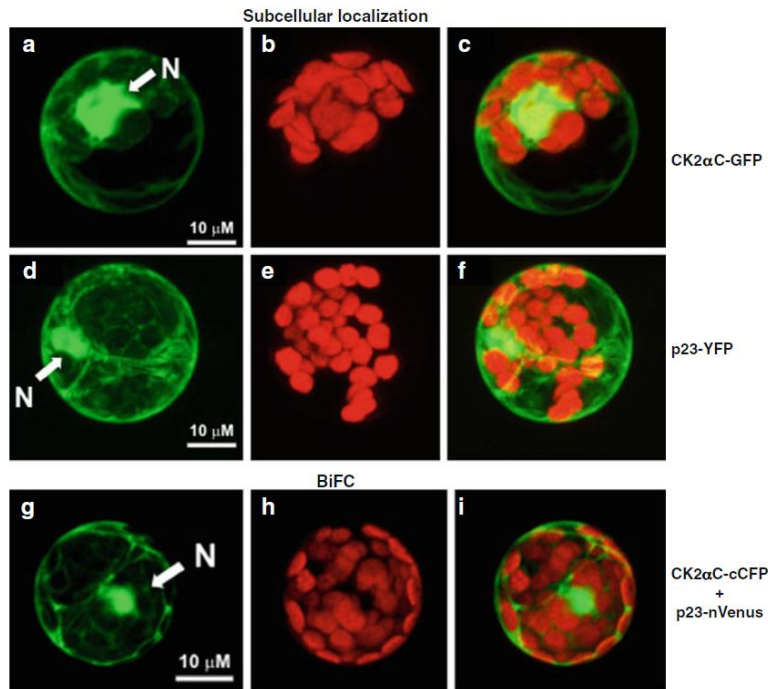


**Fig. 6** Subcellular localization of CK2 $\alpha$ C-GFP and p23-YFP and BiFC analysis in *Arabidopsis* mesophyll protoplasts. **a–c** Confocal 3D-reconstruction of a representative *Arabidopsis* mesophyll protoplast expressing the chimeric CK2 $\alpha$ C-GFP protein: **a** GFP fluorescence present in the cytoplasm and nucleus (N) of the protoplast; **b** Chlorophyll autofluorescence of the same protoplast shown in **a**; **c** Overlay image of **a** and **b**. **d–f** Confocal 3D-reconstruction of a representative *Arabidopsis* mesophyll protoplast expressing the

chimeric p23-YFP protein: **d** YFP fluorescence present in the cytoplasm and nucleus of the protoplast; **e** Chlorophyll autofluorescence of the same protoplast shown in **d**; **f** Overlay image of **d** and **e**. **g–i** Confocal 3D-reconstruction of a representative *Arabidopsis* mesophyll protoplast co-expressing the chimeric CK2 $\alpha$ C-cCFP and p23-nVenus proteins: **g** reconstituted nVenus fluorescence present in the cytoplasm and nucleus of the protoplast; **h** chlorophyll autofluorescence of the same protoplast shown in **g**; **i** Overlay image of **g** and **h**

in *Arabidopsis* cytosol a kinase responsible for the p23 phosphorylation exists; this displays typical properties of CK2, being able to phosphorylate also casein and to use GTP as phosphate donor, having the size expected for *Arabidopsis* CK2 $\alpha$ C, and being susceptible to inhibition by well-known CK2 inhibitors. Although an unequivocal demonstration of the *in vivo* association of p23 and CK2 was not achieved, we clearly showed that they colocalize in *Arabidopsis* mesophyll protoplasts, rendering their interaction quite conceivable.

This study originated from the observation that CK2 is required for the *Arabidopsis* response to SA treatment [20], and from the idea that only some specific substrates of CK2 change their phosphorylation state when SA is applied. Here we propose that p23 is a candidate for this role; however, for the time being, we can not say which isoform of p23 is really involved in the SA signaling, having

considered, in this work, only p23-2; since the other isoform, p23-1, also displays CK2 consensus sites, its phosphorylation will be also investigated in the next future. Further studies will be also required to assess if (and which) SA-dependent events make p23 protein more readily accessible to CK2-dependent phosphorylation.

In conclusion, we can presently say that the p23 co-chaperone protein is a newly identified substrate of CK2 in plants, and that, despite no specific function of this protein is known so far, its involvement in the chaperone machinery makes it quite attractive, being a potential upstream regulator of numerous client proteins, including other protein kinases as well.

**Acknowledgments** This work was supported by grants from the Italian Ministry of University and Research (PRIN-2008 to LAP) and from University of Padova (Progetto Ateneo 2009) “Ruolo dell’ossido di azoto nella risposta delle piante a stress biotici e abiotici...”.

## References

- Ahmad KA, Wang G, Unger G, Slaton J, Ahmed K (2008) Protein kinase CK2—a key suppressor of apoptosis. *Adv Enzyme Regul* 48:179–187
- Pinna LA (2002) Protein kinase CK2: a challenge to canons. *J Cell Sci* 115:3873–3878
- St-Denis NA, Litchfield DW (2009) Protein kinase CK2 in health and disease: from birth to death: the role of protein kinase CK2 in the regulation of cell proliferation and survival. *Cell Mol Life Sci* 66:1817–1829
- Trembley JH, Wang G, Unger G, Slaton J, Ahmed K (2009) Protein kinase CK2 in health and disease: CK2: a key player in cancer biology. *Cell Mol Life Sci* 66:1858–1867
- Ruzzene M, Pinna LA (2010) Addiction to protein kinase CK2: a common denominator of diverse cancer cells? *Biochim Biophys Acta* 1804:499–504
- Meggio F, Pinna LA (2003) One-thousand-and-one substrates of protein kinase CK2? *FASEB J* 17:349–368
- Pinna LA, Ruzzene M (1996) How do protein kinases recognize their substrates? *Biochim Biophys Acta* 1314:191–225
- Miyata Y (2009) Protein kinase CK2 in health and disease: CK2: the kinase controlling the Hsp90 chaperone machinery. *Cell Mol Life Sci* 66:1840–1849
- Salinas P, Fuentes D, Vidal E, Jordana X, Echeverria M, Holuigue L (2006) An extensive survey of CK2 alpha and beta subunits in *Arabidopsis*: multiple isoforms exhibit differential subcellular localization. *Plant Cell Physiol* 47:1295–1308
- Moreno-Romero J, Espunya MC, Platara M, Ariño J, Martínez MC (2008) A role for protein kinase CK2 in plant development: evidence obtained using a dominant-negative mutant. *Plant J* 55:118–130
- Espunya MC, López-Giráldez T, Hernan I, Carballo M, Martínez MC (2005) Differential expression of genes encoding protein kinase CK2 subunits in the plant cell cycle. *J Exp Bot* 56:3183–3192
- Sugano S, Andronis C, Ong MS, Green RM, Tobin EM (1999) The protein kinase CK2 is involved in regulation of circadian rhythms in *Arabidopsis*. *Proc Natl Acad Sci USA* 96:12362–12366
- Daniel X, Sugano S, Tobin EM (2004) CK2 phosphorylation of CCA1 is necessary for its circadian oscillator function in *Arabidopsis*. *Proc Natl Acad Sci USA* 101:3292–3297
- Mizoguchi T, Putterill J, Ohkoshi Y (2006) Kinase and phosphatase: the cog and spring of the circadian clock. *Int Rev Cytol* 250:47–72
- Portolés S, Más P (2007) Altered oscillator function affects clock resonance and is responsible for the reduced day-length sensitivity of CKB4 overexpressing plants. *Plant J* 51:966–977
- Moreno-Romero J, Martínez MC (2008) Is there a link between protein kinase CK2 and auxin signaling? *Plant Signal Behav* 3:695–697
- Reiland S, Messerli G, Baerenfaller K, Gerrits B, Endler A, Grossmann J, Gruissem W, Baginsky S (2009) Large-scale *Arabidopsis* phosphoproteome profiling reveals novel chloroplast kinase substrates and phosphorylation networks. *Plant Physiol* 150:889–903
- Dennis MD, Person MD, Browning KS (2009) Phosphorylation of plant translation initiation factors by CK2 enhances the in vitro interaction of multifactor complex components. *J Biol Chem* 284:20615–20628
- Kang HG, Klessig DF (2005) Salicylic acid-inducible *Arabidopsis* CK2-like activity phosphorylates TGA2. *Plant Mol Biol* 57:541–557
- Zottini M, Costa A, De Michele R, Ruzzene M, Carimi F, Lo Schiavo F (2007) Salicylic acid activates nitric oxide synthesis in *Arabidopsis*. *J Exp Bot* 58:1397–1405
- Szyska R, Grankowski N, Felczak K, Shugar D (1995) Halogenated benzimidazoles and benzotriazoles as selective inhibitors of protein kinases CK I and CK II from *Saccharomyces cerevisiae* and other sources. *Biochem Biophys Res Commun* 208:418–424
- Samo S, Vaglio P, Meggio F, Issinger O-G, Pinna LA (1996) Protein kinase CK2 mutants defective in substrate recognition. Purification and kinetic analysis. *J Biol Chem* 271:10595–10601
- Murashige T, Skoog F (1962) A revised medium for rapid growth and bioassays with tobacco tissue cultures. *Physiol Plant* 15:473–497
- Costa A, Drago I, Behera S, Zottini M, Pizzo P, Schroeder JI, Pozzan T, Schiavo FL (2010) H<sub>2</sub>O<sub>2</sub> in plant peroxisomes: an in vivo analysis uncovers a Ca(2+)-dependent scavenging system. *Plant J* 62:760–772
- Sparla F, Preger V, Pupillo P, Trost P (1999) Characterization of a novel NADH-specific, FAD-containing, soluble reductase with ferric citrate reductase activity from maize seedlings. *Arch Biochem Biophys* 363:301–308
- Zottini M, Barizza E, Costa A, Formentin E, Ruberti C, Carimi F, Lo Schiavo F (2008) Agroinfiltration of grapevine leaves for fast transient assays of gene expression and for long-term production of stable transformed cells. *Plant Cell Rep* 27:845–853
- Tzfira T, Tian GW, Lacroix B, Vyas S, Li J, Leitner-Dagan Y, Krichevsky A, Taylor T, Vainstein A, Citovsky V (2005) pSAT vectors: a modular series of plasmids for autofluorescent protein tagging and expression of multiple genes in plants. *Plant Mol Biol* 57:503–516
- Lee LY, Fang MJ, Kuang LY, Gelvin SB (2008) Vectors for multi-color bimolecular fluorescence complementation to investigate protein–protein interactions in living plant cells. *Plant Methods* 4:24
- Sheen J (2002) A transient expression assay using *Arabidopsis* mesophyll protoplasts. <http://genetics.mgh.harvard.edu/sheenweb/>
- Laemmli UK (1970) Cleavage of structural proteins during the assembly of the head of bacteriophage T4. *Nature* 227:680–685
- Ruzzene M, Di Maira G, Tosoni K, Pinna LA (2010) Assessment of CK2 constitutive activity in cancer cells. *Methods Enzymol* 484:495–514
- Ruzzene M, Brunati AM, Samo S, Donella-Deana A, Pinna LA (1999) Hematopoietic lineage cell specific protein 1 associates with and down-regulates protein kinase CK2. *FEBS Lett* 461:32–36
- Johnson JL, Beito TG, Krco CJ, Toft DO (1994) Characterization of a novel 23-kilodalton protein of unactive progesterone receptor complexes. *Mol Cell Biol* 14:1956–1963
- Zhang Z, Sullivan W, Felts SJ, Prasad BD, Toft DO, Krishna P (2010) Characterization of plant p23-like proteins for their co-chaperone activities. *Cell Stress Chaperones* 15:703–715
- Dobrowolska G, Boldyreff B, Issinger OG (2005) Cloning and sequencing of the casein kinase 2 alpha subunit from *Zea mays*. *Biochim Biophys Acta* 1129:139–140
- Samo S, Reddy H, Meggio F, Ruzzene M, Davies SP, Donella-Deana A, Shugar D, Pinna LA (2001) Selectivity of 4,5,6,7-tetrabromobenzotriazole, an ATP site-directed inhibitor of protein kinase CK2 ('casein kinase-2'). *FEBS Lett* 496:44–48
- Cozza G, Mazzorana M, Papinutto E, Bain J, Elliott M, di Maira G, Gianoncelli A, Pagano MA, Sarno S, Ruzzene M, Battistutta R, Meggio F, Moro S, Zagotto G, Pinna LA (2009) Quinalizarin as a potent, selective and cell-permeable inhibitor of protein kinase CK2. *Biochem J* 421:387–395
- Meggio F, Donella Deana A, Ruzzene M, Brunati AM, Cesaro L, Guerra B, Meyer T, Mett H, Fabbro D, Furet P, Dobrowolska G, Pinna LA (1995) Different susceptibility of protein kinases to staurosporine inhibition. Kinetic studies and molecular bases for

- the resistance of protein kinase CK2. *Eur J Biochem* 234: 317–322
39. Niefind K, Pütter M, Guerra B, Issinger OG, Schomburg D (1999) GTP plus water mimic ATP in the active site of protein kinase CK2. *Nat Struct Biol* 6:1100–1103
40. Kerppola TK (2009) Visualization of molecular interactions using bimolecular fluorescence complementation analysis: characteristics of protein fragment complementation. *Chem Soc Rev* 38:2876–2886
41. Johnson JL, Toft DO (1995) Binding of p23 and hsp90 during assembly with the progesterone receptor. *Mol Endocrinol* 9: 670–678
42. Weikl T, Abelmann K, Buchner J (1999) An unstructured C-terminal region of the Hsp90 co-chaperone p23 is important for its chaperone function. *J Mol Biol* 293:685–691
43. Weaver AJ, Sullivan WP, Felts SJ, Owen BA, Toft DO (2000) Crystal structure and activity of human p23, a heat shock protein 90 co-chaperone. *J Biol Chem* 275:23045–23052
44. Kobayashi T, Nakatani Y, Tanioka T, Tsujimoto M, Nakajo S, Nakaya K, Murakami M, Kudo I (2004) Regulation of cytosolic prostaglandin E synthase by phosphorylation. *Biochem J* 381: 59–69

***Biochemical characterization of the two isoforms of p23:***

***p23-1 co-chaperone shows a specific pattern of phosphorylation in Arabidopsis***



## ***p23-1 co-chaperone show a specific pattern of phosphorylation in Arabidopsis***

*Arabidopsis* shows two paralogues of the p23 co-chaperone encoding for two different proteins denoted as p23-1 (At4g02450) and p23-2 (At3g03773.1). We first have shown that *Arabidopsis* Hsp90 co-chaperone p23-2 is a substrate of the protein kinase CK2 and then we extended our analysis to *Arabidopsis* Hsp90 co-chaperone p23-1. Although the similarity of the two isoforms, p23-1 shows a peculiar pattern of phosphorylation.

### **Identification of p23-1 as a CK2 substrate in *Arabidopsis***

We analyzed the two protein sequences for CK2 consensus sites [Tosoni K. et al., 2011; Pinna L. A. et al. 1996] and we identified S222 as the more likely phosphorylation site by NetPhosK analysis of the kinase-specific phosphosites (Fig. II.1.A).

In order to verify whether CK2 actually phosphorylates p23-1, we cloned the coding sequence of the *At4g02450* locus into a prokaryotic expression vector to produce *pET28-T7::6xHis-p23-1* and then the recombinant protein was purified by affinity (NI-NTA) and size exclusion chromatography (see Methods). Using 0.1µg of purified recombinant protein, we performed an *in vitro* phosphorylation assay with 15 ng of the human CK2 $\alpha$  or of the maize CK2 $\alpha$ , using p23-2 as comparison (as described in Tosoni K. et al., 2011). Samples were then resolved by SDS-PAGE and the dried gel was analyzed by Cyclone Plus Storage Phosphor System (PerkinElmer). As it can be seen in Fig. II.1.B, showing the autoradiography of the phosphorylation assay, both the higher band, representing p23-1, and the lower band, representing p23-2, are efficiently phosphorylated by recombinant maize and human CK2. Furthermore, by densitometric analysis of the bands, we showed that p23-1 was phosphorylated at a lower level respect to p23-2 by both recombinant kinases.

So we demonstrated that p23-1 is phosphorylated *in vitro* by recombinant human CK2 $\alpha$  and by maize recombinant CK2 $\alpha$  that is much more similar to the *Arabidopsis* enzyme. Since most of the CK2 substrates are better phosphorylated by the tetrameric form of the kinase (CK2 $\alpha_2\beta_2$ ), while there are only few examples in which monomeric CK2 is preferred [Pinna L.A. et al. 2002], we decided to investigate which form of the kinase can phosphorylate at higher efficiency p23-1. We have previously shown that p23-2 is

preferentially phosphorylated by the monomeric catalytic subunit but, as monomeric human and maize CK2 phosphorylate at a lower rate p23-1 compared to p23-2, we investigated if the tetrameric form of the human CK2 could increase phosphorylation.

We performed an *in vitro* phosphorylation assay using the two recombinant p23s as substrates and the monomeric or the tetrameric recombinant form of the human recombinant CK2. As human tetrameric form of CK2 has a higher phosphorylation activity, we used  $\beta$ -Casein to normalize the activity and to have a similar phosphorylation level by CK2 $\alpha$  and  $\alpha_2\beta_2$ .

We found that an amount of the tetrameric human CK2 ( $\alpha_2\beta_2$ ), sufficient to produce a phosphorylation degree similar to CK2 $\alpha$  on  $\beta$ -Casein, was less efficient on p23-1 (Fig. II.1.C).

So the result shows that the monomeric catalytic subunit of CK2 is sufficient to completely phosphorylate the recombinant p23-1.

### **P23-1 phosphorylation by an Arabidopsis CK2 like activity**

Next we tested the phosphorylation activity of endogenous kinases on p23-1. To do so we used the *Arabidopsis* protein extract as source of endogenous kinases.

To this purpose we performed an *in vitro* radioactive phosphorylation assay using the soluble fraction of 10-day-old *Arabidopsis* seedlings protein extract, as source of kinases, and recombinant p23-1 as substrate.

As shown in Fig. II.2.A, p23-1 is phosphorylated by endogenous kinases, showing a different behavior in comparison with assays performed with recombinant human and maize CK2. Kinases present in the total protein extract of *Arabidopsis* seedlings phosphorylate p23-1 at a higher level compared to p23-2. As the human CK2 $\alpha$  is more processive on p23-2, this result could indicate either a different affinity between p23-1 and the *Arabidopsis* monomeric isoforms of CK2, or it could suggest that p23-1 is phosphorylated by kinases other than CK2.

In order to elucidate this point we performed a screening of the phosphorylation of p23-1 either using inhibitors specific of CK2 (TBB and CX4945) or the general inhibitor of protein kinases staurosporine, not active on CK2.

The analysis of the phosphorylation pattern of p23-1, using different inhibitors, (Fig. II.2.B) showed that p23-1 phosphorylation is mainly due to a CK2 like activity of the *Arabidopsis* seedlings protein extract. As shown in the densitometric analysis of the autoradiography, the use of CX4945, a specific inhibitor of CK2, abolished the



**Fig. II.1:** A) Sequence of the two p23 isoforms of *Arabidopsis*. ClustalW2 alignment (<http://www.ebi.ac.uk/Tools/msa/clustalw2>). The output was labeled with symbols indicating the degree of similarity (\* for exact matches, : for strong similarity, . for weak similarity) (<http://www.yeastgenome.org/help/SeqSimQuery.html>). Putative CK2 consensus sites, identified on the basis of CK2 specificity as in [Pinna et al. 1996], are bold underlined.

B) *In vitro* phosphorylation of p23-1 and p23-2 by human or maize recombinant CK2. *Arabidopsis* recombinant p23-1 or p23-2 (0.1 µg) were incubated 10 minutes at 28 °C with recombinant maize (20 ng) or human (40 ng) CK2 as indicated, in a radioactive phosphorylation mixture (total volume 20 µl). Pixel analysis of the autoradiography in which phosphorylation levels are shown as percentage of the p23-2 phosphorylation.

C) *In vitro* phosphorylation of p23-1 and β-Casein by human recombinant CK2. *Arabidopsis* recombinant p23-1 (0.1 µg) was incubated 10 minutes at 28 °C with recombinant human CK2 in the monomeric form (40 ng) or in the tetrameric form (15 ng) as indicated, in a radioactive phosphorylation mixture (total volume 20 µl). Pixel analysis of the autoradiography in which phosphorylation levels are shown as percentage of the β-Casein phosphorylation.

### Serine 222 is the only site of phosphorylation

As shown in Figure II.1.A, the principle CK2 putative site of phosphorylation of p23-1 is Serine 222. We mutated the serine 222 of p23-1 to an alanine and the recombinant protein, lacking the Serine 222, was purified. We used 0.1 µg of the recombinant mutated p23-1-S222A in an *in vitro* phosphorylation assay, using *Arabidopsis* seedling extract as source of endogenous kinases. As shown in Figure II.2.C, the recombinant phospho-defective mutant shows no phosphorylation, obtaining an even stronger inhibition of the phosphorylation compared to the use of CX4945. This result not only demonstrates that serine 222 is the site of phosphorylation by CK2 but further demonstrates that CK2 is the only kinase able to phosphorylate p23-1.

### CK2 isoforms show specificity of phosphorylation

We found that p23-1 is a specific substrate of *Arabidopsis* CK2s and the high level of phosphorylation, detected in presence of *Arabidopsis* protein extract, cannot be due to the activity of other kinases. Then, we decided to better investigate CK2 isoforms involved in the phosphorylation, as *Arabidopsis* owns 3 nuclear subunits of CK2. We observed that

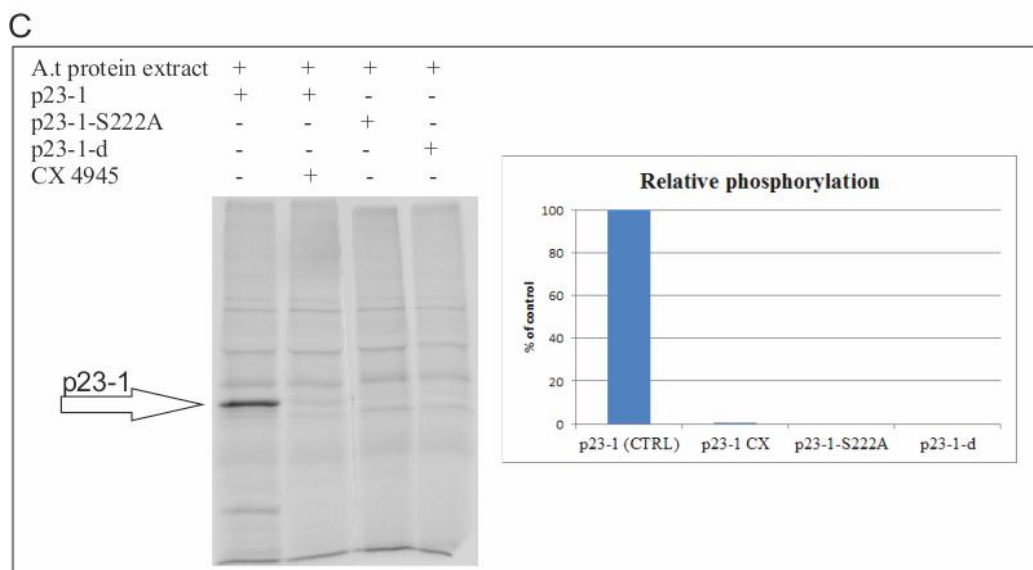
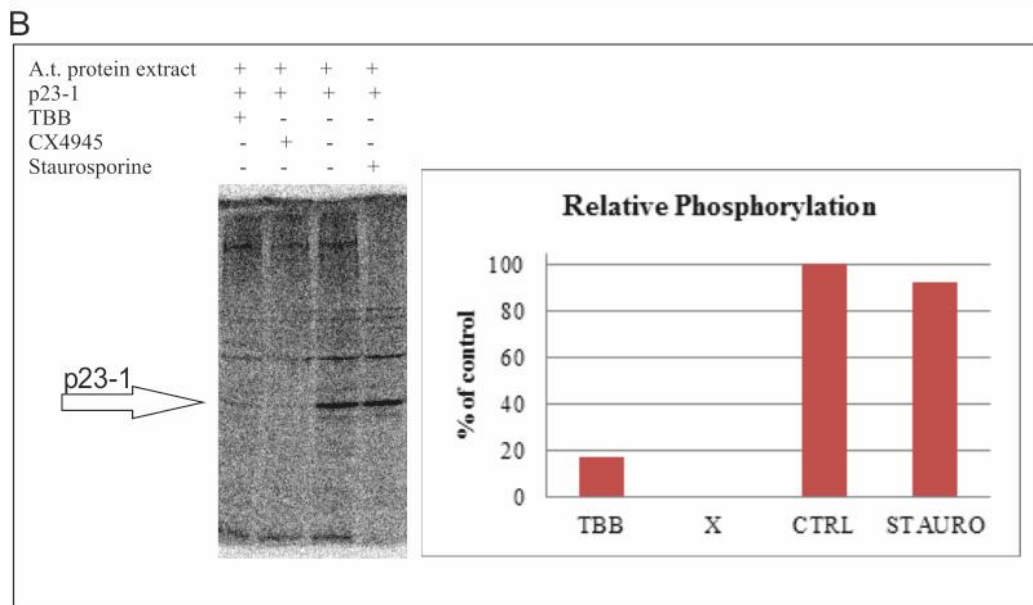
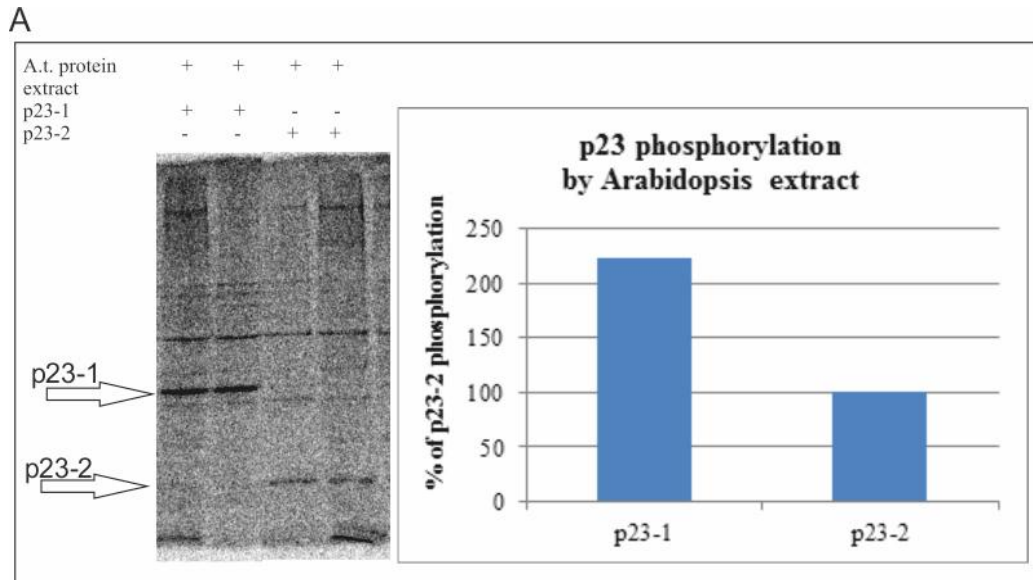


**Fig. II.2: A)** *In vitro* phosphorylation of recombinant p23-1 and p23-2 by 10-day-old *Arabidopsis* seedlings protein extract. Recombinant p23-1 and p23-2 (0.1  $\mu\text{g}$ ) were incubated with *Arabidopsis* protein extract (10 $\mu\text{g}$ ) 20 minutes at 28°C, in a radioactive phosphorylation mixture (total volume 20  $\mu\text{l}$ ). Densitometric analysis of the autoradiography in which phosphorylation levels are shown as percentage of the p23-2 phosphorylation.

**B)** *In vitro* phosphorylation of recombinant p23-1 by 10-day-old *Arabidopsis* seedlings protein extract. Recombinant p23-1 (0.1  $\mu\text{g}$ ) was incubated with *Arabidopsis* protein extract (10  $\mu\text{g}$ ) 20 minutes at 28°C, in a radioactive phosphorylation mixture (total volume 20  $\mu\text{l}$ ). Specific inhibitors of CK2: TBB (30 $\mu\text{M}$ ), CX 4945 (1  $\mu\text{M}$ ) or general inhibitors of protein kinases not active on CK2. Pixel analysis of the autoradiography in which phosphorylation levels are shown as percentage of the p23-1 phosphorylation in control conditions.

**C)** *In vitro* phosphorylation of recombinant p23-1, p23-1-S222A and p23-1-d by 10-day-old *Arabidopsis* seedlings total extract. Recombinant proteins (0.1  $\mu\text{g}$ ) were incubated with *Arabidopsis* protein extract (10  $\mu\text{g}$ ) 20 minutes at 28°C, in a radioactive phosphorylation mixture (total volume 20  $\mu\text{l}$ ). The specific inhibitor CX 4945 (1  $\mu\text{M}$ ) was used. Densitometric analysis of the autoradiography in which phosphorylation levels are shown as percentage of the p23-1 phosphorylation.

although p23-1 shows less affinity for recombinant human and maize CK2 compared to p23-2, it is phosphorylated at a higher level by *Arabidopsis* CK2s. We have already shown that p23-2 is a specific substrate of the CK2 $\alpha\text{C}$  of *Arabidopsis* and we investigated which are the isoforms of CK2 that actually phosphorylate p23-1. To assess if the kinases that actually phosphorylate p23-1 display a size consistent with *Arabidopsis* CK2 isoforms, we performed a set of in gel kinase assays, including either  $\beta$ -Casein, p23-1 or p23-2 in the gel.

We show in Figure II.3.B that there is only one band in the in gel kinase assay of p23-1, and this band has a molecular weight of about 50 kDa. This band could correspond to the high mass weight band of the  $\beta$ -Casein, reflecting the contribution of other casein kinases. *Arabidopsis* genome encodes for three nuclear isoforms of CK2 and this band could represent CK2 $\alpha\text{A}$  or CK2 $\alpha\text{B}$  respectively of 47.6 kDa and 47.2 kDa. Unfortunately, we cannot understand, directly from the in gel kinase assay, which is the CK2 isoform that actually phosphorylates p23-1 or if both isoforms are able to phosphorylate it.

In any case it is really interesting that *Arabidopsis* CK2 isoforms show specificity between p23-1 and p23-2, and we wonder if this behavior could have effects on the regulation of the HSP90 complex.

### CK2 isoforms expression levels

We have shown that *Arabidopsis* seedlings extract phosphorylates p23-1 at higher levels compared to p23-2. To assess if this behavior is due to the specificity of CK2 $\alpha$  isoforms, we investigated, by qRT-PCR, the transcript level of the three isoforms of CK2 on the whole plant, during the plant lifecycle.

As shown in Figure II.3.A the three isoforms have different transcription levels during the life cycle of the plant and CK2 $\alpha$ A is the most expressed isoform. We observe that CK2 $\alpha$ A transcript level is about three time higher than CK2 $\alpha$ C and this difference could explain why we found that p23-1 is phosphorylated at higher level respect to p23-2 by the *Arabidopsis* seedlings extract.

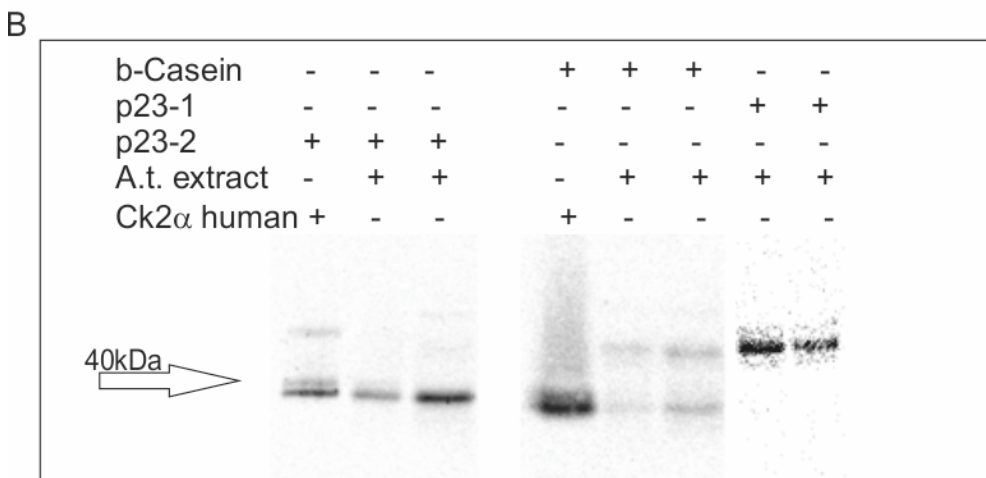
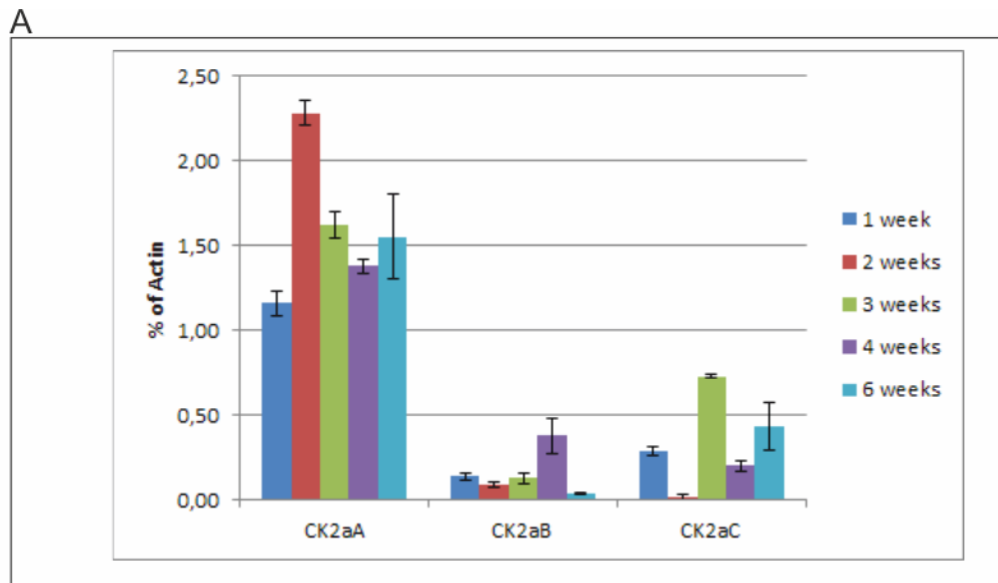


**Fig. II.3: A)** qRT-PCR of CK2 isoforms during the life of *Arabidopsis*, performed on whole plant. Data are normalized on Actin2 (At3g18780) and displayed as percentage of Actin2 transcript signal.

**B)** In gel Kinase assay.  $\beta$ -Casein (100ug), p23-1 and p23-2 (10 $\mu$ g) were included in the gel as indicated. By SDS-PAGE *Arabidopsis* seedlings protein extract were resolved by molecular mass. The whole gel was then incubated in the radioactive phosphorylation mixture for 1h at Room Temperature. Image of p23-1 in gel kinase assay is adapted on the p23-2 in gel kinase assay from Tosoni K. et al. 2011, by the use of coomassie staining.

### **Phosphorylation of p23-1-d**

So the two isoforms of p23 show a distinct pattern of phosphorylation by CK2 isoforms. The main difference between p23-1 and p23-2 is the C-terminal glycine rich (GM/MA) segment. Zang et al. have tested the binding affinity for HSP90 of the recombinant deleted protein p23-1-d (deleted of the glycine rich segment), and they have found that it has similar binding capabilities compared to full-length p23-1. We generated the deletion mutant p23-1-d as described by [Asada M. et al. 2000] and analyzed the phosphorylation pattern of the recombinant deleted p23-1-d in an *in vitro* phosphorylation assay, using the *Arabidopsis* seedlings protein extract as source of endogenous kinases. As shown in Figure II.2.C, the deleted recombinant protein shows no phosphorylation. As the recombinant deleted protein still owns the phosphorylation site, we can suggest that the glycine rich tail is essential for the correct phosphorylation of p23-1.

## Ongoing experiments

### Specificity of p23-1 for CK2 $\alpha$ A and CK2 $\alpha$ B

In order to confirm that p23-1 and p23-2 are phosphorylated by different CK2 isoforms we are selecting homozygous insertional knockout lines for CK2 $\alpha$ A, CK2 $\alpha$ B, the double knockout lines CK2 $\alpha$ A x CK2 $\alpha$ B and the triple knockout mutant [Mulekar J. J. et al., 2012]. Using the protein extract of these mutant lines as source of kinases in an *in vitro* phosphorylation assay, we should be able to understand which is the isoform that actually phosphorylate p23-1 or if both isoforms are able to phosphorylate p23-1.

### Testing the binding of p23-1 with CK2 $\alpha$ A and CK2 $\alpha$ B

Having shown that p23-2 can interact with the human CK2 $\alpha$  and with *Arabidopsis* CK2 $\alpha$ C [Tosoni K. et al., 2011] we would like to understand if p23-1 can interact with CK2 $\alpha$ A and CK2 $\alpha$ B. For this reason we have generated plasmids, based on the bimolecular fluorescent complementation [Waadt et al. 2008], in which p23-1 is upstream of the C-terminal part of the CFP while CK2 $\alpha$ A, CK2 $\alpha$ B and CK2 $\alpha$ A truncated of the N-terminal part, downstream of the N-terminal part of the CFP. By agroinfiltration of *Nicotiana Tabacum* leaves or transformation of *Arabidopsis* mesophyll protoplast, we would be able to test the interaction between these proteins.

### Effect of the phosphorylation on the binding between p23-1 and HSP90

In the introduction I have reported the considerations of Miyata Y. on the role of CK2 in the regulation of the HSP90 machine. Having shown the phosphorylation of both p23-1 and p23-2, we would test which is the impact of phosphorylation on the binding to HSP90. We have already developed different tools in order to test the binding of p23-1 to HSP90 such as recombinant *Arabidopsis* lines expressing p23-1 or p23-2 with the HA tag, under the control of the constitutive viral promoter CaMV 35S. With these tools it would be possible to perform Co-Immuno precipitation assays and to test the binding abilities of p23-1, in presence of CK2 or inhibiting it.

### **Effect of the phosphorylation on p23 function**

We have identified the only phosphorylated residue of p23-1 and we generated the phospho-defective mutant p23-1-S222A. We are now generating also the phospho-mimicking mutant p23-1-S222E and we are planning to study the phenotype of p23 dKO mutant lines complemented with the phospho-mutants of p23-1.

***Functional analysis of p23 co-chaperones of  
Arabidopsis***



## ***Functional analysis of p23 co-chaperones of Arabidopsis***

As described previously p23-1 and p23-2 are encoded by loci *At4g02450* and *At3g03773*. From bioinformatics analyses of *Arabidopsis* database (TAIR) the locus *AT3g03773* can encode two putative isoforms of p23-2: p23-2.1 and p23-2.2. The two isoforms are strongly different owning p23-2.2 a long exon 1 and a short exon 2 both absent in p23-2.1. We have tested whether the latter predicted isoform was translated by *Arabidopsis* seedlings and we found that neither exon 1 or exon 2 were translated. We concluded that the putative p23-2.2 was not present in our analysis and so we have carried out the study on p23-1 and p23-2.1.

### **Expression profile of p23-1 and p23-2**

We have analyzed the transcript levels of p23-1 and p23-2 by quantitative Real Time PCR from seedling stages (1-2 weeks) to senescence phases (6-8 weeks). We isolated mRNA from plants grown in soil from 1 to 8 weeks after germination. Doing this analysis a general picture of the levels of expression of these genes during all the life span of *Arabidopsis* was obtained.

As reported in Figure II.4.A, p23-1 is the most expressed isoform, and its expression is modulated in the different developmental stages. On the other hand, p23-2 has a much lower expression compared to p23-1, and it is stable during all the plant life cycle. Both isoforms are expressed at low levels, ranging from 0.2 to 3 % of the housekeeping Actin2 gene expression (*At3g18780*).

Then, we analyzed the expression of the transcripts of the two isoforms in different organs of the plant. In this analysis we isolated from 8 week-old plants flowers (flowers, silique, apical meristem), rosettes (leaves and stalks) and roots. The results of these experiments, shown in Figure II.4.B, show that the two isoforms of p23 are differently expressed in the organs. Both isoforms are ubiquitously expressed with stronger expression level in flowers and in roots compared to lower levels of expression in the rosette samples.

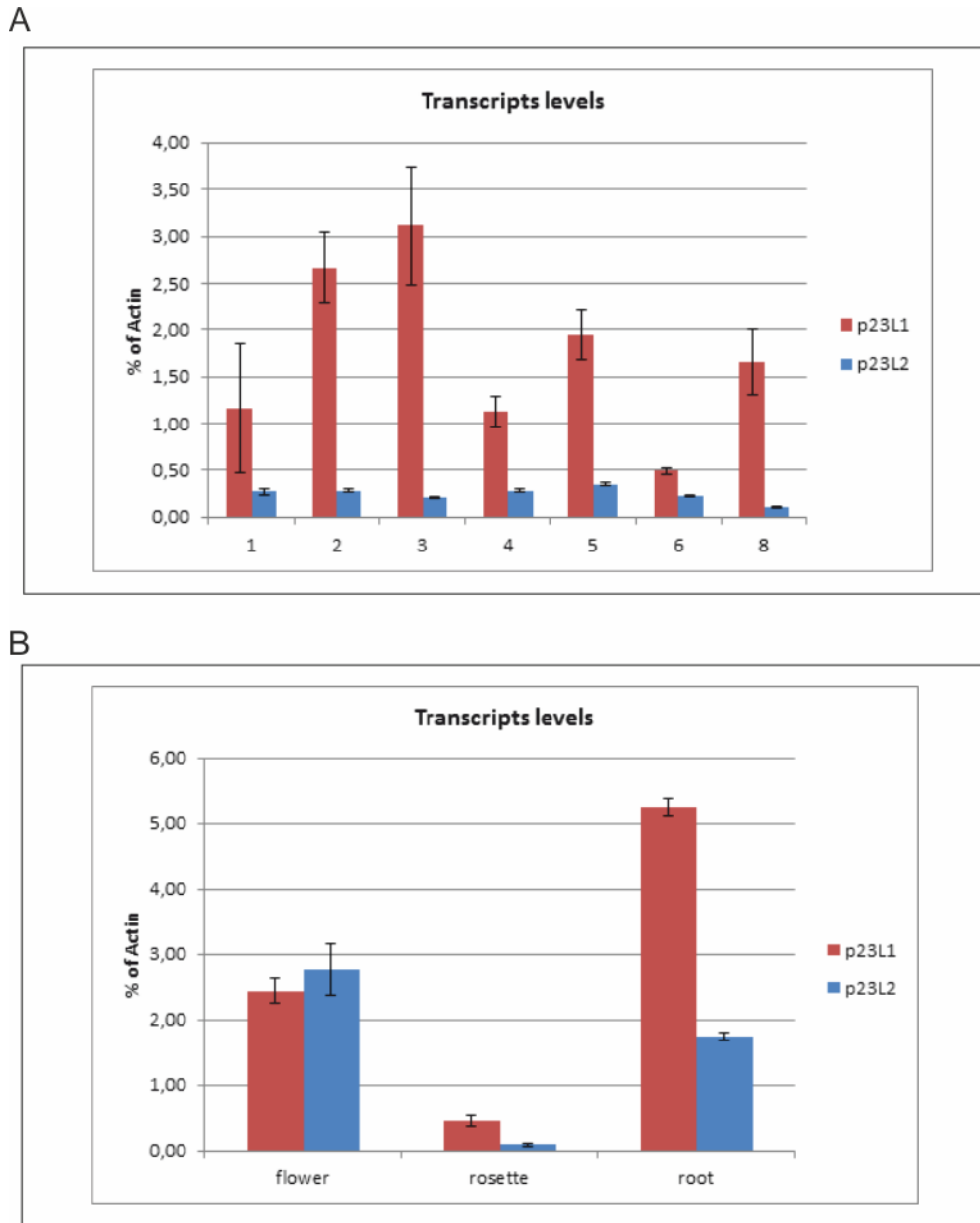


**Fig. II.4:** A) qRT-PCR of p23 isoforms during the life of *Arabidopsis* (1-8 weeks). Data are normalized on Actin2 (*At3g18780*) and displayed as percentage of Actin2 transcript signal.

B) qRT-PCR of p23 isoforms in different portions of the plants at 9 weeks. Data are normalized on Actin2 and displayed as percentage of Actin2 transcript signal.

### Promoter analysis of the two p23 isoforms

Due to qRT-PCR analyses, we obtained an overview of p23 isoforms expression. Then, in order to better define the spatio-temporal expression of the two isoforms of p23, we generated stable transformed *Arabidopsis* plants expressing the  $\beta$ -glucuronidase gene (*uid-a*) under the control of putative endogenous promoters of p23-1 and p23-2. The reporter gene  $\beta$ -glucuronidase allowed to detect the promoter activity of the two genes, by histochemical assay.

We obtained several homozygous *Arabidopsis* transgenic lines and we performed histochemical assays on seedlings and plants at different developmental stages and under different stimuli.

These analyses showed the two promoters active from early stages of development (3-5 days after germination “dag”) in the vascular tissue of the leaves and hypocotyl, while poor activity is detected in roots until 7 dag. After this time the promoter activity is localized in the vascular tissue of all analyzed plant organs.

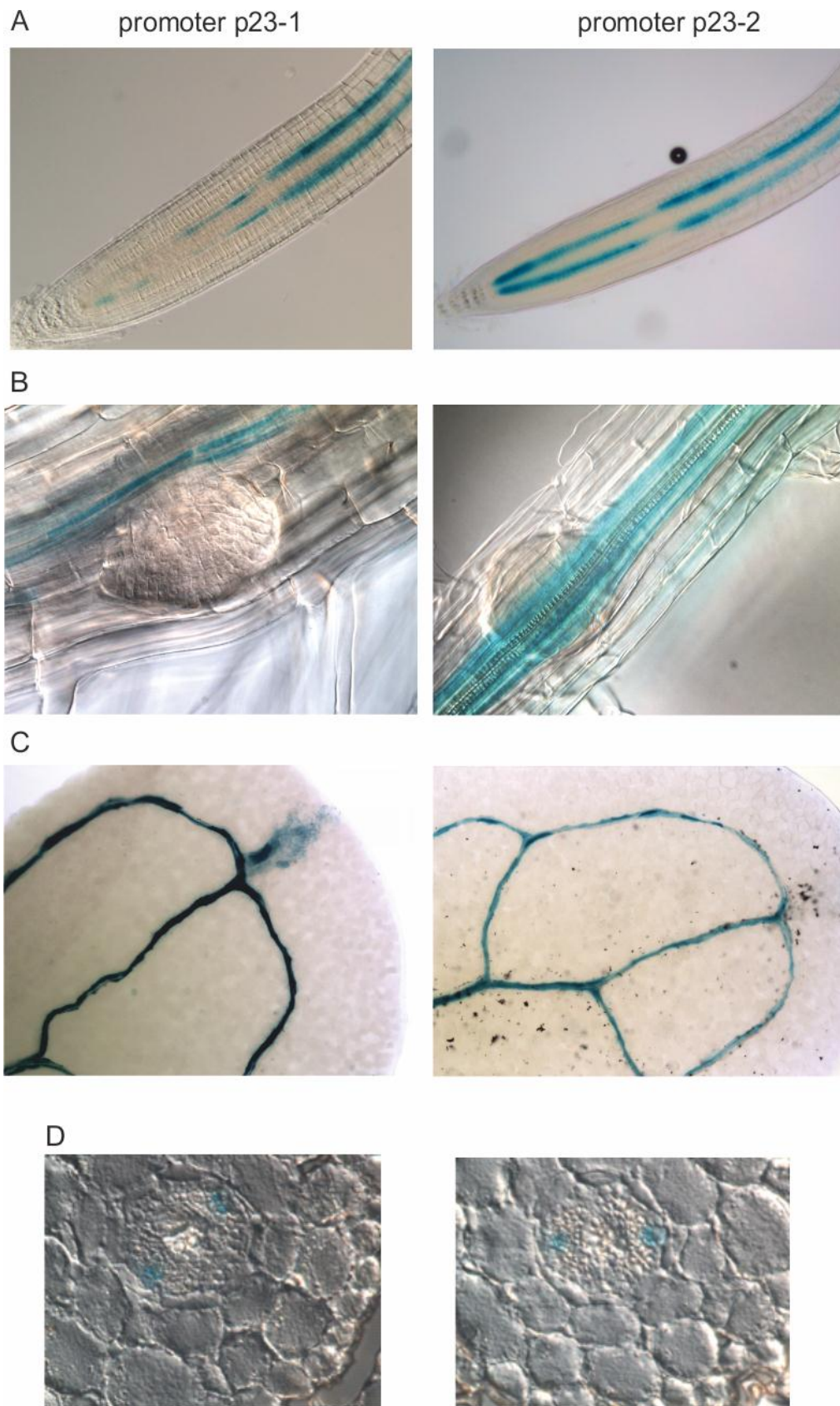
We repeated these analyses applying different abiotic or biotic stress to the transgenic lines. We applied cold stress (4°C) and heat stress (37°C or 45°C), to seedlings. In addition seedlings were treated with Salicylic acid (1mM), in order to mimic a pathogen attack, or with cadmium chloride (50, 100 and 150  $\mu$ M) to identify a possible involvement of these proteins in response to heavy metals. In none of these treatments a change in the expression pattern of the two isoforms was found. So the expression profile of the two isoforms resulted time and tissue specific but not inducible by the selected stimuli.

### Tissue localization

As shown in Figure.II.5, the blue staining in 8 day-old seedlings in the vascular cylinder, from root meristem to leaves was analyzed. The staining detection in the root meristem structure allowed us to suggest a phloematic localization for the activity of both promoters. Further, analyses on 8 week-old adult plants showed the activity of the promoters also in pollen and immature seeds. The promoter activity of the two isoforms is mainly redundant, except for few morphological structures such as: hydathode, a site of expression specific for p23-1, pollen and immature seeds that show different expression between the two isoforms. These organs, in which the two promoters are differently active, could be useful for studying specific functions of the two isoforms. The expression pattern of both isoforms seemed to be limited to the phloem in roots, hypocotyl and

leaves. To better define the pattern of expression of the two isoforms, we performed transversal sections of 8-day-old seedlings for a more accurate analysis.

In Figure II.5.D, cross-sections of the hypocotyl, embedded in Histo-resin, show in a clear way the promoters activity in the two phloematic poles, confirming the tissue specificity of the expression pattern of these two genes.



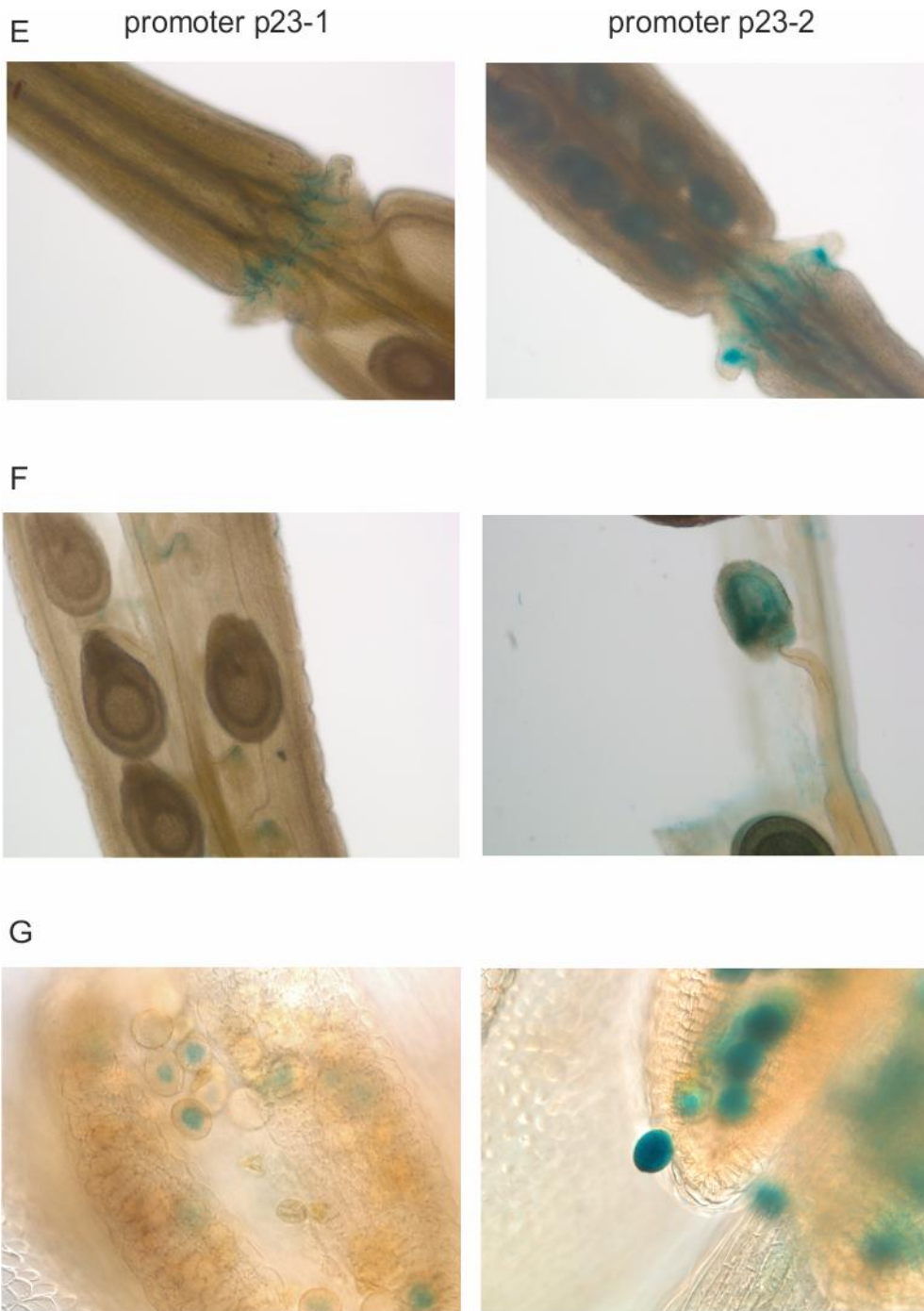


**Fig. II.5:** Histochemical assay of 10 day old seedlings: root (A, B), hypocotyls (D) and leaves (C); adults plants: silique (E, F) and anthers (G). The activity of the p23-1 or p23-2 promoter results in a blue staining of the specific tissues. D) Cross section of 10 days old seedlings embedded in resin after histochemical analysis

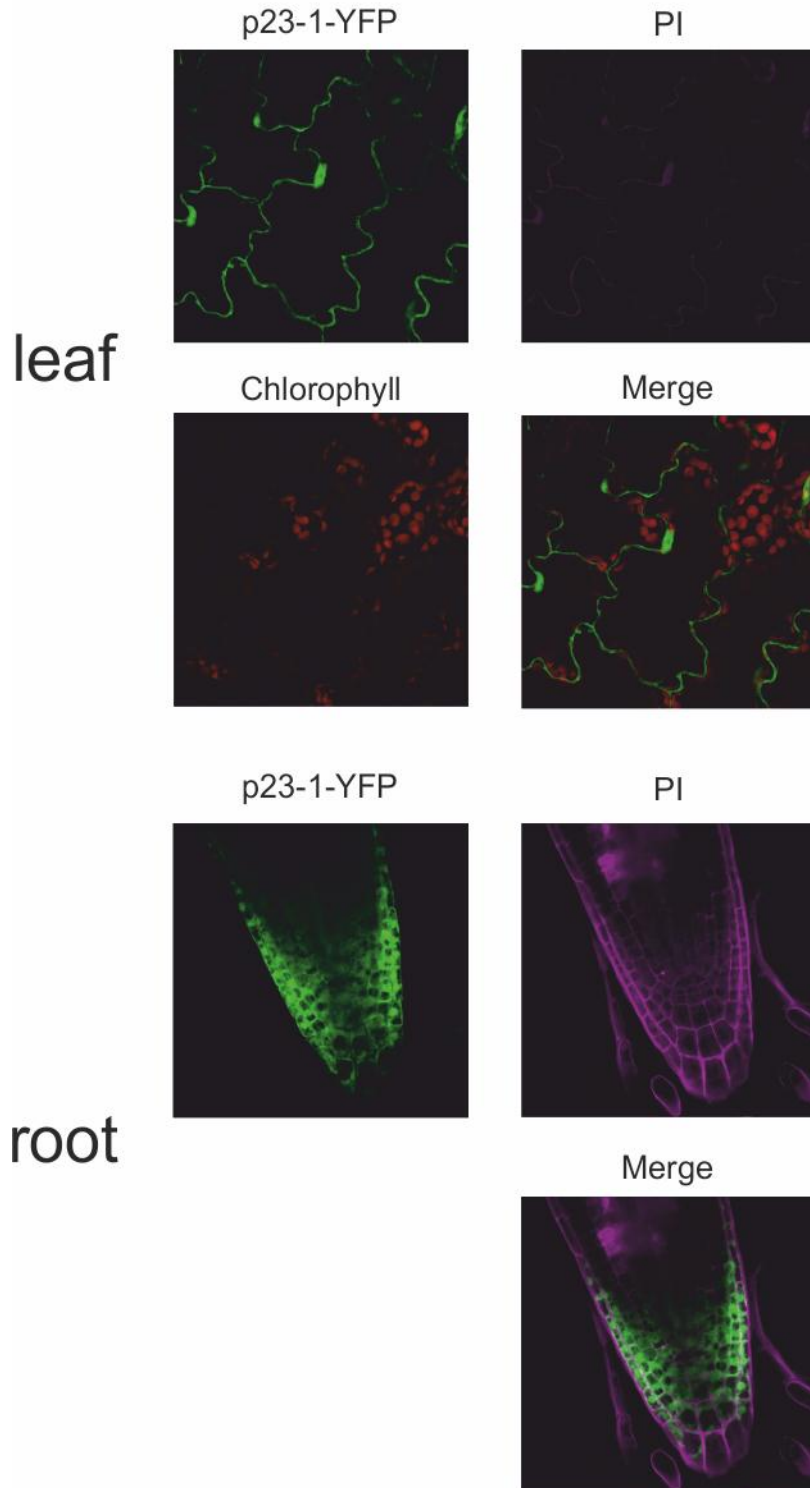
### **Subcellular localization of the two p23 isoforms**

In order to analyze the subcellular localization of the two isoforms, we generated stable transformed plants expressing the two proteins of interest under control of the constitutive viral promoter CaMV 35S. In these plants, p23-1 and p23-2 are overexpressed in all tissues and tagged at the C terminus with the yellow fluorescent protein (YFP). Analyzing different plant tissues by Confocal laser microscopy, it was possible to define the subcellular localization of the chimeric proteins.

As shown in figure II.6. A and B, the signal of the YFP is detectable in leaves and in roots of 10 day-old seedlings. In these tissues, both chimeric proteins p23-1-YFP and p23-2-YFP show cytosolic and nuclear localization.

As chimeric proteins have a molecular mass of about 50KDa, we cannot assess, directly with these experiments, if the proteins are actively transported into the nucleus or if they can passively diffuse into it.

# p23-1



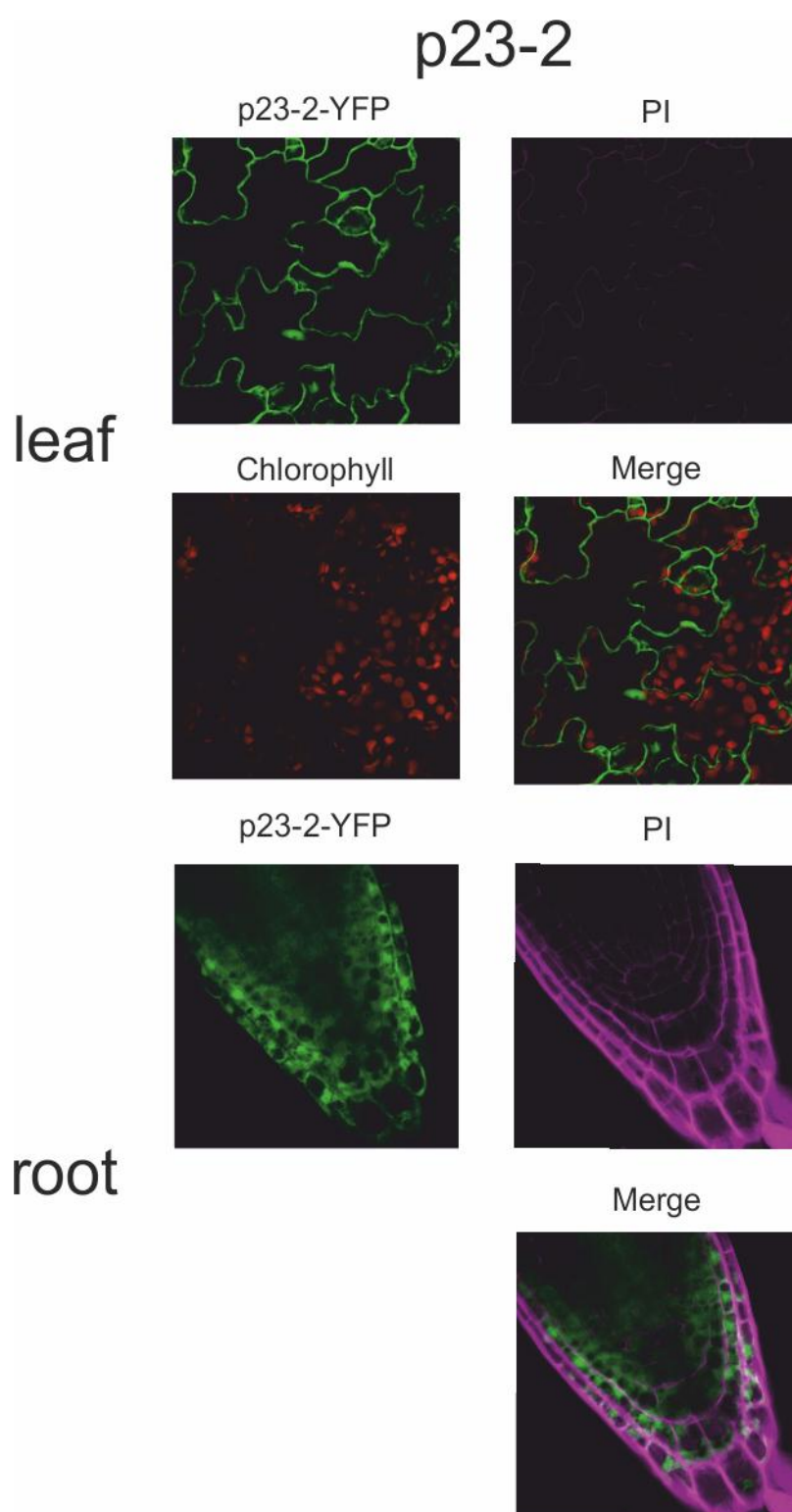


**Fig. II.6:** p23-1-YFP and p23-2-YFP. Confocal microscopy images of the epidermal layer cells of the leaf and of root meristematic zone. YFP: Excitation: 488nm, Emission: 535nm, PI: Excitation: 488nm, Emission: 635nm; Chl: Excitation: 488nm, Emission: 700 nm

## Phenotype characterization of knockout p23 mutants and overexpressing lines

In order to characterize the phenotype of knockout mutant lines of the two isoforms of p23, we analyzed the main physiological features of plants. We analyzed single knockout mutant lines of the two isoforms ( $\Delta p23-2.1$ ,  $\Delta p23-2.2$ ,  $\Delta p23-2.3$ ,  $\Delta p23-1.1$ ), and the double knockout line, obtained by crossing  $\Delta p23-2.1$  and  $\Delta p23-1.1$  (dKO). Furthermore we generated lines overexpressing p23-1 or p23-2 (OE1HA and OE2HA).

Through this analysis we observed normal features of the aerial part of the plant instead the root growth was strongly impaired in the dKO, feature detectable only from 8 days after germination (dag). In order to better characterize this behavior, we performed a more detailed analysis of the root growth on knockout and overexpressing lines (dKO and OE2HA).

In Figure II.7.A we show dKO, wild type and OE2HA lines 10 days after germination and in the lower panel the length of the primary root at 5 and 8 dag is plotted. Analyzing the root length we can observe that dKO shows shorter roots compared to the wild type, while the overexpressing line of p23-2 shows longer roots (dKO  $3.88 \pm 0.33$  cm, wt  $5.07 \pm 0.42$  cm, OE2HA  $6.09 \pm 0.45$  cm). Furthermore it is interesting to underline that the “short root phenotype” of dKO is not detectable during the first 5 days of growth while OE2HA roots are always longer than wild type. As described above the two p23 promoters are not active in the meristematic zone of the root before 7 days of growth, and the expression pattern could explain why the short root phenotype is not detectable in dKO before 8 days, strengthening the hypothesis of a role of p23 proteins in root development.

Under our experimental conditions, we could not observe secondary roots during the first 10 days of growth. In order to evaluate if the short root phenotype of dKO is affecting also secondary roots, we have grown dKO and wild type lines under long day and high light conditions (20h light – 4 h dark, 110  $\mu$ E). In these conditions plants are growing faster and secondary roots could be detected already at 10 dag.

As shown in figure II.7.B, the short root phenotype of the dKO line is more evident under high light conditions, and the impairment in the root growth affects also secondary root.

In order to characterize dKO phenotype in more details we analyzed the structure of the primary root of different lines at 8 dag by using confocal microscopy.

In Figure II.8.A is shown the analysis of the root structure using propidium iodide staining, a dye specific for cell wall. We acquired high definition images (1024x1024 64X water immersion objective) and merged 14 to 17 images by Fiji-stitching bundle.

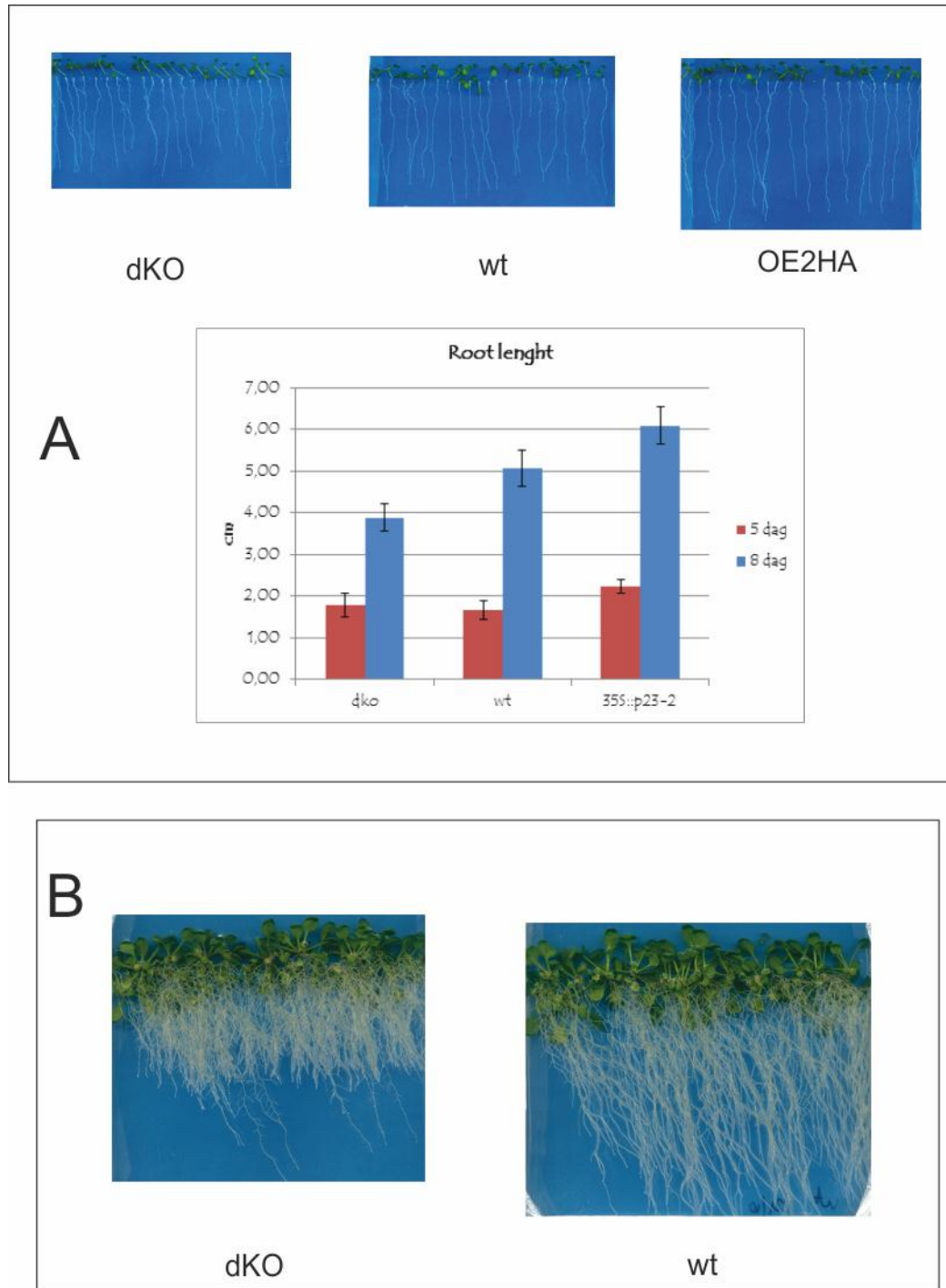


**Fig.II.7: A)** Analysis of the root length of the double knockout line (dKO), of the p23-2 overexpressing transgenic line (35S::p23-2 and oe2HA) and of the wild type. Root length is measured 5 days after germination or 8 days after germination. Bars represent 0.99 confidence interval. 25 seedlings per line. Experiment were independently repeated more than 10 times.

**B)** Comparison between dKO mutant line and the wild type. In high light (110  $\mu$ E 20h light/4h dark) conditions. The short root phenotype of the dKO is strongly enhanced and affecting also secondary roots.

We measured the root width and counted the cells between the quiescent center and the first elongating cells (marked in yellow) observing that roots of the different genotypes have a comparable width while the length of the meristematic zone was different.

dKO line shows a reduced number of cells compared to the wild type in the area under analysis, while the OE2HA line shows an increased number. These results are in agreement with the data on root length and strongly suggest that the main reason of the short-root phenotype of the dKO line could be due to a slower rate of division of the cells in the meristematic zone.

Root development is a process under control of a complex network signaling molecules and hormones and, among them, auxin and cytokinin play a pivotal role [Dello Ioio R. et al., 2008; Overoorde P. et al., 2010; Moubayidin L. et al., 2010; Sankar M. et al., 2011; Depuydt S. and Hardtke C. 2011; Santuari L. et al., 2012]. Furthermore nitric oxide is one of the most important signaling molecules in plants involved in many physiological and pathological processes (see introduction), and among these processes also root growth requires a normal level of NO. So, we wonder if NO could be involved in the short root phenotype of the dKO mutant.

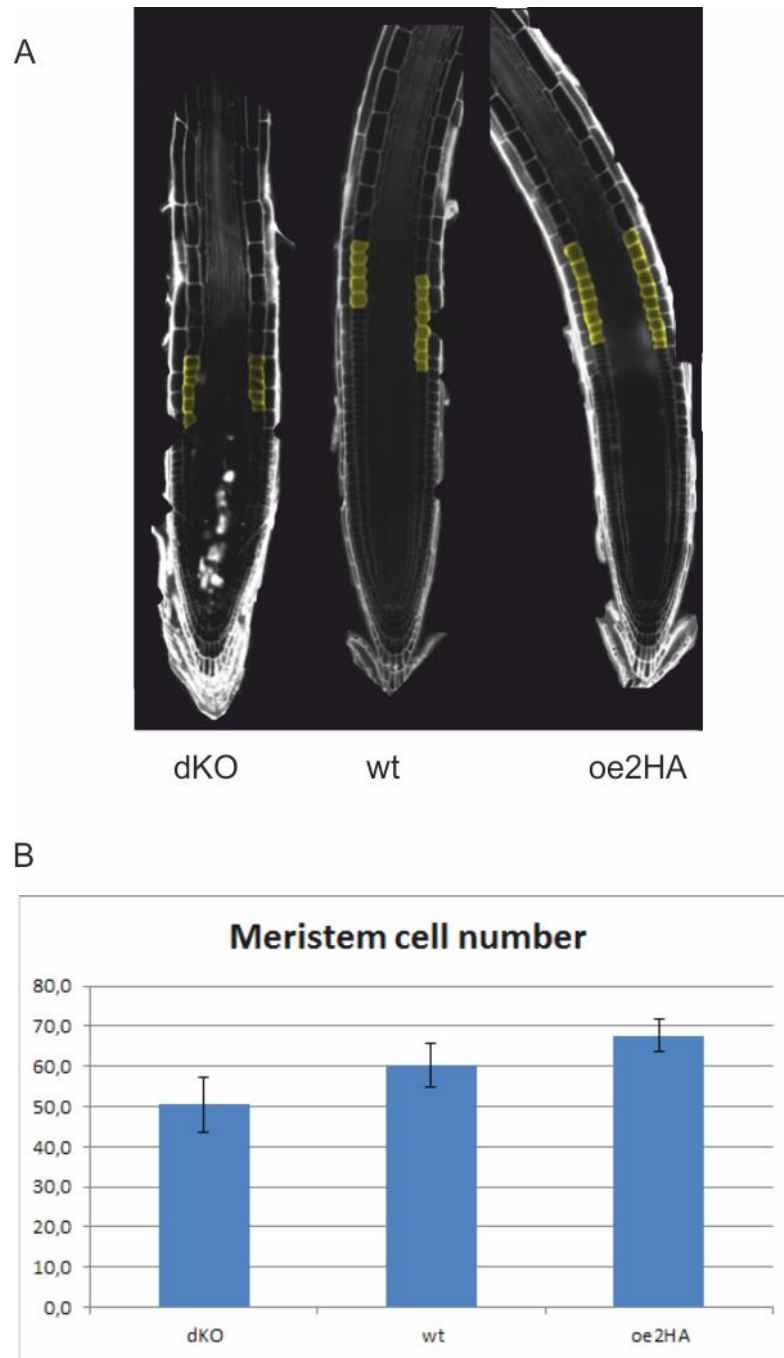


**Fig. II.8: A)** Confocal microscope analysis of Propidium iodide stained seedlings of dKO, wild type and 35S::p23-2 (OE2HA) background. First elongating cells are marked in yellow. Merge of 14-17 1024x1024 images acquired with 64X water immersion objective.

**B)** Cell number of the meristem. In particular we counted cells from the quiescent center to the first elongating cell (example in yellow in A). Bars represent 0.99 confidence interval. 8 seedlings per line.

### **dKO mutant line shows an impairment in basal NO production**

In order to test the involvement of p23 in NO production we analyzed nitric oxide levels in knockout and overexpressing lines of p23.

NO was measured in *Arabidopsis* lines by the fluorescent probe DAF-FM and by the EPR probe cPTIO. We have incubated 8 day-old seedlings in liquid culture medium in presence of the fluorescent probe (15 $\mu$ M). After two hours of incubation the fluorescence of the DAF-FM has been detected in roots by confocal analysis.

In Figure II.9 we report the analysis of the NO production of the dKO and of wild type lines. After two hours of incubation with the fluorescent probe we observed that the dKO shows a faint signal compared to wild type, especially in the upper end of the meristematic zone. These results indicate that the dKO line is strongly impaired in NO homeostasis so p23 is essential for NO production.

### **dKO mutant line shows an impairment in NO production under stress**

We found that p23 is involved in the basal NO production in root cells then we asked whether dKO is also impaired in NO production induced by a well know NO inducer molecule. Salicylic acid is a phytohormone essential for the plant defense response to pathogens, and it induces a strong NO production in root and guard cells, after 60 minute of treatment [Zottini M. et al., 2007]. Furthermore, NO production induced by SA is dependent on a NOS-like activity and on the phosphorylation due to CK2 [Zottini M. et al., 2007]. In this experiment I have also included the single knockout mutant of HSP90 (hsp90.1), the inducible and most expressed cytosolic isoform of *Arabidopsis* HSP90, to test the involvement of the HSP90 chaperone, other than p23, in the production of NO.

8 day-old seedlings of hsp90.1, dKO, OE2HA and wild type genotype were incubated with 1mM SA in presence of the specific NO fluorescent probe DAF-FM-DA. After two hours incubation, the fluorescence of the samples was analyzed by CLSM (confocal laser scanning microscopy). In Figure II.9.B, we report the analysis of the NO production carried out in the different mutant lines. Under this treatment dKO line shows a strong impairment in the SA induced NO production. The same result was obtained in hsp90.1 mutant line, suggesting the involvement of both p23 and HSP90 in NO production. On the other hand OE2HA shows no differences compared to the wild type. In particular, in the chart the DAF-FM fluorescence of the SA treated samples normalized to the basal level of fluorescence detected in control conditions is shown.

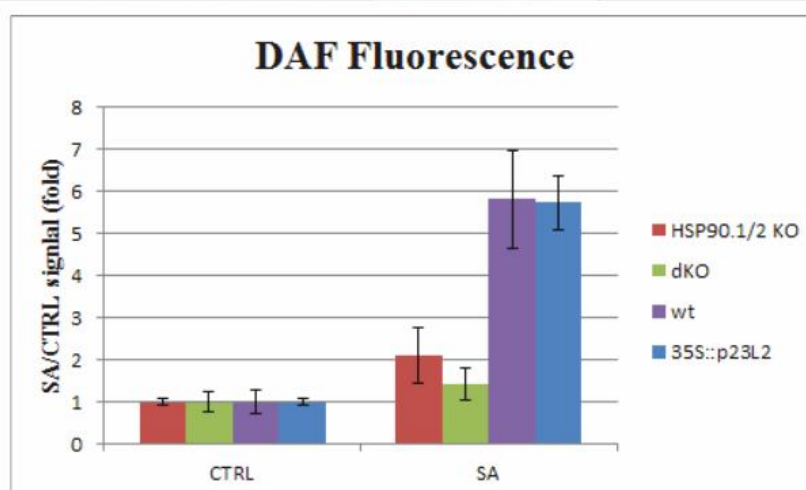
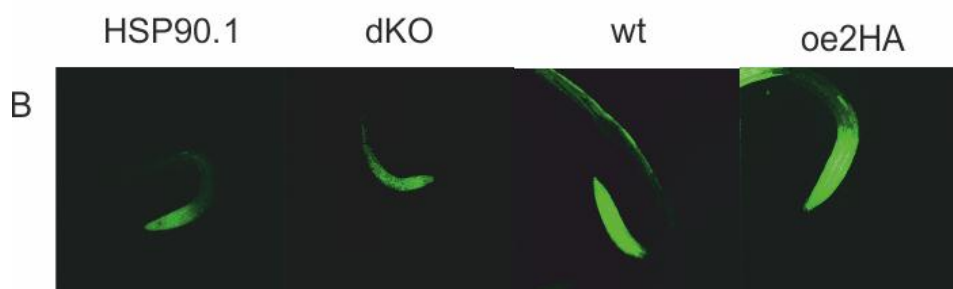
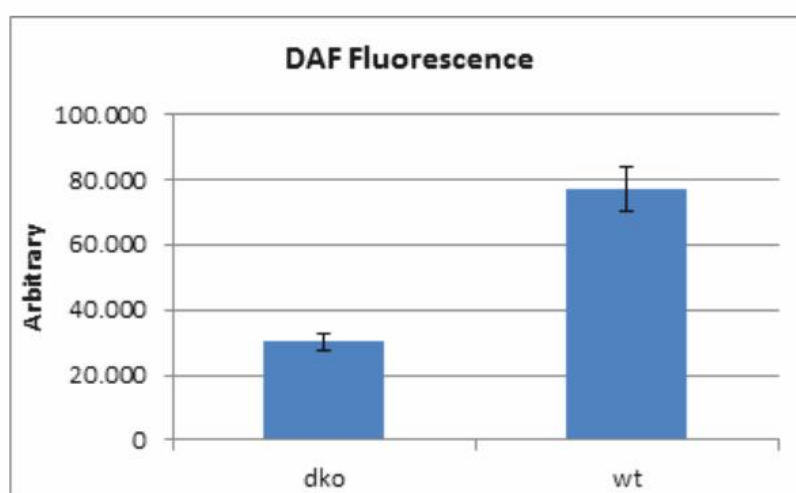
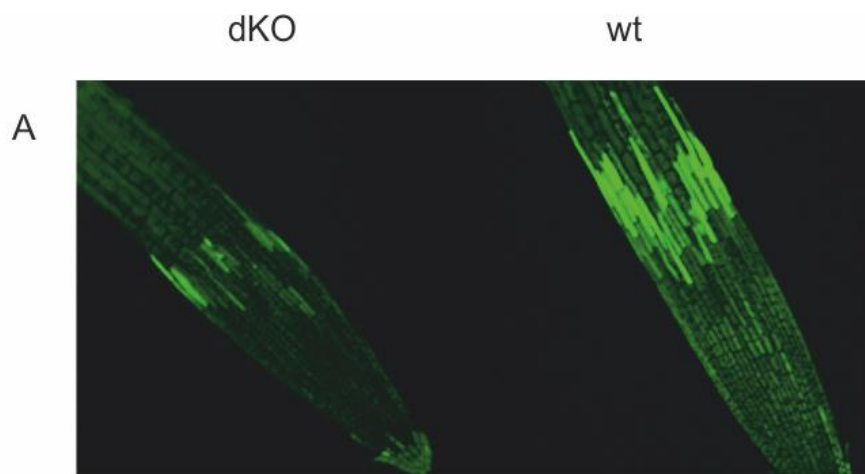


**Fig. II.9: A)** Confocal Analysis of seedling roots. DAF-FM fluorescence Ex: 488 Em: 515-530. dKO and wild type primary root meristem. Image pixel analysis of the DAF fluorescence of the different *Arabidopsis* mutant and transgenic lines. Error bars are 99% confidence intervals.

**B)** Confocal Analysis of seedlings roots. DAF-FM fluorescence. Ex: 488 Em: 515-530. dKO and wild type primary root meristem. Image pixel analysis of the DAF fluorescence of the different *Arabidopsis* mutant and transgenic lines. Error bars are 99% confidence intervals.

By this normalization, we can first of all confirm that SA induces a strong NO production in the root of 8 day-old seedlings as previously reported [Zottini M. et al., 2007]. Then, we can say that dKO and hsp90.1 lines are impaired in NO production in presence of a hormone involved in pathogen attacks as well in physiological events as leaf senescence. Thus, this experiment confirms that p23 is essential for NO production both in physiological and pathological conditions. In addition, we can say that, not only p23 but also hsp90.1 is involved in this pathway maybe in a similar molecular mechanism to animal system. Being four the cytosolic HSP90 isoforms present in *Arabidopsis*, and hsp90.1 the one impaired in the SA-induced NO production, we suggest that HSP90.1 could be the specific isoform involved in this process.

### **NO production impairment and root growth in dKO**

In order to understand if the lacking of the NO production could be the main cause of the short root phenotype of dKO mutant we treated 5 day-old seedlings of the different *Arabidopsis* lines with different NO donors: SNP, SNAP and GSNO. We chose to treat 5 day-old seedlings because we have observed that before that time the two proteins are not expressed in the meristematic zone of the root and that the short root phenotype of the dKO is appreciable only since 8 dag.

We show in figure II.10 that the application of 5  $\mu$ M SNP 5 days after germination partially rescued the short root phenotype of dKO mutant. Interestingly, dKO was the only genotype positively affected by this concentration of NO. A basal concentration of NO is essential for the root growth and auxin action [Otvos et al., 2005] while a higher concentration of NO strongly inhibits root growth [Fernandez-Marcos M. et al., 2011]. Thus this experiment confirms that wild type and the overexpressing line of p23-2 have a normal basal production of NO, and so the application of NO could be responsible of the inhibition of root growth. While dKO, having an impaired basal NO production, positively reacts to NO treatment, slightly increasing primary root length. We have so

confirmed that endogenous or low concentrations of NO are involved in the dKO short root phenotype but it is not the main actor playing in this pathway.

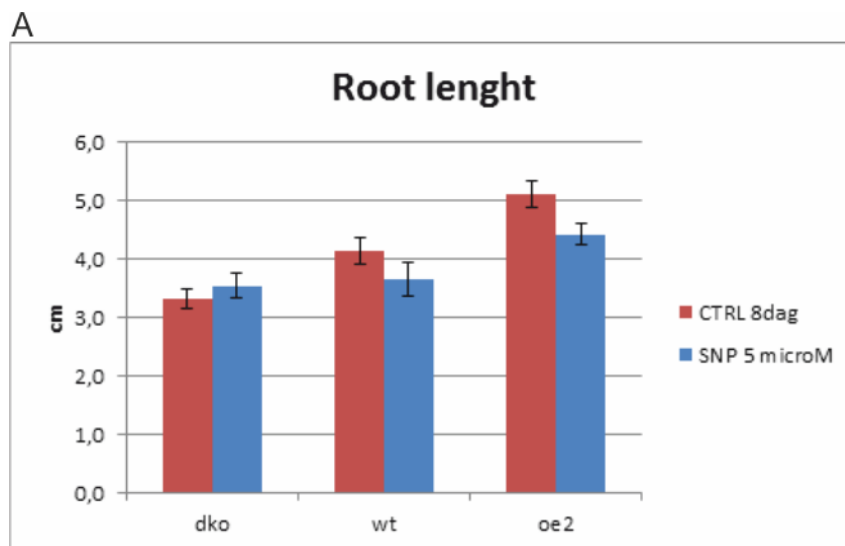


**Fig. II.10:** primary root length of wild type, dKO and oe2HA 8 day-old seedlings in control conditions (red) and treated with 5  $\mu$ M SNP at 5 day after germination (blue). Error bars are 99% confidence intervals.

## Ongoing experiments

### Role of p23 in the auxin transport

HSP90 is involved in auxin transport out of the cells through ABC transporters [Geisler M. and Bailly A. 2007]. Being p23 a likely co-chaperone of HSP90 also in plants, we wonder whether the mechanism responsible for the root growth phenotype of dKO and of overexpressing lines, could be explained through this auxin transport process. First of all we would like to test if p23 is involved in the complex regulating TWD1, the specific HSP90 co-chaperone, involved in the regulation of auxin efflux, by coimmunoprecipitation of p23 in OE1HA or OE2HA plants. Furthermore, in order to verify the homeostasis of auxin in p23 mutant we have crossed dKO and OE2HA lines with many well-known auxin reporter lines (DR5:GUS, DII-venus). Furthermore we have also crossed dKO and OE2HA with SHY2::GFP. SHY2 is a central player in the auxin-cytokinin signaling and this crossing will permit us to analyze the interplay between these two hormones in our mutants. Moreover, we have stable transformed the SHY2.2 dominant mutant line and the SHY2.31 mutant line, in order to constitutively express p23-1 or p23-2 in these genotypes. In addition we are performing immune localization experiments of auxin in dKO and wt lines and, in particular, we are beginning the characterization of PIN7, the specific auxin transporter active in phloematic tissue. The analysis of these lines would allow us to know whether p23 isoforms are indeed involved in auxin homeostasis.

### Characterization of the oe1HA root growth

We have already generated OE1HA lines, overexpressing p23-1 fused with the HA tag. We have started the analysis of the root length of these lines, but homozygous lines are not yet selected so far. By performing initial experiments on heterozygous lines it is possible to appreciate that the OE1HA lines show longer roots compared to the wild type as OE2HA, even in presence of the high standard deviation values reported. This result confirms that the two isoforms of p23 play a redundant role in the root growth pathway as thought.

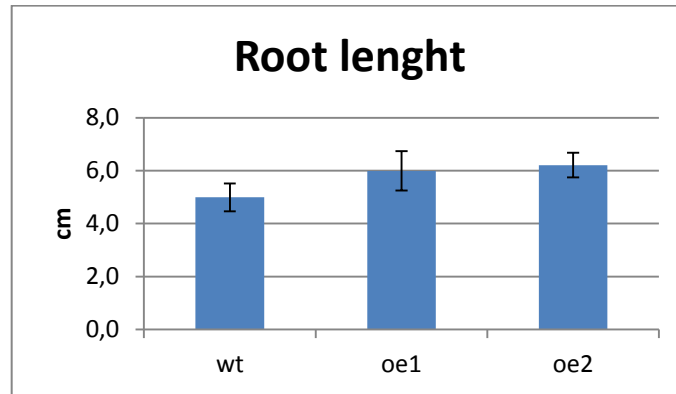


**Fig.II.11:** Primary root length of the different *Arabidopsis* mutant and transgenic lines. Error bars are 99% confidence intervals.

### Plant defense response in the dKO mutant line

We found that dKO and hsp90.1 mutant lines are impaired in NO production under SA treatment. We would like to verify if the SA-dependent defense response pathway is altered in these mutants. Salicylic acid signaling cascade strongly depends on NO, because it involves the nitrosylation of NPR1, that induces the monomerization of NPR1, condition required to move into the nucleus. Once in the nucleus, NPR1 can act as transcription factor and enhance the transcription of PR1. So we plan to perform a quantitative real time analysis to establish the transcription level of PR1, after SA treatment.

### Role of p23 phosphorylation *in planta*

We identified one of the roles of p23 *in planta*, having shown that it is essential for a correct root growth. The protein is also required for NO production, under physiological and stress conditions. A biochemical characterization of the phosphorylation pattern of p23 by CK2 was also performed. We would like to complete this work by understanding the role of the phosphorylation of p23 and the impact of the phosphorylation on the physiological role of p23. So we plan to obtain stable transformed plants of the dKO genotype, transformed with the phospho-defective mutant p23-1-S222A-HA or with the phosphor-mimicking mutant p23-1-S222E-HA. The analyses of these mutants should allow us to shed light on the role of the phosphorylation on p23 action.



***A technical note on the use of cPTIO as NO scavenger and EPR probe***



## A technical note on the use of cPTIO as NO scavenger and EPR probe

The importance of nitric oxide in plant signaling has emerged in the last decades. Despite this recognized biological role, the sensitivity and the effectiveness of the methods used for measuring nitric oxide (NO) concentration in plants are still under investigation.

Among the different methods, 4-amino-5-methylamino-2',7'-difluorofluorescein (DAF) fluorescent dyes have been widely used in combination with fluorescence microscopy and with NO scavengers, such as 2-(4-carboxyphenyl)-4,4,5,5-tetramethylimidazoline-1-oxide-3-oxide (cPTIO). However the dependence of the results on the concentrations of DAF, cPTIO and NO has not been fully investigated and may be responsible for the different results in the experiments reported from different laboratories.

cPTIO belongs to the nitronyl nitroxides (NNO) compounds which have been used also as spin traps for NO in biological samples. The reaction with NO converts the NNO in imino nitroxides (INO), allowing detection by electron paramagnetic resonance (EPR) (Figure II.12.A). Iron dithiocarbamates have been much more widely used as spin traps, due to their high affinity for NO. However, since the use of iron dithiocarbamates, either *in planta* or in cultured cells, shows interferences in the quantitative NO determination due to the presence of nitrites and nitrates, we have started a systematic study to evaluate the suitability of cPTIO for detecting NO by EPR in these systems.

### cPTIO is degraded by *Arabidopsis* cells

In order to perform real time *in vivo* analysis of NO production in plant cells using room temperature EPR spectroscopy, we set up a whole-system capillary analysis. In this experiment, cultured *Arabidopsis* cells are loaded in a 80  $\mu$ l capillary in their own medium and the whole capillary is analyzed by EPR spectroscopy. Using cPTIO as NO specific spin trap we can follow the real-time production of NO by the cells. Using different concentrations of cPTIO, ranging from 50  $\mu$ M to 1mM, we found that the EPR signal of cPTIO (NNO) disappears (Figure II.12.C) while the signal of the (INO) compound is not detectable. This is likely due to the very low amount of NO present in the cell, meaning that the quantitative disappearance of cPTIO is not due only to the reaction with NO, but also to other reactions.

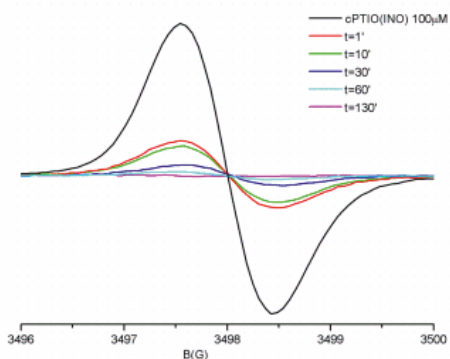
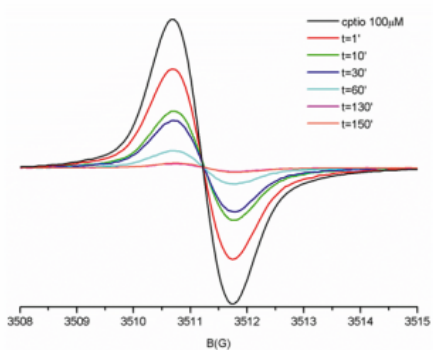
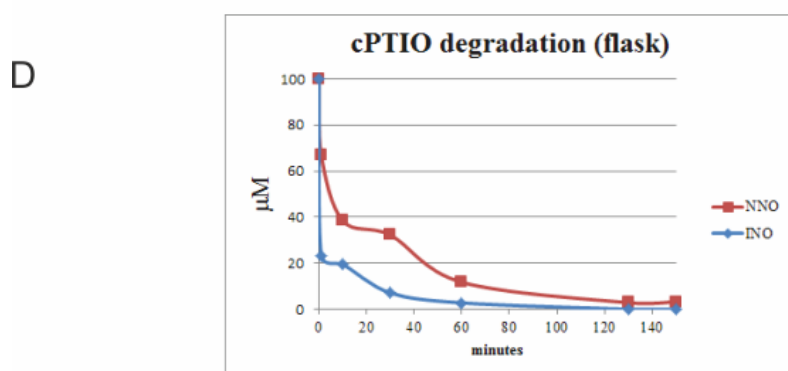
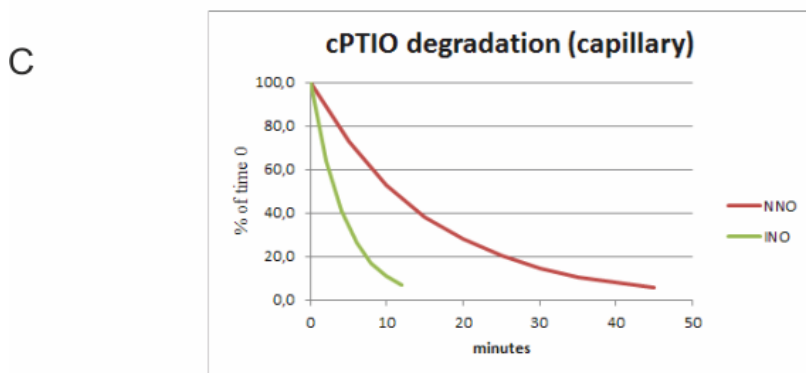
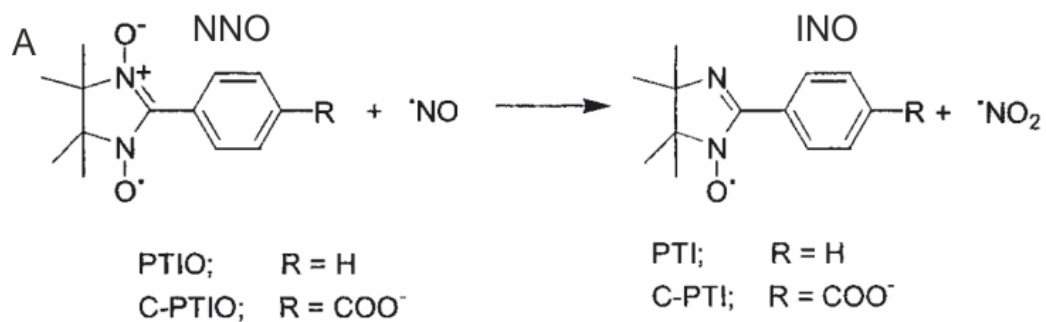


**Fig. II.12: A)** Figure adapted from [Goldstein S. et al., 2003]. PTIO and its derivative (NNO) were shown to react with NO to form the corresponding imino nitroxides (INO) and NO<sub>2</sub>.

**B)** Figure adapted from [Joseph J. et al., 1993]. Electron Spin Resonance (ESR) spectra of nytronyl and imino nitroxides. cPTIO (NNO) shows a five peak ESR spectrum while cPTIO (INO) shows the specific seven peak spectrum.

**C)** cPTIO degradation in the capillary system. cPTIO (NNO) and (INO) signals were quantified and data, normalized to the first acquisition, have been reported as percentage of the first point (2 minutes).

**D)** cPTIO degradation analysis on flask cultured cells. cPTIO (NNO) and (INO) signals were quantified, data have been normalized on 100 μM cPTIO in water and reported as concentration of cPTIO (μM). EPR spectra of the cPTIO (NNO) and (INO) signals in the different time points. In figure are shown only the third line of the cPTIO (NNO) spectrum and the first line of the cPTIO (INO) spectrum.

The capillary system allowed us to follow *in vivo* the degradation of cPTIO by the cells in their growth medium, but cells are much concentrated in the capillary compared to the normal flask culture. For this reason, we analyzed the behavior of the cPTIO incubated with suspension cell cultures, testing only the growth medium. In these conditions we found that the EPR signal of cPTIO (NNO) suffers a strong reduction if the first minute of incubation and then disappears, at a slower rate, during the incubation with *Arabidopsis* cells. As shown in Figure II.12.D, cPTIO disappearance is observed also limiting the analyses to the growth medium. The disappearance of cPTIO shows a slower rate compared to the capillary system, and this could be due to the different concentration of cells in the medium. So we have confirmed that also in normal cell growth conditions, cPTIO was fast degraded by *Arabidopsis* cells.

### **cPTIO (NNO) is stable in the absence of cells**

We tested the stability of cPTIO (NNO), in order to understand if the EPR signal is disappearing due to cell reactions. We analyzed the signal of cPTIO incubated in water, in exhausted growth medium and in presence of dead cells at room temperature for three hours. As shown in Figure II.13.A, the EPR signal of cPTIO (NNO) is stable in water and only weakly affected by the incubation in the exhausted medium or with boiled cells. This experiment demonstrated that cPTIO is stable in the media analyzed and suggests that cPTIO is degraded by a cell-linked activity.

### **cPTIO is not stored in the cells**

We analyzed cPTIO degradation by *Arabidopsis* cells both in the capillary system and analyzing only the medium of the cell culture. The capillary allowed us to measure the signal of cPTIO (NNO) in the whole system while the analyses on the growth medium, permit us to measure only the medium outside the cells. In order to confirm that, also in normal cell culture conditions, cPTIO is actually degraded and not stored inside the cells, we extracted the total soluble content from cells incubated with cPTIO. Analyzing, by EPR spectroscopy, the cell extract we found only a small signal of cPTIO (NNO) (Figure II.13.B), and this result demonstrates that cPTIO is not stored inside cells. Moreover we confirmed that cPTIO can actually enter in the cells.

### **cPTIO is degraded by *Arabidopsis* cell extract**

We powdered a sample from *Arabidopsis* Landsberg cell culture, and obtained the soluble fraction of the extract. cPTIO was incubated in the total extract and samples were analyzed at different times by EPR spectroscopy. We found that cPTIO is strongly degraded by *Arabidopsis* cell total extract suggesting that an enzymatic activity is responsible for the degradation (data not shown).

### **cPTIO (INO) is degraded by *Arabidopsis* cells**

During our analyses we observed that cPTIO (NNO) is fast degraded by *Arabidopsis* cells while the signal of cPTIO (INO) is not detectable. This could be due to the presence of only low amounts of NO in the cells, otherwise cPTIO (INO) could show a degradation similar to cPTIO (NNO). In order to understand if cPTIO (INO) is degraded by cells, we saturated cPTIO (NNO) with NO *in vitro*, by the NO donor MAHMA NONOate, and we analyzed the characteristic signal of cPTIO (INO) incubated with cell cultures. As shown in Figure II.12.C and Figure II.12.D, we found that cPTIO (INO) disappears at a faster rate compared to cPTIO (NNO) signal both in the capillary system and in the growth medium of the cell culture. This experiment explained why we never observed the signal

of the cPTIO (INO) even at low starting concentration of cPTIO (NNO). Furthermore the degradation of cPTIO (INO) by cells, at a faster rate compared to cPTIO (NNO), implies that the use of cPTIO for a quantitative *in vivo* measurement of NO is not feasible because signal of cPTIO (INO) is not stable and then does not accumulate.

### **Measuring NO production by treated cells**

Then we tested the use of cPTIO for measuring NO production in treated cells. We treated cell culture with H<sub>2</sub>O<sub>2</sub>, Salicylic acid or Cadmium chloride, three stimuli able to induce NO production [Malinouski M. et al., 2011; Zottini M. et al., 2007; De Michele et al., 2009], with different kinetics, in particular hydrogen peroxide induces a fast production of NO, SA induces the production of NO with a peak at 60 minutes while Cadmium chloride induces a slow increase in the production of NO by the cells with a peak at 48 hours. We treated cultured cell and took aliquots of the culture medium at different time (30s – 1m – 5m for the H<sub>2</sub>O<sub>2</sub>, 45m – 60m- 120m for the SA and 12h – 24h and 48h for the CdCl<sub>2</sub>). We analyzed the samples by EPR spectroscopy but we never observed the signal of cPTIO (INO) (Data not shown). This experiment further confirmed that the kinetics of degradation of the cPTIO (NNO) and (INO) impedes the quantitative measurement of NO.

### **cPTIO is degraded by *Arabidopsis* seedlings**

We demonstrated that cPTIO is degraded by *Arabidopsis* cultured cells. As cells are a simplified system compared to the whole plant we investigated the behavior of cPTIO incubated with *Arabidopsis* seedlings. We collected 5 grams of 10 day-old seedlings and put them in 30 ml of liquid growth medium, and we incubated cPTIO in this system. As shown in Figure II.13.C we found that both cPTIO (NNO) and (INO) are degraded by whole plants at a slower rate compared to cell cultures. A possible explanation to the slower rate of degradation could be ascribed to the much complex processes of uptake of cPTIO by the whole plant compared to the cell culture, but further experiments are needed.

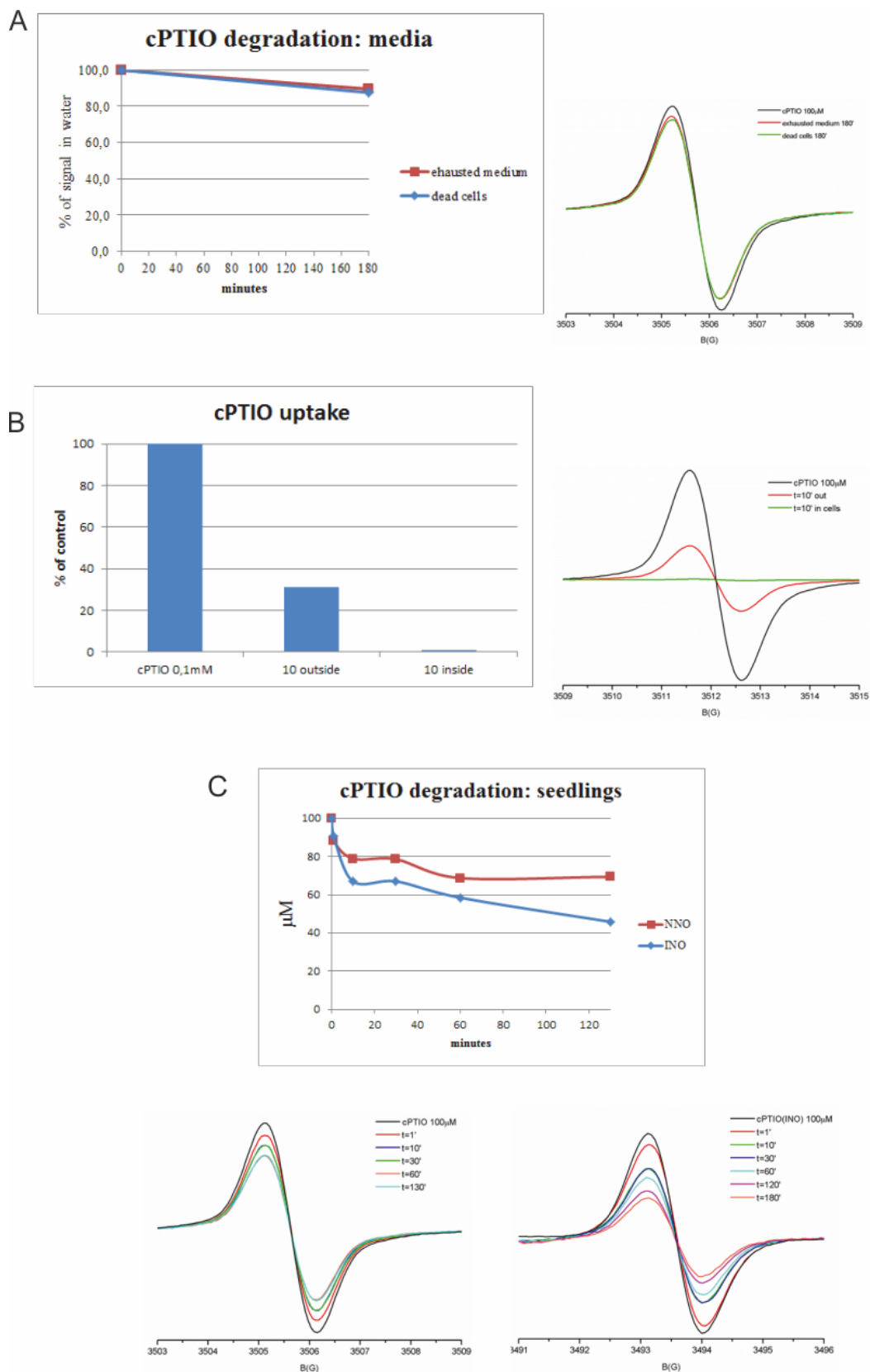


**Fig. II.13:** A) cPTIO (NNO) was incubated in water, exhaust medium or with boiled cells for 3 hours. The EPR signal was quantified and data were normalized to the signal of cPTIO incubated in water. EPR signal of cPTIO (NNO) in the different media. In figure are shown only the third line of the cPTIO (NNO) spectrum.

**B)** cPTIO (NNO) was incubated with flask cultured cells. At 10 minutes a sample from the growth medium was taken and cells were immediately frozen in liquid Nitrogen. The EPR signal of cPTIO was quantified and normalized to the signal of 100  $\mu\text{M}$  cPTIO in water. The lacking of cPTIO signal from the growth medium is not explainable by the uptake of cPTIO from cells. In figure is shown only the third line of the cPTIO (NNO) spectrum.

**C)** cPTIO degradation by Arabidopsis 8 day old seedlings. cPTIO (NNO) and (INO) signals were quantified, data have been normalized to the signal of 100  $\mu\text{M}$  cPTIO in water and reported as concentration of cPTIO ( $\mu\text{M}$ ). EPR spectra of the cPTIO (NNO) and (INO) signals at the different time points. In figure are shown only the third line of the cPTIO (NNO) spectrum and the first line of the cPTIO (INO) spectrum.

### cPTIO is degraded by human cells

In order to understand if the degradation of these molecules is a plant specific metabolic activity or if it is common in different realms, we have tested the behavior of cPTIO (NNO) and (INO) incubated with human cell cultures (293T).

We observed that cPTIO (NNO) is degraded also by human cell cultures and that cPTIO (INO) suffers a bursting reaction that completely remove the EPR signal in few seconds (Figure II.14). Due to this really fast reaction it resulted impossible, also in human cell cultures, to measure the NO production by this system.

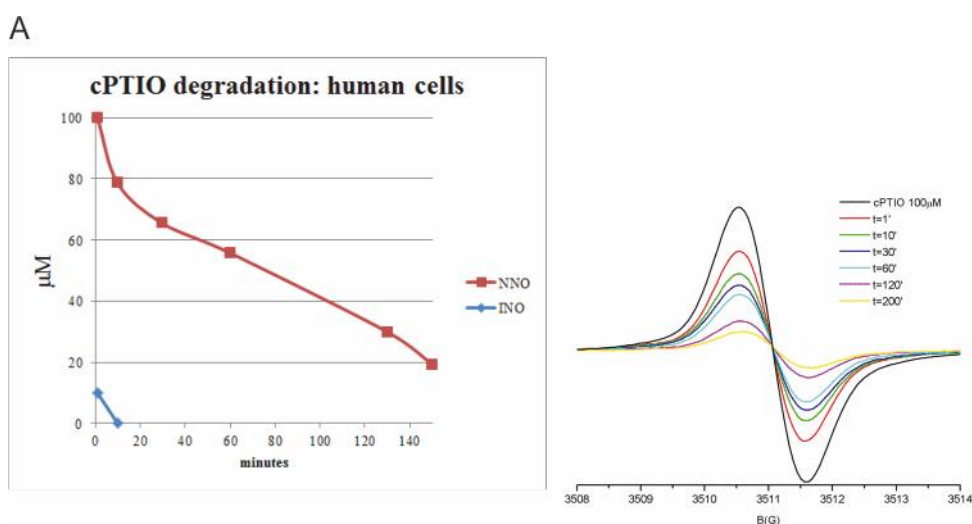


**Fig. II.14:** cPTIO degradation by 293T human cell cultures. cPTIO (NNO) and (INO) signals were quantified, data have been normalized to the signal of 100  $\mu\text{M}$  cPTIO in water and reported as concentration of cPTIO ( $\mu\text{M}$ ). EPR spectrum of the cPTIO (NNO) signals at the different time points. In figure is shown only the third line of the cPTIO (NNO) spectrum.

Our EPR analysis on *Arabidopsis* Landsberg cell cultures shows that cPTIO is degraded by cells in tens of minutes while the INO compound, produced by cPTIO and NO reaction, has not been detected by EPR either in the control or in the stressed cells. This is likely due to the very low amount present in the cell, meaning that the quantitative disappearance of cPTIO is not due only to the reaction with NO, but also to other cell reactions. Since in the cells the rate of INO degradation results to be even faster than that of cPTIO, its direct measurement by EPR is impaired. Thus these results show that this spin trap is not suitable for a quantitative measure of NO in living cells. Whole plants showed a similar behavior but with a slower rate of degradation of both cPTIO (NNO) and (INO).

In this work we also will demonstrate that the products deriving from the cell transformation of cPTIO, are not able to bind NO, and to act as scavengers. In fact, the ability of cPTIO to decrease DAF fluorescence by scavenging NO, in samples stimulated to produce NO (i.e. by hydrogen peroxide (100  $\mu$ M) or Salicylic acid (1 mM) treatment), is progressively reduced for three increasing incubation times of cPTIO, meaning that the depletion of cPTIO in the cell is not compensated by the presence of its products.

The results of this systematic work are discussed in terms of reliability of the use of nitrone nitroxides in the scavenging of NO in plant cells.

### **The product of cPTIO degradation is not able to scavenge NO**

We demonstrated that cPTIO is unsuitable for quantitative NO measurement in all system analyzed, but as the principle use of this molecule in literature is as NO scavenger, we analyzed if the products of the degradation of the cPTIO still possess scavenging abilities. As we have not identified yet the molecular species deriving from the cell metabolism of the cPTIO, we incubated the cPTIO with *Arabidopsis* cell culture for different incubation time and then we measured NO production after different stimuli measuring the fluorescence of the DAF. So we incubated for 10, 30, 60 or 120 minutes cPTIO in the cell culture in presence of 15 $\mu$ M DAF-FM-DA or DAF2 and then we treated the culture with H<sub>2</sub>O<sub>2</sub> or Salicylic acid.

Experiments done in presence of the DAF-FM-DA were analyzed by confocal microscopy and image densitometric analysis while assays done in presence of DAF2 were analyzed by measuring the fluorescence at 515 nm.

We show in Figure II.15.A the quantification of the fluorescence of the DAF-FM by image pixel analysis. We have tested two different stimuli that induce the production of NO: hydrogen peroxide (100  $\mu\text{M}$ ) and Salicylic acid (1 mM).  $\text{H}_2\text{O}_2$  induces an increase in the fluorescence of the DAF, as expected, in about one minute. So we incubated the NO scavenger cPTIO in the cell culture for 1, 30 or 120 minutes, then we treated the cell culture with  $\text{H}_2\text{O}_2$  and analyzed the sample by confocal microscopy. We can see from the data analysis that the ability of cPTIO to reduce DAF fluorescence, scavenging NO, is progressively reduced for the three incubation times. This result suggests that the non-paramagnetic molecules deriving from the transformation of cPTIO, are not able to bind NO, or at least they have a kinetic of scavenging much slower than the kinetic of reaction of DAF to NO. We repeated the same experiment with Salicylic acid, in order to confirm our results and we show that also with this treatment we see the same behavior. As Salicylic acid induces the production of nitric oxide much slower compared to  $\text{H}_2\text{O}_2$  (the peak of production is after 60 minutes), we have tested cPTIO incubated for 1 or 60 minutes in the cell culture. In figure II.15.C we report the ability of cPTIO to reduce DAF fluorescence, in which data were normalized on the effect of the cPTIO incubated for 1 minute. From this plot we can see that the incubation of the cPTIO in the cell culture, drastically reduces its ability to scavenge NO.

cPTIO is usually used as a scavenger for NO in concentration ranging from 100  $\mu\text{M}$  to 1mM, and for the experiment with DAF-FM-DA we used 100  $\mu\text{M}$  cPTIO and 15  $\mu\text{M}$  DAF-FM-DA, and we repeated the experiment using the external fluorescent probe DAF-2 (15 $\mu\text{M}$ ). The experiment, using DAF-2, was performed as described before, incubating cPTIO in the cell culture for 10, 30 or 120 minutes before treating the cells with Salicylic acid. We show in figure II.15.D the fluorescence of the DAF-2 normalized on the fluorescence of the non-treated sample. From the plot it is possible to appreciate that external DAF reports a much lower production of NO in the treated samples (2-fold of the control signal while internal DAF measured 4-fold). This was expected because NO is a high reactive species and external DAF can measure only the NO that actually exits the cells, without reacting with other molecules and permeating the membrane. In these conditions, in which cPTIO can enter the cells while DAF cannot, we can appreciate an almost complete depletion of the DAF2 signal using cPTIO incubated 10 minutes in the cell culture. As seen with the use of the internal DAF probe, also in these conditions, the incubation of the cPTIO with the cell culture causes a strong impairment in the scavenging ability of this molecule, arguing the hypothesis that cell can actually degrade cPTIO and that the deriving molecules are not able to scavenge NO.

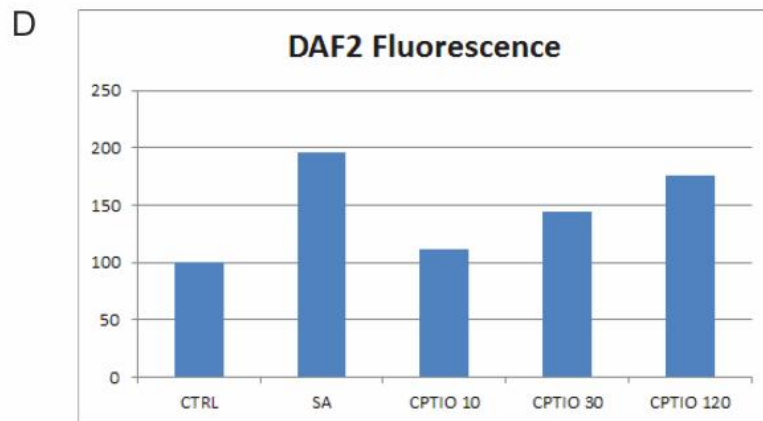
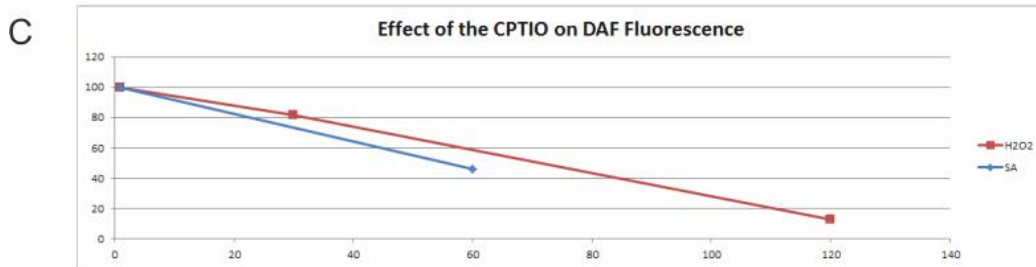
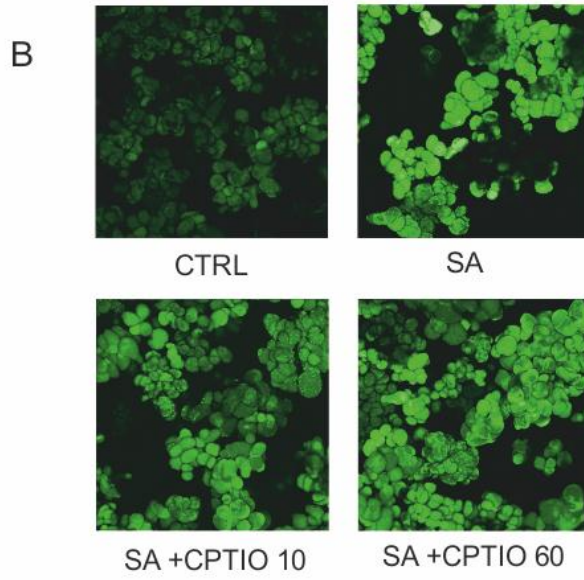
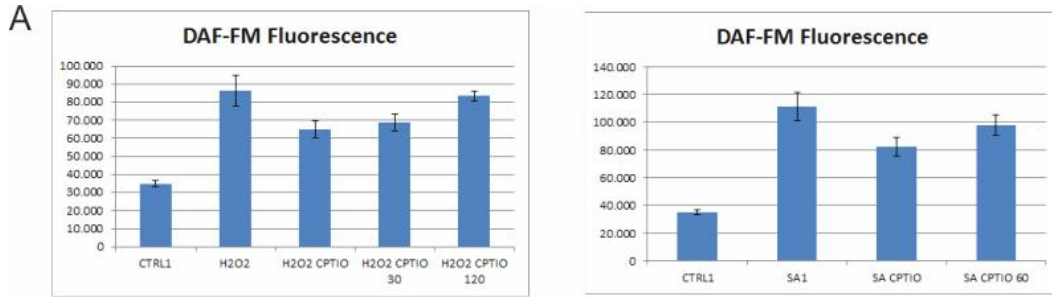


**Fig. II.15: A)** Image densitometric analysis of *Arabidopsis* cell culture treated with SA (1mM) or H<sub>2</sub>O<sub>2</sub> (100μM). cPTIO was incubated with cells for different periods and then the stimulus was somministrated. Both stimuli efficiently induced NO in cell culture and it is possible to appreciate how the incubation of cPTIO with cell culture modifies its ability to scavenge NO and reduce DAF-FM fluorescence.

**B)** CLSM images of the sample from A. Cell fluorescence was quantified by densitometric analysis of the pixel intensity and at least 20 cell per sample were singularly analyzed.

**C)** Effect of cPTIO on DAF fluorescence. the difference of fluorescence between the treated sample and the sample incubated with cPTIO was normalized on the sample at 1 minute of incubation. This chart enhance the effect of the incubation of cPTIO with cell culture.

**D)** Image densitometric analysis of *Arabidopsis* cell culture treated with SA (1mM). cPTIO was incubated with cells for different periods and then the stimulus was somministrated. Both stimuli efficiently induced NO in cell culture and it is possible to appreciate how the incubation of cPTIO with cell culture modifies its ability to scavenge NO and reduce DAF-2 fluorescence.

## **Future perspectives**

### **Analysis of the PTIO uptake**

In order to achieve a better comprehension of the reactions that transform cPTIO in a non-paramagnetic molecule, we want to use the tma-PTIO, a non-cell-permeable form of the PTIO. This molecule will permit us to understand if the degradation of the cPTIO take place inside or outside the cell.

### **Analysis of the product of the cPTIO degradation**

We want to analyze by gas chromatography the products of the reactions occurring on the cPTIO incubated with living cells. Finding the products will permit us to hypothesize the mechanism of action of the reaction.

## ***Conclusions***



## Conclusions

In this Ph.D. work I presented the result on the characterization of *Arabidopsis* p23, a key component of HSP90 complex in plant. In particular, by performing both biochemical and physiological studies, a possible role of p23 in root development can be proposed along with the explanation on how the pathway leading to NO production could be regulated.

In animal system, p23 is an essential protein, so the knockout mutation in mice leads to perinatal death. Although this protein has been well studied in animal system, literature is poor on the function played in plants. I analyzed the phenotype of the mutants on the model plant *Arabidopsis thaliana*, that is an excellent system for the study of protein function and, in parallel, I have carried out a biochemical characterization of *Arabidopsis* p23 phosphorylation, *in vitro*.

In *Arabidopsis* two isoforms of p23 are present: p23-1 (At4g02450) and p23-2 (At3g03773.1). They show a similar pattern of expression being mainly expressed in the phloematic tissue of flowers and roots although p23-1 is expressed at higher levels compared to p23-2. The specific expression in the phloematic tissue is in agreement with the tissue expression of HSP90.1, but while HSP90.1 is responsive to different stress stimuli, we found that the two isoforms are constitutively expressed and that their expression pattern does not change after different treatments.

In agreement with the similar expression pattern we found also a strong redundancy in function, as the single knockout mutants do not show phenotypical differences compared to the wild type line. Thus, we generated the double knockout mutant line by crossing each other the two single knockout mutant lines of p23 isoforms.

From the phenotype analysis of the double knockout mutant line we observed shorter roots compared to the wild type ones. This impairment in root development is not observed before of 8 days after germination (dag), likely due to the absence of p23 expression in the root meristematic zone in the first 5 dag.

On the other hand both the overexpressing line of p23-1 and of p23-2 show longer roots compared to the wild type ones, from the early stages of growing.

We also observed that the root growth impairment of dKO line affects also secondary roots.

We suggest that the alterations in the root growth is due to an impairment in the cell division at the level of the meristematic zone, in fact we observed that dKO line shows a reduced number of dividing cells in the root meristem while the overexpressing line of p23-2 shows an increased number of dividing cells.

The process of cell division in the meristematic zone is finely regulated by an equilibrium between different hormones and signaling molecules. In particular the equilibrium between auxin and other hormones play a pivotal role in root growth. Furthermore it has been demonstrated that HSP90 is involved in the extracellular transport of auxin, and the impairment of this transport caused a strong short root phenotype [Geisler M. and Bailly A., 2007]. In particular TWD1 is the co-chaperone responsible for the regulation of auxin export in the HSP90 complex, and we wonder if p23 was involved in the stability of this complex. To answer this question we are planning to test if p23 is actually involved in the complex regulating auxin export.

To do so we have crossed dKO and OE2HA lines with different auxin specific plant reporters, such as DR5::GUS, DII-Venus and SHY2::YFP. The analysis of these reporter lines will allow us to study the homeostasis of auxin in the mutant lines and understand if the root growth phenotype is linked to an alteration of the auxin homeostasis. In order to test if there were differences in the auxin levels or distribution we are also performing immune localization of auxin in the dKO and wt lines.

Nitric oxide is an important signaling molecule in plants, involved in many physiological and pathological processes and among them the auxin controlled root growth. A physiological role for NO in regulation of root growth has been described where NO diminishes primary root growth and plays a central role in determining later root development.

In our experiments, we analyzed the basal NO production in dKO, wt and OE2HA lines, by using the NO specific probe DAF-FM. We found that in dKO line the basal level of NO is lower than in wt and OE2HA lines. In order to figure out whether the difference in NO production is also observed in an experiment in which NO is induced, we tested NO production upon Salicylic acid treatment. It has been already demonstrated that SA induces NO production in *Arabidopsis* roots and this production depends on a NOS like activity and on phosphorylation by CK2. We performed the analysis of SA induced NO production on the dKO, wt, OE2HA and hsp90.1 lines. Analyzing the fluorescence of the DAF-FM probe by confocal microscopy we found that dKO is impaired also in the SA-induced NO production sharing this impairment with the single knockout mutant hsp90.1. From these analyses we concluded that p23 is essential for NO production both in physiological and stress conditions and that HSP90.1 is also involved in this pathway. An impairment in NO production is a severe phenotype as NO is necessary for many physiological and pathological pathways, and, in particular, we wonder what will be the effect on the SA signaling cascade that strictly requires NO. So we are planning to test if PR1, that is a fundamental player in the SA signaling cascade, is correctly regulated in

our mutant or if the impairment in the NO production after SA treatment affects the SA controlled plant defense responses. As mentioned before the two isoforms of p23 have a pattern of expression consistent with the one of HSP90.1 and between the seven isoforms of HSP90, HSP90.1 is the one required for NO production. We wonder if the complex of HSP90.1 and p23 is the one regulating SA-induced NO production and for this reason we would like to further deep this analysis.

As basal NO production is impaired in the dKO line, we would like to verify if this is the molecular reason underlying the root growth defect. So we provided 5  $\mu$ M SNP, a NO donor, to 5 day old seedlings of dKO, wt and OE2HA genotype, and we have analyzed the root growth. While the wt and OE2HA lines suffered a root growth inhibition, after the treatment with NO, the dKO line showed a small rescue of the root growth phenotype. This result first of all confirms that the dKO line is impaired in the basal NO production, but also suggest that NO is not the main player in this pathway. We have to perform a more accurate analysis of the NO treatment using different NO donors such as SNAP and GSNO, in order to confirm this data, but we think that the problem might be upstream of NO.

From our data we can conclude that p23 isoforms of *Arabidopsis* have a pivotal role in NO production and in root development. These pathways are of great interest in plant biology where NOS-like NO production is still controversial. In addition we have demonstrated that p23 and HSP90.1 are upstream of NO production. It is also worth to underline that root growth and root structure development are of great interest in biotechnological studies on drought stress resistance.

As reported above the phosphorylation is the main posttranslational modification regulating HSP90. In order to acquire a wide knowledge on the role of p23, we have characterized the phosphorylation profile of these proteins.

We found that both isoforms are phosphorylated by recombinant human and maize CK2 and also phosphorylated by a CK2-like activity present in a protein extract obtained from *Arabidopsis*. By the analysis of the effect of different CK2-specific or general inhibitors on the phosphorylation of p23, we demonstrated CK2 is the main kinase responsible of the phosphorylation of both isoforms.

We further demonstrated that p23 isoforms are phosphorylated by the monomeric catalytic isoform of CK2 and this result allowed us to demonstrate that CK2 isoforms show specificity between p23 isoforms. In particular, p23-2 is a specific substrate for CK2 $\alpha$ C while p23-1 is a specific substrate for CK2 $\alpha$ A or CK2 $\alpha$ B. This is an interesting results because we found that the two p23 isoforms are mainly redundant in function and

also CK2 isoforms show redundant pathways. On the other hand, the specificity of CK2 isoforms suggests a possible distinct function for the isoforms of p23.

We performed preliminary experiments on the role of the phosphorylation of p23 on the binding with HSP90 *in vitro*, and there are evidences on the negative influence of the phosphorylation on this binding.

We have further deepened the characterization of p23-1 phosphorylation and in particular we generated the phospho-defective mutant p23-1-S222A and the p23-1-d deleted of the glycine rich tail. Serine 222 is the main putative site of phosphorylation of CK2, predicted by bioinformatics analyses and we demonstrated that S222 is the actual site of phosphorylation by CK2 and further confirmed that p23-1 is a specific client of CK2.

We are now generating the phospho-mimicking mutant p23-1-S222E in order to transform the p23 dKO line with both phospho-mimicking and phospho-defective mutants and to observe the phenotype of these complemented lines. The results of these experiments together with the information deriving from the in-vitro analysis will allow us to delineate the role of the phosphorylation of p23 *in planta*.

We analyzed the phosphorylation of the recombinant p23-1-d and we found that the glycine rich tail is essential for the phosphorylation of p23-1. This result demonstrates that the specificity of phosphorylation by the different isoforms of CK2 is not dependent on the glycine rich tail and suggests specificity for the phospho-site.

During the Ph.D. project NO resulted an essential component in pathways where p23 was involved. Despite the recognized biological role, the sensitivity and the effectiveness of the methods used for measuring nitric oxide (NO) concentration in plants are still under discussion. For this reason, we tested the use of EPR spectrometry and NO specific spin trap for *in vivo* NO measurements. We found that Iron dithiocarbamates, that have been widely used as spin traps, due to their high affinity for NO, show interferences in the quantitative NO determination due to the presence of nitrites and nitrates *in planta*. So we started a systematic study to evaluate the suitability of cPTIO for detecting NO by EPR in these systems. Literature already presents attempts to measure NO production *in vivo* by the use of this probe, but the quantification of a clear NO signal is still controversial. For the first time we report that cPTIO is degraded by different species, including human and *Arabidopsis* cell culture and *Arabidopsis* seedlings, and that cPTIO (INO) is degraded faster than the cPTIO (NNO) in all system analyzes. For these reasons we strongly argue that cPTIO cannot be used as probe for the quantification of NO *in vivo*.

As cPTIO is a well-known NO specific scavenger molecule, and it is largely used in biological and medical literature, we have analyzed the effect of the degradation of this

molecule on the scavenging abilities and we show that the scavenging abilities of cPTIO are impaired due to the cellular reactions.

The analysis we report here is not only a drawback on the use of the CPTIO as EPR probe for *in vivo* measurements of NO, but it is useful for calibrating the use of cPTIO as scavenger of NO. The analysis, we have performed, elucidated that in order to have a real depletion of NO, at least in the tissues analyzed, it has to be taken in count that cPTIO is degraded by living cells. So the behavior of these molecules could finally explain why cPTIO is not always able to completely scavenge NO especially for treatments that induce a gradual and continuous production of NO.



# *Chapter III:*

## *Materials and Methods*



## Plant material

### *Arabidopsis thaliana* lines

All *Arabidopsis thaliana* plants used in this work belong to the ecotype *Columbia 0*, except Shy2.2 and Shy 2.31 mutant line.

### Insertional mutant lines:

Locus	NASC	Name
<i>At3g03773.1</i>	SALK_003076	$\Delta p23-2.1$
<i>At3g03773.1</i>	SALK_126538C	$\Delta p23-2.2$
<i>At3g03773.1</i>	SAIL CS817617	$\Delta p23-2.3$
<i>At4g02450.1</i>	SAIL 245_H06	$\Delta p23-1.1$
<i>At5g67380</i>	SALK_N521073	$\Delta CK2\alpha A$
<i>At3g50000</i>	SALK_126662	$\Delta CK2\alpha B$
<i>At2g23080</i>	SALK_151200	$\Delta CK2\alpha C$

$\Delta p23-2.1$  was crossed with  $\Delta p23-1.1$  to obtain the double mutant Insertional line dKO. Homozygous lines of all Insertional lines were obtained.

### Transgenic lines:

Plasmid	Name	Generation
pGreen (0029)-35Sx2::p23L1-YFP	OE1-YFP	T3
pGreen (0029)-35Sx2::p23L2-YFP	OE2-YFP	T3
pGreen (0029)-prom.p23L1::GUS	GUSp23-1	T3
pBI121-prom.p23L2::GUS	GUSp23-2	T3
pGreen (0179)-35S::p23L1-HA	OE1-HA	T2
pGreen (0179)-35S::p23L2-HA	OE2-HA	T3
pGreen (0029)- prom.p23L1::p23L1-YFP in dKO	L1YFP	T1
pGreen (0029)- prom.p23L2::p23L2-YFP in dKO	L2YFP	T1
pGreen (0179)-35S::p23L1-HA in Shy 2.2		T1
pGreen (0179)-35S::p23L2-HA in Shy 2.2		T1
pGreen (0179)-35S::p23L1-HA in Shy 2.31		T1
pGreen (0179)-35S::p23L2-HA in Shy 2.31		T1

Transgenic lines were obtained by floral dip transformation [Clough S. J. and Bent A. F., 1998].

Crossed lines:

Parental lines	Generation
dKO x 35S::DII-Venus	F1
OE2-HA x 35S::DII-Venus	F1
dKO x DR5:GUS	F1
OE2-HA x DR5:GUS	F1
dKO x 35S::modified DII-Venus	F1
OE2-HA x 35S::modified DII-Venus	F1
dKO x prom. SHY2::YFP	F1
OE2-HA x prom. SHY2::YFP	F1
dKO x prom. BRX::GUS	F1
OE2-HA x prom. BRX::GUS	F1
dKO x Hsp18.2::GUS	F2
OE2-HA x Hsp18.2::GUS	F1

### **Growth conditions:**

Flask culture:

Suspension cell culture was generated from hypocotyls dissected from young plantlets of *Arabidopsis* (ecotype Landsberg erecta) and subcultured in AT3 medium [Desikan et al., 1996]. For subculture cycles, 2 mL of packed cell volume was placed in 100-mL Erlenmeyer flasks containing 50 mL of liquid medium. Cells were subcultured in fresh medium at 7-d intervals and maintained in a climate chamber on a horizontal rotary shaker (80 rpm) at 25°C with a 16-/8-h photoperiod and a light intensity of 70 mmol m<sup>-2</sup> s<sup>-1</sup>. Treatments with filter-sterilized solutions of CdCl<sub>2</sub>, Salicylic acid or H<sub>2</sub>O<sub>2</sub> were carried out with 5-d-old cultures.

Plates:

Seeds of *Arabidopsis* were surface sterilized by vapor-phase Chloride or by washing with EtOH 70% Triton X 100 0.05%. After the sterilization they were grown on MS – ½ medium supplemented with 0.5 g/l MES-KOH pH 5.7, 0.8% Plant Agar, and 1% Sucrose. After 48h of vernalization at 4 °C in the dark, plates were put in a growing chamber at 24

°C and long day light period (16h light/ 8h dark). The plates were kept vertically. Seedlings of 5, 8 or 10 days were used for the experiments.

#### Soil:

Plants were grown in plastic trays with steamed-sterilized Jiffy Pot (<http://jiffypot.com/jiffy/catalogue/jiffypot>). *Arabidopsis* seeds were sowed on the top of the jiffy and after 48h of vernalization at 4 °C in the dark, the trays were transferred to the growth room at 22°C, 70µmol m<sup>-2</sup> s<sup>-1</sup> white light, 70% relative humidity, and long day period (16h light/ 8h dark). Trays were regularly rotated and watered. Plants 5-week old were used for the experiments.

### Medium Compositions:

MS - ½: half concentrations of the Murashige & Skoog medium in double distilled purified water

AT3: MS medium, 30 g/L sucrose, 0.5 mg/L NAA, 0.05 mg/L Kinetin, pH 5,5

LB: Luria Bertani medium (10 g/l triptone, 5 g/l yeast extract, 10 g/l NaCl)

SOC: 20 g/l triptone, 5 g/l yeast extract, 0.5 g/l NaCl, MgCl<sub>2</sub>, MgSO<sub>4</sub>, Glucose

YEP: 10 g/l yeast extract, 10g/l peptone, 5 g/l NaCl

DMEM: Dulbecco's Modified Eagle Medium (DMEM), commercial composition

### Plasmids:

*pGreen (0029) – promoter p23-1::GUS*

The putative promoter region of the *At4g02450.1* locus (-300 to -1 bases from the start codon ATG) was cloned upstream of the uid-a gene in the *pGreen (0029) – GUS* vector. The putative promoter was PCR-amplified from the genomic DNA using Phusion DNA polymerase in GC buffer. We used the primers:

5'-CATGGAATTCCTCAAATTTGGCTAAAAAAGAAAAAGA-3'

5'-CATGGAATTCGTTTACTGGAAAAGTGTGAAGGAGAACC-3'

*pBII21-promoter p23-2::GUS*

The putative promoter region of the *At3g03773.1* locus (-1800 to -1 bases from the start codon ATG) was cloned upstream of the uid-a gene in the *pBII21* vector. The putative promoter was PCR-amplified from the genomic DNA using Phusion DNA polymerase in GC buffer. We used the primers:

5'-CATGAAAGCTTTCGCACGAAGGCATCTCCATCAG-3'

5'-CATGGGATCCGTTTTCAGCCAAGTGTAGATTTTGGATA-3'

*pGreen (0029) – CaMV 35Sx2::p23-1-YFP*

The coding sequences of the *At4g02450.1* locus was cloned in the *pGreen (0029) – 35Sx2::YFP*, upstream of the fluorescent reporter gene YFP. The coding sequence was PCR-amplified from the cDNA using Phusion DNA polymerase. We used the primers:

5'-CATGCCATGGCCATGAGTCGTCATCCTGAAGTGAAGT-3'

5'-CATGCCATGGCTGCCTTGTCTTCCTAACAGATGTTGT-3'

*pGreen (0029) – CaMV 35Sx2::p23-2-YFP*

The coding sequences of the *At3g03773.1* locus was cloned in the *pGreen (0029) – 35Sx2::YFP*, upstream of the fluorescent reporter gene YFP. The coding sequence was PCR-amplified from the cDNA using Phusion DNA polymerase. We used the primers:

5'-CATGCCATGGCCATGAGTCGTAATCCGGAGGTTCTT-3'

5'-CATGCCATGGCCGCCTTGTTCCTTGCCTTTTCCA-3'

*pGreen (0029) – promoter p23-1::p23-1-YFP*

The putative promoter region of the locus *At4g02450.1* was cloned upstream of the p23L1-YFP coding sequence in the *pGreen (0029)* vector. The putative promoter was subcloned from *pGreen (0029) – pp23L1::GUS* by digestion with EcoRI. The plasmid was transformed in dKO lines by floral dip and only phenotype-complemented lines were selected.

*pGreen (0029) – promoter p23-2::p23-2-YFP*

The putative promoter region of the locus *At3g03773.1* was cloned upstream of the p23L2-YFP coding sequence in the *pGreen (0029)*. The putative promoter was subcloned from *pBII21-pp23L2::GUS* by digestion with KpnI & BamHI. The plasmid was

transformed in dKO lines by floral dip and only phenotype-complemented lines were selected.

*pGreen (0179) – CaMV 35S::p23-1-HA*

The coding sequence of the *At4g02450.1* locus was PCR-amplified from *pGreen (0029) – 35Sx2::p23L1–YFP* using Phusion DNA polymerase, and cloned downstream of the CaMV 35S constitutive promoter in the *pGreen (0029)-35Scassette*. The reverse primer was designed in order to add the HA tag to the C terminus of the coding sequence. We used the primers:

5'-CATGGAATTCATGAGTCGTCATCCTGA-3'

5'-CATGGAATTCCTATGCGTAGTCGGGGACGTCGTAGGGGTACTTGTCTT  
CCTTAACAGATG-3'

The whole 35S-Cassette was then amplified by PCR using Phusion DNA polymerase and cloned in the *pGreen(0179)* vector. We used the primers:

5'-CATGGGTACCGATATCGTACCCCTACTCCAAAAT-3'

5'-CATGGGATCCGATATCGATCTGGATTTTAGTA-3'

*pGreen (0179) – CaMV 35S::p23-2-HA*

The coding sequence of the *At3g03773.1* locus was PCR-amplified from *pGreen (0029) – 35Sx2::p23L2–YFP* using Phusion DNA polymerase, and cloned downstream of the CaMV 35S constitutive promoter in the *pGreen (0029)-35Scassette*. The reverse primer was designed in order to add the HA tag to the C terminus of the coding sequence. We used the primers:

5'-CATGGGATCCATGAGTCGTAATCCGGAGGTTCTT-3'

5'-CATGGAGCTCCTATGCGTAGTCGGGGACGTCGTAGGGGTACTTGT  
TTCTTGCCTTTTC-3'

The whole 35S-Cassette was then amplified by PCR using Phusion DNA polymerase and cloned in the *pGreen(0179)* vector. We used the primers:

5'-CATGGGTACCGATATCGTACCCCTACTCCAAAAT

5'-CATGGGATCCGATATCGATCTGGATTTTAGTA

*pET28 – T7::6xHIS-p23-1*

In order to purify the recombinant protein p23L1 the coding sequence of the *At4g02450.1* locus was PCR-amplified from *pGreen (0029) – 35Sx2::p23L1-YFP* using Phusion DNA polymerase, and cloned in the *pET28* vector downstream of the 6xHIS tag.

5'-CATGCCATATGATGAGTCGTCATCCTGA-3'

5'-CATGCCTCGAGTCACTTGTCTTCCTAAC-3'

*pET28 – T7::6xHIS-p23-2*

In order to purify the recombinant protein p23L2 the coding sequence of the *At3g03773.1* locus was PCR-amplified from *pGreen (0029) – 35Sx2::p23L2-YFP* using Phusion DNA polymerase, and cloned in the *pET28* vector downstream of the 6xHIS tag.

5'-CATGCCATATGAGTCGTAATCCGGAGGTTCTT-3'

5'-CATGCCATATGCTACTTGTTCCTTGCCTTTTCCA-3'

*pScyce-MAS::p23-1-cCFP*

The coding sequences of the *At4g02450.1* locus was cloned in the *pScyce-MAS::cCFP* vector upstream of the C terminal part of the CFP. The coding sequence was PCR-amplified from the *pGreen (0029) – 35Sx2::p23-1-YFP* using Phusion DNA polymerase. We used the primers:

5'-CATGTCTAGAATGAGTCGTCATCCTGAAGTGAAG-3'

5'-CATGGGTACCCTTGTCTTCCTAACAGATGTTGT-3'

*pScyne- CaMV 35S::CK2αA-nCFP*

The coding sequences of the *At5g67380* locus was cloned in the *pScyne-35S::nCFP* vector upstream of the N terminal part of the CFP. The coding sequence was PCR-amplified from the cDNA using Phusion DNA polymerase. We used the primers:

5'-CATGGGATCCATGATAGATACGCTTTTCTTC-3'

5'-CATGGGAGCTCTCATTGACTTCTCATTCTGCT-3'

pScyne- *CaMV* 35S::CK2 $\alpha$ A $\Delta$ N-nCFP

The coding sequences of the *At5g67380* locus was cloned in the pScyne-35S::nCFP vector upstream of the N terminal part of the CFP. The coding sequence was PCR-amplified from the cDNA using Phusion DNA polymerase. We used the primers:

5'-CATGGGATCCATGTCGAAAGCTCGTGT-3'

5'-CATGGAGCTCTCATTGACTTCTCATTCTGCT-3'

pScyne- *CaMV* 35S::CK2 $\alpha$ B-nCFP

The coding sequences of the *At3g50000* locus was cloned in the pScyne-35S::nCFP vector upstream of the N terminal part of the CFP. The coding sequence was PCR-amplified from the cDNA using Phusion DNA polymerase. We used the primers:

5'-CATGGGATCCATGCACCTAATCTTCTTCTTC-3'

5'-CATGGAGCTCCTATTGAGTCCTCATTCTGCT-3'

## Sum table of primers:

Primer		
AC40	GCGAACTGATCGTTAAAACACTGC	
AC43	TGGTTCACGTAGTGGGCCATCG	
AC49	CATGGGTACCGATATCGTACCCCTACTCCAAAAAT	KpnI
AC50	CATGGGATCCGATATCGATCTGGATTTTAGTA	BamHI
AC59	GCAAAGACGCTCCAATGTTTGTTG	
AC60	GAAGCACCTTCCGACAGCCTTG	
AC 61	GCCTTTTCAGAAATGGATAAATAGCCTTGCTTCC	
AC 72	TTCTTCCGATATTCCTGCATC	
AC 73	TAAAACACTATTGGGGCCCAATG	
AC74	TCAAGTGGAAAGTAACCATTCG	
AC75	AACCGGAAGAGATAGGTGGTC	
AC84	TGCATTTTGTTGAGGAACAAAG	
AC85	GGAGTCTTTGATTTCTCTGCG	
AC95	CATGccatggcCATGAGTCGTCATCCTGAAGTGAAGT	NcoI
AC96	CATGccatggcTGCCTTGTCTTCCTTAACAGATGTTGT	NcoI
AC97	CATGccatggcCATGAGTCGTAATCCGGAGGTTCTT	NcoI
AC98	CATGccatggcCGCCTTGTTTCTTGCCTTTTCCA	NcoI
AC114	CATGgaattcCTCAAATTTTGGCTAAAAAAGAAAAAGA	EcoRI
AC115	CATGgaattcGTTTACTGGAAAACGTTGAAGGAGAACC	EcoRI
AC117	CATGcatatgAGTCGTAATCCGGAGGTTCTT	NdeI
AC118	CATGcatatgCTACTTGTTTCTTGCCTTTTCCA	NdeI
AC128	CATGgaagcttTCGCACGAAGGCATCTCCATCAG	HindIII
AC129	CATGggatccGTTTTTCAGCCAAGTGTAGATTTTGGATA	BamHI
AC 130	ATCTGTTGGTTGCATGTCTCAA	
AC 131	GCCAGTCGATCAATTTTCTACTA	
AC132	CATGggatccATGAGTCGTAATCCGGAGGTTCTT	BamHI
AC133	CATGgagctcCTATGCGTAGTCGGGGACGTCGTAGGGGTTACTTGTCTTCTT GCCTTTTC	SacI
AC140	CATGgagctcAATGATAGATACGCTTTTCTTCT	SacI
AC141	CATGggatccCTGCTTGACTTCTCATTCTGCT	BamHI
AC142	CATGgagctcCATGTACAAGGAACGTAGTGGA	SacI
AC143	CATGggatccCTGCTGGTTTGTGTACCTTGAA	BamHI
AC144	CATGgagctcATGAGTCGTAATCCGGAGGTTCTT	SacI
AC145	CATGggatccCCGCCTTGTTTCTTGCCTTTTCCA	BamHI
AC148	CATGgagctcAATGCACCTAATCTTCTTCTTCTCCT	SacI
AC149	CATGggatccCTGCTTGAGTCCTCATTCTGCTGCT	

		BamHI
AC150	CATGgagctcAATGTCGAAAGCTAGGGTTTATAACAGAT	SacI
AC151	CATGggtaccCTGCCTGAGTTCGTAGTCTGCTGCT	BamHI
AC152	CATGccatggccATGTGTGATAGGTATCGTTTCAAAGGT	NcoI
AC153	CATGggtaccTCGGCCACAATTAGAGATTTTATTTTACA	BamHI
AC213	TTCCTCTCCGCTTTGAATTGTCTCG	
AC214	GCCTTACCATAACCGGTACCATTG	
AC237	CATGcatatgATGAGTCGTCATCCTGA	NdeI
AC238	CATGctcgagTCACTTGTCTTCCTTAAC	XhoI
AC245	CATGctcgagTCGCACGAAGGCATCTCCATCAG	XhoI
AC246	CATGctcgagGTTTTTCAGCCAAGTGTAGATTTTGGATA	XhoI
SD9	CTCGGGTGAAACTAAGTGCTG	
SD10	GTGAACAGCAAGGAGAAGTGTC	
SD11	TCTTCTATGGCCATGACAACC	
SD12	TGTGTGATTTTTGAACGCTTG	
SD13	GCAAGCCTAAGAGGGTCATTC	
SD14	TCTCTGCGGCTTTAACTTGAG	
SD17	GAGCGCTTTGAATTCAGCTT	
SD18	GAGGCTGTTTCAGAGTTGACC	
SD19	GTCAATGTTGAGGAAAGCAAAATCAAC	
SD20	CGAGAAATCCATTCCCTTCCATTCC	
SD23	CTTGAAATATCTTGAGGCAACACG	
SD24	CTATGCGGTGGGCCAAAT	
SD25	AGCTGTTGAAGGCTTTGGACT	
SD26	TTGATGATCATAACCGGAGCA	
SD27	AGCTTCTGAAGGCATTGGATT	
SD28	TCATTGGTTCCCAACACCTT	
SD29	CATGgaattcATGAGTCGTCATCCTGA	EcoRI
SD30	CATGgaattcCTATGCGTAGTCGGGGACGTCGTAGGGGTTACTTGTCTTCCT TAACAGATG	EcoRI
SD31	CATGtctagaATGAGTCGTCATCCTGAAGTGAAG	
SD32	CATGggtaccCTTGTCTTCCTTAACAGATGTTGT	
SD37	CATGggtaccATGATAGATACGCTTTTCTTC	BamHI
SD38	CATGgagctcTCATTGACTTCTCATTCTGCT	SacI
SD39	CATGggtaccATGTCGAAAGCTCGTGT	BamHI
SD40	CATGggtaccATGCACCTAATCTTCTTCTTC	BamHI
SD41	CATGgagctcCTATTGAGTCCTCATTCTGCT	SacI
SD49	GGAAGAGTTTGAAGACGCTGATGATGAAGAAG	
SD52	GATATGGATATGGCAGGAATGGCATGGAAGAGTTTGAAG	
SD55	GTAGGTGCTCTTGTCTTCCC	
SD56	CACATAATCCCACGAGGATC	

## Methods:

Identification and cloning of the promoter region:

The genes sequences obtained from TAIR ([www.arabidopsis.org](http://www.arabidopsis.org)) were analyzed with Softberry TSSP (<http://linux1.softberry.com>) using a threshold of 0.02. The putative promoters were cloned by PCR from genomic DNA of *Arabidopsis Columbia 0* genotype.

Cloning of the coding sequences

The coding sequence of the proteins of interest were cloned by PCR from cDNA of *Arabidopsis Columbia 0* ecotype. RNA was extracted by TRIZOL method, treated by DNase, and retrotranscribed by ImProm RT or Superscript II RT using oligo dT primers.

Recombinant proteins expression and purification

The vector pET28-p23-1, pET28-p23-2, pET28-p23-1-S222A and pET28-p23-1-d, described previously, were transformed in BL21(DE3) *E. coli* cell for expression. The 6His-tagged proteins were expressed and purified by nickel affinity chromatography (HIS-Select® Nickel Affinity Gel, from Sigma-Aldrich) starting from 1 L cultures. His tag has not been removed from the purified recombinant proteins. The affinity-purified proteins were subjected to gel filtration (Superdex 200 HR 10/30 or HR 16/60 column, GE Healthcare, equilibrated in 30 mM Tris-HCl, pH 8, 150 mM NaCl elution buffer). For each purification, the eluted fractions were pooled together and concentrated by centrifugal filters (Vivaspin® Centrifugal Concentrators, 10,000 MWCO, from Sartorius Stedim Biotech) giving rise to a final concentration ranging from 100 µg/ml to 4 mg/ml. Purified proteins were analyzed by 12% SDS-PAGE, or Bradford protein quantification.

In vitro Phosphorylation assays

Protein substrates (p23-1 or  $\beta$ -casein) were incubated at 30°C with recombinant human monomeric or tetrameric CK2 or maize CK2, or at 28°C with *Arabidopsis* seedlings protein extract. The reaction take place in a phosphorylation mixture containing 50 mM Tris-HCl pH 7.5, 10 mM MgCl<sub>2</sub>, 20 µM ATP, [ $\gamma$ <sup>33</sup>P] ATP (1000/2000 cpm/pmol) according to the K<sub>m</sub> value for ATP of human CK2 (10µM), in a total volume of 20 µl. Samples were loaded on a SDS-PAGE, which was stained with Coomassie Blue and then

analyzed by autoradiography with the Cyclone Plus Storage Phosphor System (Perkin Elmer).

#### In gel Kinase assay

A protein substrate was included into a 11% SDS-PAGE (500µg/ml β-Casein or 10 µg/ml p23-1). Then cytosolic protein extract (5-40 µg) from *Arabidopsis* seedlings were resolved by electrophoresis. SDS was removed and protein renatured, as described in [Ruzzene M. et al., 2010]. Then the whole gel was incubated in a phosphorylation mixture containing 50mM Tris-HCl pH 7.5, 10 mM MgCl<sub>2</sub>, 20 µM ATP, [ $\gamma$ <sup>33</sup>P] ATP (1000/5000 cpm/pmol). After Coomassie blue staining the gel was analyzed by autoradiography for the detection of the radioactive bands.

#### qRT-PCR

cDNA of the different samples was analyzed by qRT-PCR using following primers:

Actin2 For: 5'-TTCCTCTCCGCTTTGAATTGTCTCG-3'

Actin2 Rev: 5'-GCCTTCACCATAACCGGTACCATTG-3'

P23-1 For: 5'-GTCAATGTTGAGGAAAGCAAAATCAAC-3'

P23-1 Rev: 5'-CGAGAAATCCATTCCTTCCATTCC-3'

P23-2 For: 5'-GAGCGCTTTGAATTCAGCTT-3'

P23-2 Rev: 5'-GAGGCTGTTTCAGAGTTGACC-3'

CK2αA For: 5'-CTTGAAATATCTTGAGGCAACACG-3'

CK2αA Rev: 5'-CTATGCGGTGGGCCAAAT-3'

CK2αB For: 5'-AGCTGTTGAAGGCTTTGGACT-3'

CK2αB Rev: 5'-TTGATGATCATACCGGAGCA-3'

CK2αC For: 5'-AGCTTCTGAAGGCATTGGATT-3'

CK2αC Rev: 5'-TCATTGGTTCCCAACACCTT-3'

PR1 For: 5'-GTAGGTGCTCTTGTTCTTCCC-3'

PR1 Rev: 5'-CACATAATTCCCACGAGGATC-3'

Cycle adopted for the amplification reaction was:

Denaturing

50°C 2 min  
95°C 10 min

Amplification 40X:

95°C 15 sec  
60°C 1 min

Melting:

95°C 15 sec  
60°C 15 sec  
95°C 15 sec  
60°C 15 sec

Confocal analysis

The confocal microscope analyses were performed using a Nikon PCM2000 (Bio-Rad, Germany) laser scanning confocal imaging system, or with a LEICA SP5 confocal imaging system. Excitation and Emission wavelength are reported in the image captions. Image pixel analyses were done with Fiji – Imagej bundle software.

$\beta$ -Glucuronidase (GUS) histochemical assay

Gus histochemical staining was performed at different developmental stages. Samples were analyzed for GUS activity following the protocol described by Jefferson (1987). The samples were incubated for variable time (1h to O/N) at 37°C in the following medium: 2mM X-Gluc, 0.05% Triton X-100, 2.5 mM  $K_3Fe(CN)_6$ , 2.5mM  $K_4Fe(CN)_6$  3xH<sub>2</sub>O, 10 mM EDTA and 50 mM sodium phosphate buffer pH 7.0. Experiment were performed at least 3 times and each sample consists of 10 seedlings.

Propidium Iodide Staining

*Arabidopsis* seedlings of 8-10 days old were mounted in a 2% (20 $\mu$ g/ml) Propidium iodide solution, on a microscope slide and observed by confocal microscopy. Propidium iodide stains cell walls and permits to count cells in the root meristem. 10 to 20 high definition images (1024x1024 acquired with 64X water immersion objective) were merged using stitching plugins of the Fiji – Imagej bundle software.

Experiment were performed at least 3 times and each sample consists of 10 seedlings.

#### DAF-FM staining

DAF-FM is the evolution of the DAF2 fluorescent dye for NO. It is more resistant to pH changes and the fluorescence quantum yield upon NO binding has been increased. DAF-FM DA (diacetate) is cell-permeant and passively diffuses across cellular membranes. Once inside cells, it is deacetylated by intracellular esterases to become DAF-FM. The fluorescence quantum yield of DAF-FM is ~0.005, but increases about 160-fold, to ~0.81, after reacting with nitric oxide with excitation/emission maxima of 495/515 nm. *Arabidopsis* seedlings of 8-10 days old were incubated in liquid MS - ½, 15µM DAF-FM-DA for 20 minutes and then washed with MS - ½, and incubated 2h in MS - ½. During the incubation it is possible to treat plants with a stimulus. Sample were observed by confocal microscopy using the 488 Argon line for excitation. Experiment were performed at least 3 times and each sample consists of 10 seedlings.

#### Deletion and mutagenesis

The deletion protein p23-1-d and the site-directed mutated protein p23-1-S222A were obtained as described in Asada M. et al 2000. The single primer single step mutagenesis were performed with the sequent primers:

P23-1-d: GATATGGATATGGCAGGAATGGCATGGAAGAGTTTGAAG

P23-1-S222A: GTAGGTGCTCTTGTCTTCCC

#### Analysis of the root growth

*Arabidopsis* seeds of the different genotypes were sewed on the solid growth medium, and put in vertical growth as described previously. Plates were analyzed at different development stages by image pixel analysis with Fiji – Imagej bundle software. Experiment were performed at least 10 times and each sample consists of 25 seedlings.

#### Embedding in Leica Historessin and sectioning

*Arabidopsis* seedlings were fixed overnight in the fixing solution (1% glutaraldehyde, 4% formaldehyde, 50mM Sodium phosphate pH7.2). Then samples were dehydrated by ethanol gradient and incubated overnight with solution A (basic resin solution, 1% hardener powder, 2% PEG 400) 1:1 in EtOH. Samples were then incubated in 100% Solution A for three hours and placed in the holders. Once sample are correctly disposed on the holders hardener solution (Solution A 15:1 hardener liquid). Holders can be

combined and fused by adding hardener solution. Samples were sectioned with semiautomatic Leica microtome.

#### Electron paramagnetic resonance (EPR)

Room-temperature continuous-wave EPR spectra were collected using a Bruker Elexsys E580-X-band spectrometer equipped with a ER4102ST cavity. Acquisition parameters were the following: microwave frequency = 9.38 GHz; modulation = 0.1 mT, microwave power = 6.0 mW; time constant = 163.84 ms; conversion time = 81.92 ms; number of data points = 4096 (scan range = 700 mT) or 1024 (scan range = 100 mT).

#### Analysis of cPTIO degradation

cPTIO was diluted from a 10mM stock solution directly in the growth medium of flask cultured cells, to the final concentration of 100  $\mu$ M (depending on the experiment). For the capillary analysis a sample from the cell culture was loaded into the capillary and the degradation of cPTIO was followed *in vivo* by EPR spectrometry. For the analysis of the growth medium, aliquots of the medium were taken at different incubation time and then analyzed by EPR spectrometry.

## **Collaborations**

Maria Ruzzene Ph.D., and Sofia Zanin

Collaboration on the biochemical analysis of the phosphorylation of p23

Prof. Donatella Carbonera, Bianca Posocco and Georgia Zahariou Ph.D.

Collaboration on the EPR analysis of cPTIO degradation

Prof. Christian Hardtke and David Pacheco Villalobos Ph.D.

Collaboration on the analysis of auxin homeostasis in p23 dKO and OE2HA lines

## **Acknowledgments**

I would like to thank:

Mariana Corigliano Ph.D. for the antibody of *Arabidopsis* HSP90.2

Prof. Christian Hardtke and all the members of his laboratory for kind hospitality and useful discussions

Michela Zottini and Alex Costa for the support during the Ph.D. and the proof reading of the thesis



# *Bibliography*



- Akaike, T. and Maeda, H.** (1996) Quantitation of nitric oxide using 2-phenyl-4,4,5,5-tetramethylimidazoline-1-oxyl 3-oxide (PTIO) *Methods Enzymol.*, **268**, 211-221.
- Ali, M.M., Roe, S. M., Vaughan, C. K., Meyer, P., Panaretou, B., Piper, P. W., Prodromou, C. and Pearl, L. H.** (2006) Crystal structure of an Hsp90-nucleotide-p23/Sba1 closed chaperone complex *Nature*, **440**(7087), 1013-1017.
- Bailly, A., Sovero, V. and Geisler, M.** (2006) The twisted dwarf's ABC: How immunophilins regulate auxin transport *Plant. Signal. Behav.*, **1**(6), 277-280.
- Bailly, A., Sovero, V. and Geisler, M.** (2006) The TWISTED DWARF's ABC: How immunophilins regulate auxin transport *Plant Signaling & Behavior*, **1**(6), 277-280.
- Bali, P., Pranpat, M., Bradner, J., Balasis, M., Fiskus, W., Guo, F., Rocha, K., Kumaraswamy, S., Boyapalle, S., Atadja, P., Seto, E. and Bhalla, K.** (2005) Inhibition of histone deacetylase 6 acetylates and disrupts the chaperone function of heat shock protein 90: A novel basis for antileukemia activity of histone deacetylase inhibitors *J. Biol. Chem.*, **280**(29), 26729-26734.
- Battistutta, R., Sarno, S., De Moliner, E., Marin, O., Issinger, O. G., Zanotti, G. and Pinna, L. A.** (2000) The crystal structure of the complex of zea mays alpha subunit with a fragment of human beta subunit provides the clue to the architecture of protein kinase CK2 holoenzyme *Eur. J. Biochem.*, **267**(16), 5184-5190.
- Besson-Bard, A., Pugin, A. and Wendehenne, D.** (2008) New insights into nitric oxide signaling in plants *Annu. Rev. Plant. Biol.*, **59**, 21-39.
- Besson-Bard, A., Courtois, C., Gauthier, A., Dahan, J., Dobrowolska, G., Jeandroz, S., Pugin, A. and Wendehenne, D.** (2008) Nitric oxide in plants: Production and cross-talk with Ca<sup>2+</sup> signaling *Mol. Plant.*, **1**(2), 218-228.
- Blakeslee, J.J., Bandyopadhyay, A., Lee, O. R., Mravec, J., Titapiwatanakun, B., Sauer, M., Makam, S. N., Cheng, Y., Bouchard, R., Adamec, J., Geisler, M., Nagashima, A., Sakai, T., Martinoia, E., Friml, J., Peer, W. A. and Murphy, A. S.** (2007) Interactions among PIN-FORMED and P-glycoprotein auxin transporters in arabidopsis *Plant Cell*, **19**(1), 131-147.
- Buchner, J.** (1999) Hsp90 & co. - a holding for folding *Trends Biochem. Sci.*, **24**(4), 136-141.
- Chadli, A., Bouhouche, I., Sullivan, W., Stensgard, B., McMahon, N., Catelli, M. G. and Toft, D. O.** (2000) Dimerization and N-terminal domain proximity underlie the function of the molecular chaperone heat shock protein 90 *Proc. Natl. Acad. Sci. U. S. A.*, **97**(23), 12524-12529.
- Chantalat, L., Leroy, D., Filhol, O., Nueda, A., Benitez, M. J., Chambaz, E. M., Cochet, C. and Dideberg, O.** (1999) Crystal structure of the human protein kinase CK2 regulatory subunit reveals its zinc finger-mediated dimerization *Embo j.*, **18**(11), 2930-2940.
- Clough, S.J. and Bent, A. F.** (1998) Floral dip: A simplified method for agrobacterium-mediated transformation of arabidopsis thaliana *Plant J.*, **16**(6), 735-743.

- Cooney, R.V., Harwood, P. J., Custer, L. J. and Franke, A. A.** (1994) Light-mediated conversion of nitrogen dioxide to nitric oxide by carotenoids *Environ. Health Perspect.*, **102**(5), 460-462.
- Cox, M.B., Riggs, D. L., Hessling, M., Schumacher, F., Buchner, J. and Smith, D. F.** (2007) FK506-binding protein 52 phosphorylation: A potential mechanism for regulating steroid hormone receptor activity *Mol. Endocrinol.*, **21**(12), 2956-2967.
- Crawford, N.M.** (2006) Mechanisms for nitric oxide synthesis in plants *J. Exp. Bot.*, **57**(3), 471-478.
- De Michele, R., Vurro, E., Rigo, C., Costa, A., Elviri, L., Di Valentin, M., Careri, M., Zottini, M., Sanita di Toppi, L. and Lo Schiavo, F.** (2009) Nitric oxide is involved in cadmium-induced programmed cell death in arabidopsis suspension cultures *Plant Physiol.*, **150**(1), 217-228.
- Delledonne, M., Zeier, J., Marocco, A. and Lamb, C.** (2001) Signal interactions between nitric oxide and reactive oxygen intermediates in the plant hypersensitive disease resistance response *Proc. Natl. Acad. Sci. U. S. A.*, **98**(23), 13454-13459.
- Depuydt, S. and Hardtke, C. S.** (2011) Hormone signalling crosstalk in plant growth regulation *Curr. Biol.*, **21**(9), R365-73.
- Desikan, R., Hancock, J. T., Coffey, M. J. and Neill, S. J.** (1996) Generation of active oxygen in elicited cells of arabidopsis thaliana is mediated by a NADPH oxidase-like enzyme *FEBS Lett.*, **382**(1-2), 213-217.
- Durner, J. and Klessig, D. F.** (1999) Nitric oxide as a signal in plants *Curr. Opin. Plant Biol.*, **2**(5), 369-374.
- Durner, J., Wendehenne, D. and Klessig, D. F.** (1998) Defense gene induction in tobacco by nitric oxide, cyclic GMP, and cyclic ADP-ribose *Proc. Natl. Acad. Sci. U. S. A.*, **95**(17), 10328-10333.
- Echtenkamp, F.J., Zelin, E., Oxelmark, E., Woo, J. I., Andrews, B. J., Garabedian, M. and Freeman, B. C.** (2011) Global functional map of the p23 molecular chaperone reveals an extensive cellular network *Mol. Cell*, **43**(2), 229-241.
- Espunya, M.C., Lopez-Giraldez, T., Hernan, I., Carballo, M. and Martinez, M. C.** (2005) Differential expression of genes encoding protein kinase CK2 subunits in the plant cell cycle *J. Exp. Bot.*, **56**(422), 3183-3192.
- Fernandez-Marcos, M., Sanz, L., Lewis, D. R., Muday, G. K. and Lorenzo, O.** (2011) Nitric oxide causes root apical meristem defects and growth inhibition while reducing PIN-FORMED 1 (PIN1)-dependent acropetal auxin transport *Proc. Natl. Acad. Sci. U. S. A.*, **108**(45), 18506-18511.
- Floryszak-Wieczorek, J., Milczarek, G., Arasimowicz, M. and Ciszewski, A.** (2006) Do nitric oxide donors mimic endogenous NO-related response in plants? *Planta*, **224**(6), 1363-1372.

- Garcia-Mata, C. and Lamattina, L.** (2003) Abscisic acid, nitric oxide and stomatal closure - is nitrate reductase one of the missing links? *Trends Plant Sci.*, **8**(1), 20-26.
- Geisler, M. and Bailly, A.** (2007) Tete-a-tete: The function of FKBP in plant development *Trends Plant Sci.*, **12**(10), 465-473.
- Geisler, M. and Murphy, A. S.** (2006) The ABC of auxin transport: The role of p-glycoproteins in plant development *FEBS Lett.*, **580**(4), 1094-1102.
- Geisler, M., Blakeslee, J. J., Bouchard, R., Lee, O. R., Vincenzetti, V., Bandyopadhyay, A., Titapiwatanakun, B., Peer, W. A., Bailly, A., Richards, E. L., Ejendal, K. F., Smith, A. P., Baroux, C., Grossniklaus, U., Muller, A., Hrycyna, C. A., Dudler, R., Murphy, A. S. and Martinoia, E.** (2005) Cellular efflux of auxin catalyzed by the arabidopsis MDR/PGP transporter AtPGP1 *Plant J.*, **44**(2), 179-194.
- Goldstein, S., Russo, A. and Samuni, A.** (2003) Reactions of PTIO and carboxy-PTIO with \*NO, \*NO<sub>2</sub>, and O<sub>2</sub>-\* *J. Biol. Chem.*, **278**(51), 50949-50955.
- Hecker, M., Walsh, D. T. and Vane, J. R.** (1991) On the substrate specificity of nitric oxide synthase *FEBS Lett.*, **294**(3), 221-224.
- Hess, D.T., Matsumoto, A., Kim, S. O., Marshall, H. E. and Stamler, J. S.** (2005) Protein S-nitrosylation: Purview and parameters *Nat. Rev. Mol. Cell Biol.*, **6**(2), 150-166.
- Ignarro, L.J.** (1999) Nitric oxide: A unique endogenous signaling molecule in vascular biology *Biosci. Rep.*, **19**(2), 51-71.
- Johnson, J.L., Beito, T. G., Krco, C. J. and Toft, D. O.** (1994) Characterization of a novel 23-kilodalton protein of unactive progesterone receptor complexes *Mol. Cell. Biol.*, **14**(3), 1956-1963.
- Joseph, J., Kalyanaraman, B. and Hyde, J. S.** (1993) Trapping of nitric oxide by nitronyl nitroxides: An electron spin resonance investigation *Biochem. Biophys. Res. Commun.*, **192**(2), 926-934.
- Kadota, Y. and Shirasu, K.** (2011) The HSP90 complex of plants *Biochim. Biophys. Acta*, .
- Kadota, Y., Amigues, B., Ducassou, L., Madaoui, H., Ochsenein, F., Guerois, R. and Shirasu, K.** (2008) Structural and functional analysis of SGT1-HSP90 core complex required for innate immunity in plants *EMBO Rep.*, **9**(12), 1209-1215.
- Kolbert, Z., Bartha, B. and Erdei, L.** (2008) Exogenous auxin-induced NO synthesis is nitrate reductase-associated in arabidopsis thaliana root primordia *J. Plant Physiol.*, **165**(9), 967-975.
- Kovacs, J.J., Murphy, P. J., Gaillard, S., Zhao, X., Wu, J. T., Nicchitta, C. V., Yoshida, M., Toft, D. O., Pratt, W. B. and Yao, T. P.** (2005) HDAC6 regulates Hsp90 acetylation and chaperone-dependent activation of glucocorticoid receptor *Mol. Cell*, **18**(5), 601-607.

- Krishna, P. and Gloor, G.** (2001) The Hsp90 family of proteins in arabidopsis thaliana *Cell Stress Chaperones*, **6**(3), 238-246.
- Lamotte, O., Gould, K., Lecourieux, D., Sequeira-Legrand, A., Lebrun-Garcia, A., Durner, J., Pugin, A. and Wendehenne, D.** (2004) Analysis of nitric oxide signaling functions in tobacco cells challenged by the elicitor cryptogein *Plant Physiol.*, **135**(1), 516-529.
- Lees-Miller, S.P. and Anderson, C. W.** (1989) Two human 90-kDa heat shock proteins are phosphorylated in vivo at conserved serines that are phosphorylated in vitro by casein kinase II *J. Biol. Chem.*, **264**(5), 2431-2437.
- Li, J., Soroka, J. and Buchner, J.** (2012) The Hsp90 chaperone machinery: Conformational dynamics and regulation by co-chaperones *Biochim. Biophys. Acta*, **1823**(3), 624-635.
- Malinouski, M., Zhou, Y., Belousov, V. V., Hatfield, D. L. and Gladyshev, V. N.** (2011) Hydrogen peroxide probes directed to different cellular compartments *PLoS One*, **6**(1), e14564.
- Mimnaugh, E.G., Worland, P. J., Whitesell, L. and Neckers, L. M.** (1995) Possible role for serine/threonine phosphorylation in the regulation of the heteroprotein complex between the hsp90 stress protein and the pp60v-src tyrosine kinase *J. Biol. Chem.*, **270**(48), 28654-28659.
- Miyata, Y.** (2009) Protein kinase CK2 in health and disease: CK2: The kinase controlling the Hsp90 chaperone machinery *Cell Mol. Life Sci.*, **66**(11-12), 1840-1849.
- Miyata, Y., Chambraud, B., Radanyi, C., Leclerc, J., Lebeau, M. C., Renoir, J. M., Shirai, R., Catelli, M. G., Yahara, I. and Baulieu, E. E.** (1997) Phosphorylation of the immunosuppressant FK506-binding protein FKBP52 by casein kinase II: Regulation of HSP90-binding activity of FKBP52 *Proc. Natl. Acad. Sci. U. S. A.*, **94**(26), 14500-14505.
- Moreno-Romero, J. and Martínez, M. C.** (2008) Is there a link between protein kinase CK2 and auxin signaling? *Plant Signaling & Behavior*, **3**(9), 695 <last\_page> 697.
- Moreno-Romero, J., Carme Espunya, M., Platara, M., Ariño, J. and Carmen Martínez, M.** (2008) A role for protein kinase CK2 in plant development: Evidence obtained using a dominant-negative mutant *The Plant Journal*, **55**(1), 118 <last\_page> 130.
- Moubayidin, L., Perilli, S., Dello Ioio, R., Di Mambro, R., Costantino, P. and Sabatini, S.** (2010) The rate of cell differentiation controls the arabidopsis root meristem growth phase *Curr. Biol.*, **20**(12), 1138-1143.
- Mulekar, J.J., Bu, Q., Chen, F. and Huq, E.** (2012) Casein kinase II alpha subunits affect multiple developmental and stress-responsive pathways in arabidopsis *Plant J.*, **69**(2), 343-354.
- Otvos, K., Pasternak, T. P., Miskolczi, P., Domoki, M., Dorjgotov, D., Szucs, A., Bottka, S., Dudits, D. and Feher, A.** (2005) Nitric oxide is required for, and promotes auxin-mediated activation of, cell division and embryogenic cell formation

- but does not influence cell cycle progression in alfalfa cell cultures *Plant J.*, **43**(6), 849-860.
- Overvoorde, P., Fukaki, H. and Beeckman, T.** (2010) Auxin control of root development *Cold Spring Harb Perspect. Biol.*, **2**(6), a001537.
- Pearl, L.H. and Prodromou, C.** (2006) Structure and mechanism of the Hsp90 molecular chaperone machinery *Annu. Rev. Biochem.*, **75**, 271-294.
- Pinna, L.A.** (2002) Protein kinase CK2: A challenge to canons *J. Cell. Sci.*, **115**(Pt 20), 3873-3878.
- Pinna, L.A. and Ruzzene, M.** (1996) How do protein kinases recognize their substrates? *Biochim. Biophys. Acta*, **1314**(3), 191-225.
- Planchet, E. and Kaiser, W. M.** (2006) Nitric oxide (NO) detection by DAF fluorescence and chemiluminescence: A comparison using abiotic and biotic NO sources *J. Exp. Bot.*, **57**(12), 3043-3055.
- Rahman, A., Bannigan, A., Sulaman, W., Pechter, P., Blancaflor, E. B. and Baskin, T. I.** (2007) Auxin, actin and growth of the arabidopsis thaliana primary root *Plant J.*, **50**(3), 514-528.
- Ruzzene, M., Di Maira, G., Tosoni, K. and Pinna, L. A.** (2010) Assessment of CK2 constitutive activity in cancer cells *Methods Enzymol.*, **484**, 495-514.
- Salinas, P., Fuentes, D., Vidal, E., Jordana, X., Echeverria, M. and Holuigue, L.** (2006) An extensive survey of CK2 alpha and beta subunits in arabidopsis: Multiple isoforms exhibit differential subcellular localization *Plant Cell Physiol.*, **47**(9), 1295-1308.
- Sangster, T.A. and Queitsch, C.** (2005) The HSP90 chaperone complex, an emerging force in plant development and phenotypic plasticity *Curr. Opin. Plant Biol.*, **8**(1), 86-92.
- Sangster, T.A., Salathia, N., Lee, H. N., Watanabe, E., Schellenberg, K., Morneau, K., Wang, H., Undurraga, S., Queitsch, C. and Lindquist, S.** (2008) HSP90-buffered genetic variation is common in arabidopsis thaliana *Proc. Natl. Acad. Sci. U. S. A.*, **105**(8), 2969-2974.
- Sangster, T.A., Bahrami, A., Wilczek, A., Watanabe, E., Schellenberg, K., McLellan, C., Kelley, A., Kong, S. W., Queitsch, C. and Lindquist, S.** (2007) Phenotypic diversity and altered environmental plasticity in arabidopsis thaliana with reduced Hsp90 levels *PLoS One*, **2**(7), e648.
- Sankar, M., Osmont, K. S., Rolcik, J., Gujas, B., Tarkowska, D., Strnad, M., Xenarios, I. and Hardtke, C. S.** (2011) A qualitative continuous model of cellular auxin and brassinosteroid signaling and their crosstalk *Bioinformatics*, **27**(10), 1404-1412.
- Santuari, L., Scacchi, E., Rodriguez-Villalon, A., Salinas, P., Dohmann, E. M., Brunoud, G., Vernoux, T., Smith, R. S. and Hardtke, C. S.** (2011) Positional

information by differential endocytosis splits auxin response to drive arabidopsis root meristem growth *Curr. Biol.*, **21**(22), 1918-1923.

**Scroggins, B.T., Robzyk, K., Wang, D., Marcu, M. G., Tsutsumi, S., Beebe, K., Cotter, R. J., Felts, S., Toft, D., Karnitz, L., Rosen, N. and Neckers, L.** (2007) An acetylation site in the middle domain of Hsp90 regulates chaperone function *Mol. Cell*, **25**(1), 151-159.

**Sidera, K. and Patsavoudi, E.** (2008) Extracellular HSP90: Conquering the cell surface *Cell. Cycle*, **7**(11), 1564-1568.

**Stamler, J.S., Lamas, S. and Fang, F. C.** (2001) Nitrosylation. the prototypic redox-based signaling mechanism *Cell*, **106**(6), 675-683.

**Sud, N., Sharma, S., Wiseman, D. A., Harmon, C., Kumar, S., Venema, R. C., Fineman, J. R. and Black, S. M.** (2007) Nitric oxide and superoxide generation from endothelial NOS: Modulation by HSP90 *Am. J. Physiol. Lung Cell. Mol. Physiol.*, **293**(6), L1444-53.

**Szyska, R., Kramer, G. and Hardesty, B.** (1989) The phosphorylation state of the reticulocyte 90-kDa heat shock protein affects its ability to increase phosphorylation of peptide initiation factor 2 alpha subunit by the heme-sensitive kinase *Biochemistry*, **28**(4), 1435-1438.

**Terrile, M.C., Paris, R., Calderon-Villalobos, L. I., Iglesias, M. J., Lamattina, L., Estelle, M. and Casalongue, C. A.** (2012) Nitric oxide influences auxin signaling through S-nitrosylation of the arabidopsis TRANSPORT INHIBITOR RESPONSE 1 auxin receptor *Plant J.*, **70**(3), 492-500.

**Tosoni, K., Costa, A., Sarno, S., D'Alessandro, S., Sparla, F., Pinna, L. A., Zottini, M. and Ruzzene, M.** (2011) The p23 co-chaperone protein is a novel substrate of CK2 in arabidopsis *Mol. Cell. Biochem.*, .

**Waadt, R. and Kudla, J.** (2008) In planta visualization of protein interactions using bimolecular fluorescence complementation (BiFC) *CSH Protoc.*, **2008**, pdb.prot4995.

**Yamasaki, H., Sakihama, Y. and Takahashi, S.** (1999) An alternative pathway for nitric oxide production in plants: New features of an old enzyme *Trends Plant Sci.*, **4**(4), 128-129.

**Yang, Y., Rao, R., Shen, J., Tang, Y., Fiskus, W., Nechtman, J., Atadja, P. and Bhalla, K.** (2008) Role of acetylation and extracellular location of heat shock protein 90alpha in tumor cell invasion *Cancer Res.*, **68**(12), 4833-4842.

**Yong, W., Yang, Z., Periyasamy, S., Chen, H., Yucel, S., Li, W., Lin, L. Y., Wolf, I. M., Cohn, M. J., Baskin, L. S., Sanchez, E. R. and Shou, W.** (2007) Essential role for co-chaperone Fkbp52 but not Fkbp51 in androgen receptor-mediated signaling and physiology *J. Biol. Chem.*, **282**(7), 5026-5036.

**Zhang, Z., Sullivan, W., Felts, S. J., Prasad, B. D., Toft, D. O. and Krishna, P.** (2010) Characterization of plant p23-like proteins for their co-chaperone activities *Cell Stress Chaperones*, **15**(5), 703-715.

**Zhao, Y.G., Gilmore, R., Leone, G., Coffey, M. C., Weber, B. and Lee, P. W.** (2001) Hsp90 phosphorylation is linked to its chaperoning function. assembly of the reovirus cell attachment protein *J. Biol. Chem.*, **276**(35), 32822-32827.

**Zhu, S. and Zhou, J.** (2006) Effects of nitric oxide on fatty acid composition in peach fruits during storage *J. Agric. Food Chem.*, **54**(25), 9447-9452.

**Zottini, M., Costa, A., De Michele, R., Ruzzene, M., Carimi, F. and Lo Schiavo, F.** (2007) Salicylic acid activates nitric oxide synthesis in arabidopsis *J. Exp. Bot.*, **58**(6), 1397-1405.

---

*Bibliography*



Esposizione riassuntiva

## CARATTERIZZAZIONE BIOCHIMICA E FUNZIONALE DI P23: UNA CO-CHAPERONE REGOLATORIA DI HSP90 IN *ARABIDOPSIS*

In questo lavoro di tesi è stata eseguita l'analisi della funzione della co-chaperone p23 di HSP90, analizzando diversi aspetti dell'espressione, regolazione e funzione, in modo da riuscire ad ottenere una caratterizzazione di ampio raggio della proteina.

HSP90 e p23 sono proteine fortemente conservate in tutti gli eucarioti, ma gli studi sono stati condotti, finora, principalmente in ambito animale. Questo lavoro ha lo scopo di individuare il ruolo ricoperto da p23 in pianta, organismo nel quale HSP90 stessa ha dimostrato di avere un pattern funzionale solo in parte simile a quello animale, e ricco di funzioni caratteristiche per il regno vegetale.

In *Arabidopsis thaliana* sono presenti due isoforme di p23 e la caratterizzazione della proteina è stata condotta su entrambe le isoforme parallelamente, studiando l'espressione *in planta* e la regolazione tramite fosforilazione.

Innanzitutto è stato dimostrato che entrambe le proteine sono fosforilate specificamente dalla forma monomeric della chinasi CK2, e che le due isoforme di p23 sono fosforilate da diverse subunità catalitiche di CK2. Questo comportamento suggerisce nuove ipotesi sulla fosforilazione da parte di CK2 in pianta, in quanto finora le diverse isoforme di CK2 presenti in pianta avevano mostrato solo funzioni ridondanti.

Sebbene questi studi *in vitro*, dovranno essere confermati dalla caratterizzazione *in vivo* della fosforilazione, rivelano che p23 possiede una regolazione post-trascrizionale specifica, individuano la chinasi responsabile della fosforilazione ed indentificano il residuo fosforilato di p23-1 nella Serina 222.

La regolazione delle proteine è stata studiata anche tramite l'analisi dell'espressione *in planta*, sia analizzando i livelli dei messaggeri, sia identificando i presunti promotori delle due proteine ed ottenendo piante reporter stabilmente trasformate. Entrambe le analisi sono state effettuate a diversi stadi dello sviluppo e su diversi organi, ed hanno permesso di ottenere un quadro completo dell'espressione delle due proteine in pianta. Le due proteine sono espresse nei tessuti floematici in tutta la pianta: dal meristema radicale alle foglie, ed i due promotori hanno mostrato attività fortemente tessuto specifica. L'analisi del livello dei trascritti tramite qRT-PCR ha evidenziato che p23-1 è espressa a livelli maggiori di p23-2, e ha confermato che le due proteine hanno lo stesso pattern di espressione. I trattamenti effettuati, inoltre, non hanno indotto cambiamenti nel pattern di

espressione. È stata inoltre studiata la localizzazione subcellulare delle due proteine tramite l'utilizzo di piante stabilmente trasformate esprimenti le proteine fuse ad un reporter fluorescente, sotto il controllo di un promotore costitutivo. L'analisi tramite microscopia confocale delle piante reporter ha rivelato la localizzazione citosolica e nucleare di entrambe le proteine.

Lo studio funzionale di p23 è stato, inoltre, condotto tramite la generazione di diversi strumenti genetici come il doppio mutante knockout e i singoli mutanti overesprimenti. Per questo tipo di studi sono stati generati mutanti che overesprimono singolarmente le due proteine fuse al tag HA. L'analisi di questi mutanti ha portato alla scoperta di un ruolo di p23 nella crescita e nello sviluppo sia della radice primaria che delle radici secondarie, infatti il doppio mutante knockout mostra radici più corte, rispetto al wild type, mentre le linee overesprimenti mostrano radici più lunghe. Inoltre p23 sembra avere un ruolo anche nella produzione del monossido d'azoto, un importante molecola segnale nel regno vegetale. Sono stati condotti esperimenti preliminari per testare se la crescita ridotta del mutante knockout fosse dovuta alla minore produzione di NO, ma i risultati suggeriscono che il monossido di azoto sia coinvolto nella crescita delle radici ma non sia il fattore principale nel fenotipo mostrato dal mutante di p23.

È stata inoltre testata la capacità del doppio mutante knockout di produrre NO sotto elicitazione con acido salicilico, ed è stato dimostrato che sia la mancanza di p23 sia la mancanza dell'isoforma HSP90.1, impediscono la corretta produzione di NO, quindi si ipotizza che il signalling del acido salicilico, un ormone vegetale coinvolto nella risposta all'attacco di patogeni, sia compromessa nel mutante doppio knockout di p23.

Durante il lavoro di tesi è stato inoltre condotto un approfondimento tecnico sul comportamento di una ben nota molecola scavenger del monossido di azoto, il cPTIO, in presenza di cellule o tessuti vivi. È stato quindi dimostrato che questa molecola subisce delle reazioni che ne fanno scomparire il segnale EPR, quando incubata in presenza di materiale vivo. Questa nota tecnica risulta particolarmente utile, in quanto in base alle cinetiche di degradazione mostrate, si potrà decidere quali sono le concentrazioni più appropriate in base alla durata degli esperimenti.

Il progetto ha approfondito la conoscenza della funzione di p23 sia tramite l'analisi biochimica della fosforilazione da parte di CK2 di p23, sia analizzando il comportamento dei diversi mutanti. È stato individuato un ruolo centrale per p23 nella produzione di NO e nello sviluppo della radice. In particolare viene mostrato che la crescita subnormale delle radici del mutante knockout di p23 dipende da un alterata crescita del meristema radicale. Il meristema radicale è controllato da un fine meccanismo dipendente

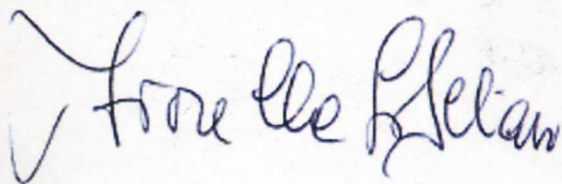
dall'equilibrio fra citochinine ed auxina, è il progetto sta ora evolvendo verso l'analisi dell'equilibrio di questi ormoni nei diversi mutanti.



Medaglione Stefano D'Alessandro

In his PhD thesis, Stefano D'Alessandro presents the characterisation, biochemically and functionally, of the p23 protein in *Arabidopsis thaliana*, a model plant organism. This protein, a co-chaperon of HSP90, is well known in animal but poorly investigated in plant. Stefano addressed the biochemical analysis of the protein working in a tight collaboration established between Prof. Pinna's and our lab, showing good capacity and autonomy in organising and carrying out his work. In our lab, working on the functional aspects of the protein, Stefano carried out the molecular and cell biology characterization of p23, acquiring deep knowledge in several molecular, cell biological and imaging techniques. During the last year, Stefano spent few months in the lab of prof. Christian Hardtke, chairman of the Plant Molecular Biology Department, at the University of Lausanne. In this period he generated numerous *Arabidopsis* lines useful for testing the hypothesis of a possible involvement of p23 in auxin transport.

Stefano D'Alessandro has been a very good PhD student, highly motivated, a good reader of the scientific literature, capable of projecting and organising his scientific work in an autonomous way and then now ready to begin his career as a brilliant young scientist. For these reasons my opinion on him is excellent.

A handwritten signature in blue ink, reading "Fiorella Lo Schiavo". The signature is written in a cursive style with a large initial 'F'.

Prof. Fiorella Lo Schiavo





UNIL | Université de Lausanne  
Département de biologie moléculaire  
végétale  
bâtiment Biophore bureau 5426  
CH-1015 Lausanne

Lausanne, January 21st, 2012

Subject: evaluation, Ph.D. thesis submitted by Mr. Stefano d'Alessandro

---

To whom it may concern,

Stefano d'Alessandro submits a Ph.D. thesis that revolves around the characterization of the p23 co-chaperone in plants. p23 is a regulator of the conserved eukaryotic chaperone HSP90, and equally conserved among eukaryotes. Next to nothing is known however about the role of p23 in plants, and this thesis set out to clarify this issue. Clearly, this is a timely subject for a thesis, which is both of general interest to biologists and particular interest to plant biologists.

Although extensive literature on the role of p23 in animal systems exists, these findings are frequently not directly transferable to plants beyond the purely biochemical facts. The thesis therefore concentrated on confirming the biochemical and cell biological activities of p23 in the model plant Arabidopsis, such as interaction with the Arabidopsis HSP90, and on deciphering the biological role of p23 in the cellular and developmental context. Thus, an introductory part of the thesis investigates the potential regulation of p23 activity by the conserved eukaryotic casein kinase 2, while the bulk of the thesis aims to embed p23 activity in the established framework of root growth control, with special attention to the relation with hormone pathways as well as nitric oxide perception. These investigations were motivated by the observation that mutation and transgenic over-expression of p23 isoforms results in a reduced and rare enhanced root growth phenotype, respectively, as well as an alteration in nitric oxide homeostasis. While the part on casein kinase 2 regulation has been published, the observations on p23 activity in development presented in the subsequent chapters are not, but from the data set I believe a first author paper for Mr. d'Alessandro is definitely a realistic prospect.

Overall, the thesis gives a bit of a fragmented impression, it contains a nice set of useful data that appear to have been acquired meticulously, but they do not yet connect very well towards a coherent story. However, in my experience this often occurs in the type of reverse genetics approach chosen here, and I have little doubt that with some extra effort the loose ends can be connected to give a consistent idea of p23 activity and its developmental role in Arabidopsis. As such, I therefore support the award of a Ph.D. for this work and I wish all the best to Stefano d'Alessandro for his future career.

With best wishes,



Christian Hardtke

Faculté de biologie et de médecine  
Département de biologie moléculaire végétale

Tél.+41 21 692 42 51 | Fax.+41 21 692 41 95 | Christian.Hardtke@unil.ch



## EVALUATION REPORT

THESIS TITLE: BIOCHEMICAL AND FUNCTIONAL CHARACTERIZATION OF P23  
A REGULATORY CO-CHAPERONE OF HSP90 IN *ARABIDOPSIS*.

PhD Student: Stefano D'Alessandro

In this the thesis work the author addressed many aspects related to the biochemical regulation of p23 activity, and he has initiated the study of the putative involvement of p23 in the regulation of different biological signaling pathways. P23 is a co-chaperone of the HSP90 complex, which is found in all eukaryotes.

Regarding the studies on the regulation of p23 activity, the author presents data about p23 gene expression in Arabidopsis, both at different stages of Arabidopsis development and in different organs of adult Arabidopsis plants, studies performed by measuring the accumulation of transcript levels by qRT-PCR. In addition, he performed promoter analysis, using fusions of p23 promoter with the gene reporter GUS. These data reveal similar patterns of expressions for the two p23-encoding genes in Arabidopsis, although one of the genes appears to be much highly expressed than the other.

Moreover, the author also demonstrates that p23 is phosphorylated in vitro by protein kinase CK2. The two isoforms of p23 (p23-1 and p23-2) might be phosphorylated by different isoforms of CK2, which raises interesting questions and hypothesis about the role of this phosphorylation. Although these studies should be confirmed by studies of phosphorylation in vivo, these experiments reveal a post-transcriptional regulation of p23 and they identify the kinase responsible of the phosphorylation, as well as the residue of p23 that is phosphorylated.

The functional studies have been addressed by generating several genetic tools, such as knock-out mutants and overexpressing lines for the two p23-encoding genes, and by using mutants of protein kinase CK2. The author has studied the phenotypes of the p23 mutants, and has related these data with nitric oxide-signaling and salicylic acid-signaling pathways. Although still preliminary, the results presented in the thesis work point out to a function of p23 in the biosynthesis of nitric oxide, and also a role in the SA-signaling and auxin-signaling biological pathways.

The thesis work also presents a technical note regarding the quantification of nitric oxide in plants, which is of great interest in this field.

The amount of work performed by Mr. D'Alessandro is impressive. He has used a great amount of different techniques in the fields of biochemistry, cellular biology, and genetic engineering. He has used the most actual approaches to answer biological

questions (use of gene reporters, transgenic plants, mutants, etc...) as well as other, more classical techniques, in biochemistry. In this sense, I think he has acquired a very good expertise in the laboratory and he will be able in the future to apply them to any project. In addition, he got interesting results that contribute to the knowledge in plant biology. Thus, the work performed by Mr. D'Alessandro has the standard levels to get his PhD degree. My opinion is that it is an excellent work and that is well presented in its written form.

*M. Carmen Martínez*  
←

M. Carmen Martínez, PhD

Biochemistry and Molecular Biology Department

Autonomous University of Barcelona



Universitat Autònoma de Barcelona

Departament de Bioquímica  
i de Biologia Molecular

Unitat de Bioquímica de Biociències



UNIVERSITÀ  
DEGLI STUDI  
DI PADOVA

SCUOLA DI DOTTORATO  
IN BIOSCIENZE E BIOTECNOLOGIE  
INDIRIZZO DI BIOTECNOLOGIE

**Estratto del verbale del Collegio**

**Scuola di Dottorato in Bioscienze e Biotecnologie**

**Indirizzo di BIOTECNOLOGIE**

**Seduta dell' 11 Dicembre 2012**

Alle ore 14.00 del giorno 11 Dicembre 2012 nell'aula seminari del 5° piano sud del Dipartimento di Biologia, si è riunito il Collegio dei Docenti dell'Indirizzo di Biotecnologie della Scuola di Dottorato in Bioscienze e Biotecnologie.

Risultano presenti:

Nome	Presenze	Assenze giustificate	Assenze
Mariano Beltramini		X	
Pietro Benedetti	X		
Elisabetta Bergantino	X		
Luigi Bubacco	X		
Francesco Filippini	X		
Fiorella Lo Schiavo	X		
Stefano Mammi	X		
Emanuele Papini		X	
Patrizia Polverino De Laureto	X		
Andrea Squartini		X	
Giorgio Valle	X		
Paola Venier	X		
Giuseppe Zanotti	X		
Chiara Fecchio ( <i>Rappresentante dei dottorandi</i> )	X		

Il Coordinatore dell'Indirizzo, Prof. Giorgio Valle, riconosce valida la seduta e la dichiara aperta per trattare, come dall'avviso di convocazione, il seguente ordine del giorno:

1. Comunicazioni.
2. Ammissione dei dottorandi del 26° e 27° ciclo all'anno successivo.
3. Ammissione dei dottorandi del 3° anno all'esame finale.
4. Progetti di dottorato da assegnare ai dottorandi del 28° ciclo.
5. Pratiche dottorandi.

...omissis...



UNIVERSITÀ  
DEGLI STUDI  
DI PADOVA

SCUOLA DI DOTTORATO  
IN BIOSCIENZE E BIOTECNOLOGIE  
INDIRIZZO DI BIOTECNOLOGIE

**Oggetto 3: Ammissione dei dottorandi del 3° anno all'esame finale.**

Il Collegio, dopo avere sentito le presentazioni dei dottorandi, visto le loro relazioni scritte e sentito il parere dei rispettivi supervisori e tutori, discute in merito all'ammissione dei dottorandi all'esame finale, prendendo in considerazione individualmente ogni singolo caso.

Dopo adeguata discussione il Collegio delibera quanto segue:

Albiero: è ammesso all'esame finale di dottorato in Biotecnologie;  
Andreazza: è ammessa all'esame finale di dottorato in Biotecnologie;  
Beneventi: è ammessa all'esame finale di dottorato in Biotecnologie;  
Bisogno: è ammesso all'esame finale di dottorato in Biotecnologie;  
Cappellini: è ammessa all'esame finale di dottorato in Biotecnologie;  
D'Alessandro: è ammesso all'esame finale di dottorato in Biotecnologie;  
De Pascale: è ammesso all'esame finale di dottorato in Biotecnologie;  
De Pittà: è ammesso all'esame finale di dottorato in Biotecnologie;  
Fedeli: è ammessa all'esame finale di dottorato in Biotecnologie;  
Giannetti: è ammessa all'esame finale di dottorato in Biotecnologie;  
Minute: è ammesso all'esame finale di dottorato in Biotecnologie;  
Plotegher: è ammessa all'esame finale di dottorato in Biotecnologie;  
Rossi: è ammesso all'esame finale di dottorato in Biotecnologie.

...omissis...

Non essendoci altri punti da discutere, il verbale viene approvato seduta stante e la seduta del Collegio si conclude alle ore 13,30.

Prof. Giorgio Valle  
Coordinatore dell'Indirizzo